LAB-SCALE FEASIBILITY OF IN-SITU CARBONATION OF ALKALINE INDUSTRIAL WASTES

LAURENS A.D.R. THUY

MSC. THESIS

LAB-SCALE FEASIBILITY OF IN-SITU CARBONATION OF ALKALINE INDUSTRIAL WASTES

Student Name: Laurens Thuy

Student Number: 3399346

Home Institute: Utrecht University, Utrecht, The Netherlands

Receiving Institute: Tor Vergata University, Rome, Italy

Research Topic: Accelerated In-Situ Carbonation of Alkaline Industrial Wastes

In the framework of the project: HOMBRE, Holistic Management of Brownfield Areas

Mentor Utrecht University: Dr. Ruud Schotting

Mentor Tor Vergata University: Dr. Renato Baciocchi

Cooperating Phd student: Oriana Capobianco

Cooperating Bachelor student: Elisa Magliocci

ABSTRACT

The need for inventive techniques to address current soil- and water pollution problems has sparked research on remediation methods such as accelerated carbonation technology (ACT). However, the majority of research has focused on optimising the process by applying highly enhanced and energy-intensive conditions, thereby making large-scale application unfeasible. The HOMBRE project is working on integrated techniques to make redevelopment of polluted Brownfield areas faster, more profitable and more sustainable. In line with this, the current work investigated the feasibility of accelerated in-situ carbonation of industrial wastes under more ambient conditions with as objective to improve the materials environmental behaviour. Special focus was on stainless steel slags. The experimental research consisted of a full physical and chemical characterisation of the material with subsequent carbonation experiments. Initially, batch experiments were conducted to determine the maximal CO_2-uptake of the material whereas in a later stage column carbonation was performed according to a new direct-carbonation set-up. Results indicated that performance of the column set-up was similar to more widely-used methods under similar conditions: a CO_2-uptake of 5.5% was found for a reaction time of 8h in the column. Post-carbonation analysis pointed out that treatment indeed had significantly altered the slags mineralogy. The main effects of this were an increased buffering capacity, a reduced alkalinity, and significant changes in the leaching concentration of hazardous metals.

NOMENCLATURE LIST

ACT: Accelerated Carbonation Technique

ANC: Acid Neutralization Capacity

AOD: Argon Oxygen Decarburization

AOD-L: Argon Oxygen Decarburization Lance

AOGCM: Atmosphere-Ocean Coupled General Circulation Model

APC: Air Pollution Control

BF: Brownfield

BOF: Basic Oxygen Furnace

CCS: Carbon Capture & Storage

CCT: Clean Coal Technology

CFC: Chlorofluorocarbon

CKD: Cement Kiln Dust

DC furnace: Direct-Current furnace

EAF: Electric Arc Furnace

GCM: General Circulation Model

GHG: Greenhouse Gas

GWP: Global Warming Potential

HOMBRE: Holistic Management of Brownfield Regeneration

HTT: Holistic Technology Train

IC: Inorganic Carbon

ICP-OES: Inductively Coupled Plasma- Optical Emission Spectrum

MSWI: Municipal Solid Waste Incineration

O.M.: Organic Matter

PAH: Polycyclic Aromatic Hydrocarbon

PCC: Precipitated Calcium Carbonate

PFA: Pulverized Fly Ash

PSD: Particle Size Distribution

S/S: Solidification / Stabilization

SICC: Solid Inorganic Carbon Content

SS: Stainless slag

SSS: Stainless steel slag

TCLP: Toxicity Characterization Leaching Procedure

TT: Technology Train

TCO_2-uptake: Theoretical CO_2-uptake

ECO_2-uptake: Effective CO_2-uptake

UP water: Ultra-Pure water

VOC: Volatile Organic Carbon

XRD: X-ray Diffraction

LISTS OF FIGURES

LISTS OF TABLES

ACKNOWLEDGMENTS

TABLE OF CONTENTS

1 **INTRODUCTION**

Worldwide, soils in widespread areas are characterised by elevated concentrations of polluting substances due to anthropogenic activities. In particular, the presence of elevated concentrations of heavy metals can be of a large importance for human health due to the fact that they are non-biodegradable and accumulative in nature, leading to harmful effects in the long-term (Škrbic & Mladenovic, 2010). Possible solutions for remediation of this pollution may be divided into 2 major categories: off-site treatment, with which the affected soil is excavated, followed by post-processing of the soil in another location, or on-site treatment, for which the soil is remediated without excavation and thus in-situ.

The aim of the research is to investigate the applicability of in-situ carbonation of alkaline wastes through CO_2-injection in soils or land-filled areas as a means of an engineering practice for the environmental treatment of potentially harmful pollutants.

This thesis focuses on lab-scale carbonation of alkaline waste materials such as steel slags, with a focus on stainless steel slag. As was acknowledged by Baciocchi et al. (2009), research done on wet carbonation of stainless steel slags, to examine the effect of different carbonation extents on slag properties, is still rather sparse. Therefore, lab-scale tests were performed to investigate the feasibility of field-scale in-situ accelerated carbonation of these wastes. The research was performed within the framework of the international HOMBRE (HOlistic Management of Brownfield REdevelopment) project. The main products of this carbonation process are inorganic alkali (earth) carbonates. Research will be done to investigate the feasibility of applying in-situ accelerated carbonation technique (ACT) upon alkaline industrial (steel) wastes through the use of CO_2-injection, originating from industrial activities or generated by other remediation techniques, such as ECO-GROUT. Carbonation of these waste slags could serve as an engineering practice for environmental treatment of hazardous material by stabilizing and reinforcing the matrix through carbonate formation in order to limit the leaching and spreading of heavy metals and other potentially harmful substances into

13

the environment. In addition to this it could be possible to use these carbonated wastes as a substitute for other raw carbonates in certain applications, thereby reducing the consumption of raw materials and reducing the volume of waste to be landfilled without further use. Examples of this are the use of the carbonated material as a filler for road construction, as a component in cement or in paper- or rubber production (U.S. Department Of The Interior, 2005). A positive side-effect would be the dual reduction in GHG emissions: at one hand as avoided emissions through reuse and limited raw material consumption, and on the other hand through CO_2 uptake of the material, what may provide a safe and long-term solution for CO_2 storage. This could contribute to the efforts in combating global climate warming.

The in-situ carbonation feasibility will be assessed according to lab research tests on a specific kind of slag, making use of a new carbonation setup. On behalf of the tests, the sampled material will be fully characterized in terms of particle size distribution, initial humidity, the total inorganic carbon content, environmental behaviour through the analysis of the leachate (concentration of chlorides, heavy metals and other elements of interest), its chemical phases, and elemental composition. The carbonation tests will be performed on different fractions of the material to track differences in leaching concentration and behaviour for specific elements. Carbonation tests will be initially performed in a stainless steel container submerged in a warm water bath to identify the optimal carbonation conditions for the specific slag and to determine the maximal extent of carbonation. After this, the carbonation of the material will occur in a glass column to simulate more realistic, field-like conditions, with flow of CO_2 through the porous medium. After the tests, the extent of carbonation will be validated through gravimetric and TIC analysis whereas the change in elemental composition and environmental behaviour of the material will be examined through ICP-OES and leachate testing.

This dissertation will be structured as follows. In Chapter 2, the topic of water and soil pollution is being discussed through further elaboration of the topic by revealing the true extent of the problem, the contaminant sources, and their potential dangerous effect on the environment. Together with this, the concept of a Brownfield is introduced along with the possible remediation techniques to this worldwide phenomenon. Emphasis is laid on the HOMBRE project, which is seeking innovative and integrated solutions to the problem of water and soil pollution and the remediation of Brownfield areas. During a side-step, the

problem of global climate change is shortly discussed, with special focus on the primary drivers of this problem, which are co-causers of the water-and soil pollution issues on whom this work is dedicated. Therefore, solutions to the latter might be part of the solution for the former problem. This solution might be in the form of ACT remediation, a technique which is discussed in Chapter 3, where an overview on the topic is given by compiling essential information through a literature review of previous research on the topic of industrial waste carbonation. Emphasis is strongly put on the lab-scale remediation of steel slags. Throughout the chapter, the scope of interest narrows down to a specific type of slags, stainless steel slags, on which the current research was performed.

The contaminated slag material was fully analysed in terms of its physical and chemical properties, and subsequently tested during a series of experiments according to two main set-ups: batch and column. The technical part of the whole analysis process and the experimental phase is described throughout Chapter 4: 'Materials and Methods'. Finally, the outcomes of the research are presented in Chapter 5. Here, the obtained results on the properties and the environmental behaviour of the material are put forward. Next to this, the effect of the applied carbonation techniques is evaluated through the changes in properties and composition that occurred with respect to the untreated material. Besides this, also the effectiveness of the lab carbonation setup is discussed.

2 WATER – AND SOIL POLLUTION AND REMEDIATION

2.1 Pollution worldwide

Soil pollution is a kind of chemical degradation that can be caused by many processes or activities such as the accumulation of industrial or urban wastes, an excessive use of manure or pesticides for agriculture or horticulture, the settling and acidification of airborne pollutants, or the spilling of harmful substances. Soil pollution tends to be more common or more severe in or near densely populated areas, accompanied by intensified industrial activities, although contamination of more remote regions may occur through airborne deposition as well (Oldeman, 1992). In Europe, pollution by industrial and bio-industrial activities is the dominant type of human-induced soil degradation, however quantitative estimates are sparse. In 1992, about 22 million ha worldwide was known to be degraded by pollution, although this figure was most certainly an under-estimation since 19 million ha of this were located in Europe (Oldeman, 1992). Contamination by means of metals forms one of the more severe types of soil pollution as a consequence of the toxic properties of several metals and their persistence and long-lasting character in the environment. Human-induced soil contamination with metals occurs mostly by the introduction of the elements of lead, cadmium, tin and mercury in the environment. This introduction of the aforementioned and other polluting substances may happen through different processes such as: fuel combustion (transport vehicles), residential services, industrial- and agricultural activities (chemical treatments, ploughing), solid or liquid waste disposal (municipal and industrial), the use of wastewater for irrigation, or by direct contact and abrasion (e.g. tires) (Khan et al., 2008). Contamination may also occur due to settling of airborne material originating from coal- or fuel combustion, waste incineration and steel industry (Khan et al., 2008; Zhang et al., 2008). Steel production on its own causes elevated concentrations of especially Cr, Cu, Mn, Fe and Nb through the settling of airborne particles (Cannon & Horton, 2009). Smelting operations produce iron and steel from iron ores and may also extract copper and other base metals. Next to through the deposition of the mentioned airborne metals, asbestos, and sulfur compounds, contamination from the steel industry also occurs through improper management of the waste

products and non-precautious storage or disposal may lead to direct soil and groundwater pollution (HOMBRE, 2010).
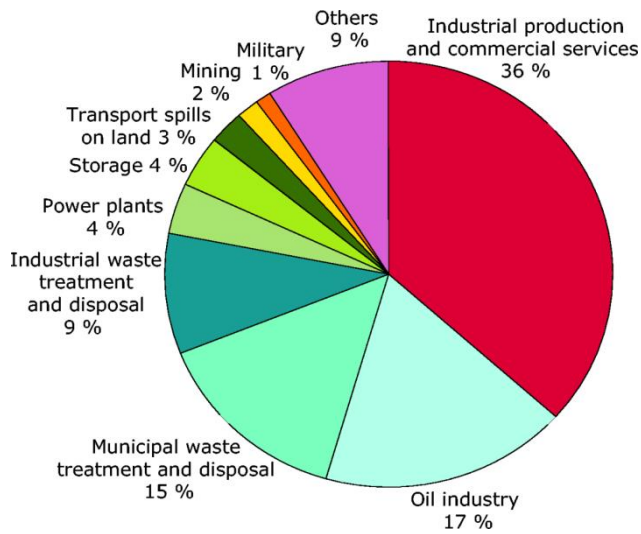
Figure 2.1: An overview of the nature of activities causing soil-pollution casualties (EEA, 2012a).
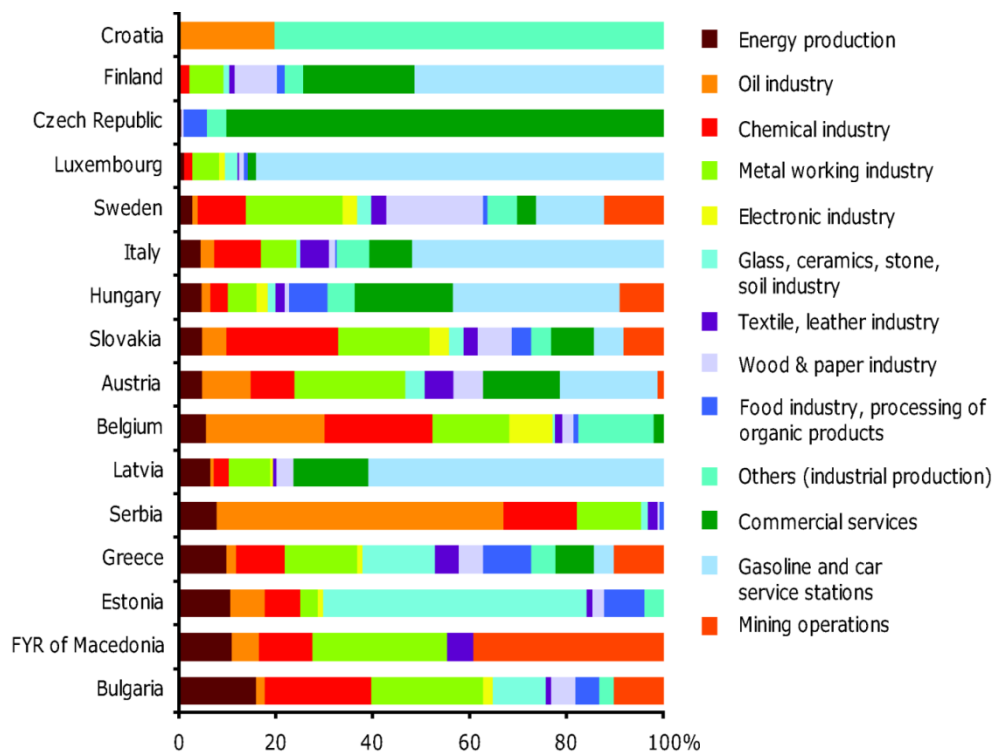
Figure 2.2: Individual contribution of activities in the industrial and commercial sector to soil contamination (EEA, 2012b).

It can be seen from Figure 2.2 that the share of the different industrial and commercial activities is very different per country, but in general it can be seen that the sources of contamination are the oil- and chemical industries, mining- and metal industries and that as a point-source, the share of gasoline and car service stations is remarkably high. Responsible for the large contribution of industrial and commercial activities to pollution are mostly the unintended handling losses, storage tank and pipelines leakages, and accidents (EEA, 2007).

According to figures of the EEA (2007) there are approximately 250.000 sites with soil contamination requiring clean-up in its member countries. It is estimated that "potentially polluting activities" took place at 3 million sites. Following the current trends, it may be expected that by 2025, the number of sites in need for clean-up will have increased to 375.000 and over. In addition, there are 130.000 known cases of groundwater pollution and another 3 million sites are potential sources of groundwater contamination. It is expected that the former value will more than double, reaching 270.000 sites with effective groundwater pollution by 2025. In most cases, the problem is caused by historical pollution, which occurred decades ago but which are identified now due to better monitoring techniques, while only in a minor amount of cases pollution is due to present activities and accidents. The nature of pollution is variable, with heavy metals and mineral oils most often being the instigators of soil pollution whereas in the case of groundwater pollution, mineral oil and chlorinated hydrocarbons are more common as can be seen in Figure 2.3 (EEA, 2007).
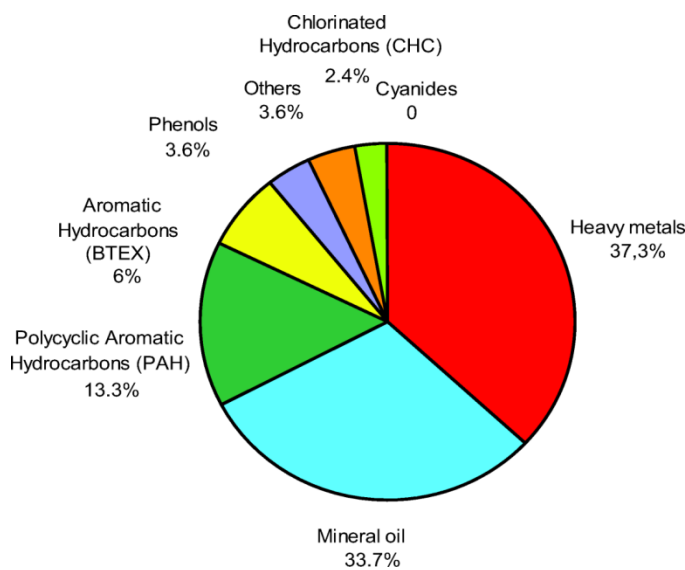
Figure 2.3: Regularity of occurrence (%) of chemical contaminants in soil –and groundwater pollutants (EEA, 2012c)

Knowing that during the last three decades, about 80.000 sites with soil pollution have been effectively cleaned, it can be seen that there is still a long way to go.

Soil composition is very important for the distribution of heavy metals. It appears that often the organic components in sediments are found to be enriched in trace elements such as B, V, Mn, Co, Ni, Cu, Zn, As, Mo, Ag, Cd, Sb, Hg and Pb, for a concentration of more than 3 times the magnitude of the concentration found in the bulk soil matrix (Hirner et al., 1990). Natural spatially-varying conditions lead to heterogeneous soils with discontinuous or variable values for physical properties such as permeability, porosity, texture (determined by content of sand-silt-clay), structure, bulk density, or hydraulic conductivity, and chemical properties such as pH, salinity, elemental composition, and so on. Soils represent a three-dimensional system, formed by the interactions of both the solid and liquid phase. Therefore, the aforementioned physical characteristics of the solid matrix as well as the state of the liquid phases (through for example the pH) determine the behaviour of the contaminant (e.g. metals) and its interaction with the solid and liquid phases. In general, clay soils generally adsorb metals less readily, whereas soils rich in oxides and organic material have a higher affinity for heavy metals. Also the presence of dissolved O.M. may increase the solubility of metals and increase adsorption (Zovco & Romic, 2011). The chemical properties of the system control processes such as dissolution, oxidation/reduction, hydrolysis, acid-base reactions, precipitation, adsorption, biochemical degradation or complex formation of heavy metals (Page & Berger, 2006). Metals may be present in the system in different states: dissolved in the aqueous soil phase, as precipitated metals, bound to clay minerals, in oxides and hydroxides, adsorbed to O.M., or present in the solid matrix. However, governing the mobility of the pollutant, the form in which the metal is present (in terms of ionic charge) is also of crucial importance (Zovco & Romic, 2011). The latter is generally governed by the pH which determines the electric charges of the particles -at low pH the presence of metals as ions is more likely- and the specific surface area of the matrix (m²/g) (Page & Berger, 2006). Because of this also the retainment- and leaching properties of heavy metals and other pollutants in soils may vary spatially (Škrbic & Mladenovic, 2010). It needs to be addressed that the severity of the pollution (in posing a risk to human health) is a function of multiple variables, such as the quantitative total concentration, the elements present and the fraction of bio-available or mobile element phases present (Škrbic & Mladenovic, 2010; Wuana & Okieimen, 2011) It should be remarked that only metals, present in the aqueous soil solution

are available for plant uptake (Zovco &Romic, 2011). The greatest risk for accumulation in living organisms is posed by lipophilic compounds in opposition to hydrophilic compounds (Mirsal, 2008). The accumulation of heavy metals in soils through irrigation with wastewater or excessive accumulation through air deposition increases heavy metal uptake by crops, introducing these substances into the food chain, eventually transferring it to humans (Muchuweti et al., 2006; Wuana & Okieimen, 2011). Especially nutritionally non-essential metals such as lead, mercury and the inorganic cadmium and arsenic may pose a threat to human health. Despite the fact that lethal effects following inhalation, ingestion or skin contact are very rare and only possible under the intake of high doses which are normally not present in consumers products, their bio-accumulative nature leads to accumulation in target organs and long-term intake may lead to clinical effects (Goyer et al., 2004).

The concentration of pollutants in regional soils provides a reference value to which other measured values in areas of higher anthropogenic activity can be put into perspective. However, it is likely that this reference value of the surface soil is already elevated with respect to the original and natural value of pristine soils if it were not that they were contaminated due to long-distance atmospheric transport of airborne material or regional activities.

2.2 Brownfield Areas

2.2.1 BF Characteristics

Generally, with the term Brownfield area (BF), one refers to an area which is affected or potentially affected by contamination. A more official definition comes from the 'Concerted Action on Brownfields and Economic Regeneration' Network or 'CABERNET'. They defined brownfields as "sites that have been affected by the former uses of the site and surrounding land; are derelict and underused; may have real or perceived contamination problems; are mainly located in developed urban areas; and require intervention to bring them back to beneficial use" (Lee Oliver et al., n.d.). However, as can be noticed by reading this definition, it may be differently interpreted and that is the reason why data on brownfields in Europe is hardly comparable, due to the lack of consensus on what exactly should be classified as a brownfield and what not. In any case, brownfield areas come into existence when the estimated economic, social and/or environmental costs of an area are higher than the

revenues or return-flow expected for the area on a longer term basis. This leads to unattractive prospects for investors and stake-holders, and may often lead to a cessation of the use of the area and abandonment. (HOMBRE, 2012a).

The ease with which the area may enrol into a new life-cycle depends on the projected costs and return-flow during the new life-cycle, with another land use and management. When these prospects are positive, the BF may easily proceed towards a new land-use cycle, under more negative prospects this may be more difficult or nearly impossible. At the base of this are many other incentives which may determine whether a project/area may be attractive for investments or not. Brownfield density covers generally about 0.25-0.5% of the total land surface of a nation, with countries as France and Sweden having lower (0.01 and 0.04%) and Poland and Romania markedly higher figures (2.5 and 3.8%) although the latter is partly because of the fact that also in-use areas are contained in the BF definition (Oliver et al., n.d.). However it should be noted that many EU countries do not dispose of a national database keeping track of polluted BF areas. The primary sources or causes of BF's are the same pollution-causing industries or activities listed in Figure 2.2.

The main aim for BF remediation is the mitigation of health- and environmental risks for its future use. The more these risks can be reduced, the larger the possibilities for future use of the area and the better the BF can enrol into its new life-cycle.

2.2.2 BF problems

Besides the above-mentioned pollution of soils, there is also a large quantity of waste generated during BF regeneration by the demolition and clearing of structures present at the site. This waste may consist of concrete, ceramics, steel, bricks, and other materials. It may be possible to reuse part of these materials and therefore proper sorting of the material is needed. On the other hand, part of this waste may be toxic or have undesirable environmental properties (asbestos, chemical solvents), making proper management and post-processing necessary to make these substances harmless. Therefore it is necessary to sort or separate these materials carefully at the BF site, so that toxic materials become separated of benign and recyclable materials in order to make the recycling process more efficient and faster. Materials which can be easily recycled are for example plastics, steel, paper/wood and glass.

A key challenge for the success of sustainable remediation is that the different scientific, technical and socio-economic aspects have to be integrated with each other to a higher level. Brownfield problems are mostly labour-intensive and the project planning and approval takes

time due to the necessity to deal with often complex environmental, economic, legal, social, and land use issues for a given property (Page & Berger, 2006).

It should be remarked that the presence of contamination in the subsurface most often has a delaying effect on the development of an area. This is due to the need to take measures for the pollution to remain contained and controlled, what implies constraints on the redevelopment activities. Therefore it could be preferred to attempt to remove or stabilize all pollution in the subsurface before the start of the construction phase.

2.2.3   BF opportunities

Often, the first incentive for redevelopment is due to economic incentives, i.e. generating revenues and profits out of the area, by means of selling the site and letting it enrol its new life-cycle. The outcome of the economic analysis seems to be determined by 2 driving factors: competiveness; based on economic performance, government efficiency, business efficiency and infrastructure (IMD, 2004) and population density, since the latter determines the availability of greenfields and the land-use intensity. According to this, the chance for redevelopment of a BF is largest in western European countries which are characterized by a high population density and a high competitiveness leading to high ground prices and making it economically more interesting to redevelop BF's (Oliver et al., n.d.).

Concretely stated, the reason these sites (and their redevelopment) are often interesting is for example (World Bank, 2010; EEA, 2007; Wedding & Brown, 2007):
- They are often situated in cities or strategic locations, where there is large demand for residential/commercial space;
- They can generate new private and public revenues through economically stimulating and tax-generating activities;
- The environmental and social advantages of their regeneration;
- The remediation efforts of existent pollution help to achieve better environmental standards;
- This may transform dull and disadvantaged neighbourhoods to reviving communities with better prospects and prevent further decline of the area;
- Redevelopment is crucial in the combat against the never-ending urbanization and intensive land-use;

- It reduces the demand for new greenfield development thus conserving non-urbanized area;
- May help to safe-guard public health.

Several European countries have made commitments to reduce their greenfield consumption for the construction of new residential, commercial and industrial area and to turn towards brownfield redevelopment. For example Germany targets to bring down its daily greenfield consumption from 93 to 30 ha by 2020. In the UK, from 1990-2005, the share of new buildings constructed on previously-developed sites increased from 54 to 73% (EEA, 2007). This is beneficially from both an economical and environmental point of view, since untouched sites are becoming scarcer, more valuable, and more expensive. Another beneficial economic aspect which should be taken into account is that Brownfield rehabilitation creates jobs and stimulates (new) businesses (ENEA, 2006).

Next to these incentives, there is also the possibility to reuse wastes from the BF sites and to re-incorporate the material into new products. This may lead to a strong diminution of the waste volume generated and the raw resources consumed in construction. This could be reached through a better planning and a more efficient cooperation with other sectors, to reuse the material in the construction plans at the site or off-site to take opportunity of the generated waste. To really have a significant impact or be implemented on a large scale, the development of new, low-cost and efficient techniques is needed to establish a solid market for low-value 'waste' products. Changes in legislation could play an important role here as well, for example by increasing charges on the disposal of waste (Lackner et al., 1997). In practice, material that is excavated or demolished and would normally be landfilled, can be transformed into aggregates in some situations, making reuse possible and at the same time potentially eliminating its hazardous properties. These materials can originate from on-site or off-site locations, but could eventually be used for the redevelopment of the site: for example for landscaping purposes (elevation of planned buildings, paths, or barriers) or for the construction of roads. Besides reusing the waste materials, it is also possible to incorporate / store the CO_2, produced in waste-incineration plants, or generated though fossil fuel combustion (such as through energy production), in the aggregates by means of ex-situ granulation or in-situ carbonation and stabilization procedures (Grotenhuis et al., 2012).

2.3   Remediation techniques

The number of soil- and groundwater treatment techniques is very diverse; application of a certain technique often depends upon site-specific conditions. Factors which determine the best-suitable method are for example the physical, chemical and biological conditions of the site, the severity of the pollution (type of contaminant and its concentration), and the time-horizon over which remediation may or must take place (Andrade et al., 2010). An overview of general remediation techniques is presented in Table 2.1.

Table 2.1: Advantages and disadvantages of several remediation techniques. (Own elaboration from Bastão de Souza et al., 2013 and Mulligan et al., 2001; Environment Canada, 2002).

	TECHNOLOGY	ADVANTAGES	DISADVANTAGES
In –Situ	Containment and/or Solidification/Stabilization:	-Cost-effective -Large soil Volume can be treated -Very recommended for metals	-Only immobilization, no treatment (short-lived) -Volume increases upon treatment -Interference contaminant/binding agents -Process hindered by the depth of the contaminant
	Advanced Oxidation Processes (AOP)	-Cost-effective -Mineralization capacity -Recommended for highly permeable soils -Different reagents may be used	-Mass transfer of adsorbed to aqueous phase -Risk of contamination by non-recovered solvent -Limitations for large-scale application -Use of strong acids destructs soil structure
	Thermal desorption or extraction with supercritical CO_2	-Highly efficient for volatile compounds -Soil aeration can facilitate bioremediation -Fast -Low environmental	-Low efficiency for soils with low permeability -Not suited for saturated areas -Treatment of released vapour is required

		impact
Bioventing	-Less permeable areas oxygenated -Minimal disturbance -Low cost	-Not for shallow soils -Monitoring of volatile gases needed -Slow
Vapour extraction	-Vapour migration controlled: reduced inhalation risk	-Not for impermeable and/or highly humid soils -Treatment of resulting liquid -Costly
Adsorption with clay	-Cost-effective -Minimal disturbance of site -Can be combined with other techniques	-Long-term monitoring required -Limited by buffer capacity soil -Selectivity for specific ions
Biodegradation	-Low cost -Minimal disturbance -Highly accepted-May be combined with other techniques	-May increase contaminant mobility -Less suited for highly heterogeneous soils -and pollution distribution -Slow
Phyto-extraction (plant root uptake)	-Low cost -Large area may be treated	-Limited depth of treatment -Not for high contaminant concentrations -Disposed plants must be properly processed
Electrokinetic	-High efficiency -Can be combined with other techniques	-Treatment time depends on the distance between the electrodes -pH changes near the electrode -Costly

			-Lower efficiency in soils with low permeability
Ex-Situ	Incineration	-Highly efficient -Fast -May be used where other processes are not effective	-Expensive -Releases secondary compounds to the atmosphere -Monitoring required
	Soil Washing	-Fast -High acceptance	-Less suited for soils rich in clay and high in OM -Wastewater treatment needed -Expensive
	Chemical Extraction	-Applicable to wide spectrum of contaminants	-Residual solvent may require additional treatment -Expensive
	Bioremediation	-High level of control over processes -Simple to implement -High acceptance	-Disruption of soil integrity -High costs -Atmospheric emissions -Slow
	Thermal Desorption	-Treats wider array of contaminants than vapour treatment	-Volatile atmospheric emission -Less suited for high-moisture soils -Expensive
	Vitrification	-Resistant to leaching -Permanent	-Disposal of solid product -High cost -High power needs

The 'containment' techniques isolate the contaminated matrix physically, by encapsulation, or vitrification. With the use of different techniques (physical obstruction with walls or covers, solidifying chemicals or electrical energy) the contamination is immobilized and contained. Ex-situ techniques imply the removal of the polluted matrix and subsequent treatment by for example incineration, soil washing or physical separation and are generally more expensive but much faster. When only groundwater treatment is desirable, pump and treat may be

applied. In-situ treatment allows for the matrix to stay relatively undisturbed in place and remediation is possible by means of several processes such as: the use of reactive barriers, bioremediation, electrokinetic treatment, soil flushing, and so on, depending on the exact concentration and location of the pollution (Grotenhuis et al, 2012; Mulligan et al., 2001). An example of Advanced Oxidation Processes is RedOx which process is based on the ameliorating of the chemical and biological conditions through injection of specific reagents into the matrix to speed up the rate chemical or biological degradation. Bioremediation on the other hand takes place through decomposition of the harmful substances into benign ones by the aid of micro-organisms or through phytoremediation, where plants sequester the contaminants. The use of reactive barriers may occur through the placement of a permeable barrier, containing reactive substances, in the flow path of a contamination plume to neutralize the contamination through several chemical neutralization reaction (Yeung & Gu, 2011). As can be seen, a large number of techniques are available, many of which however are too expensive to apply on large volumes of material.

In practice, it is also possible to combine multiple of these treatment techniques in technology trains, such as for example making use of naturally-occurring degradation and retardation processes in the subsurface (natural attenuation, NA), together with in-situ remediation. In this way, it seems possible to deal with more complex pollution problems, for example in situations where multiple contaminants with different properties are present. The concept of these technology trains will be described in more detail in the para. 2.4.2.

In order to conclude the array of treatment techniques, in Figure 2.4 the frequency of application of the most common soil treatment techniques can be seen, for some European countries of whom data was available. From this it may be seen that generally the traditional dig & dump or containment techniques are still widely applied and that the more 'innovative' remediation techniques are applied in-situ as well as ex-situ at a comparable amount of sites (taking into account the heterogeneous trends for individual countries).
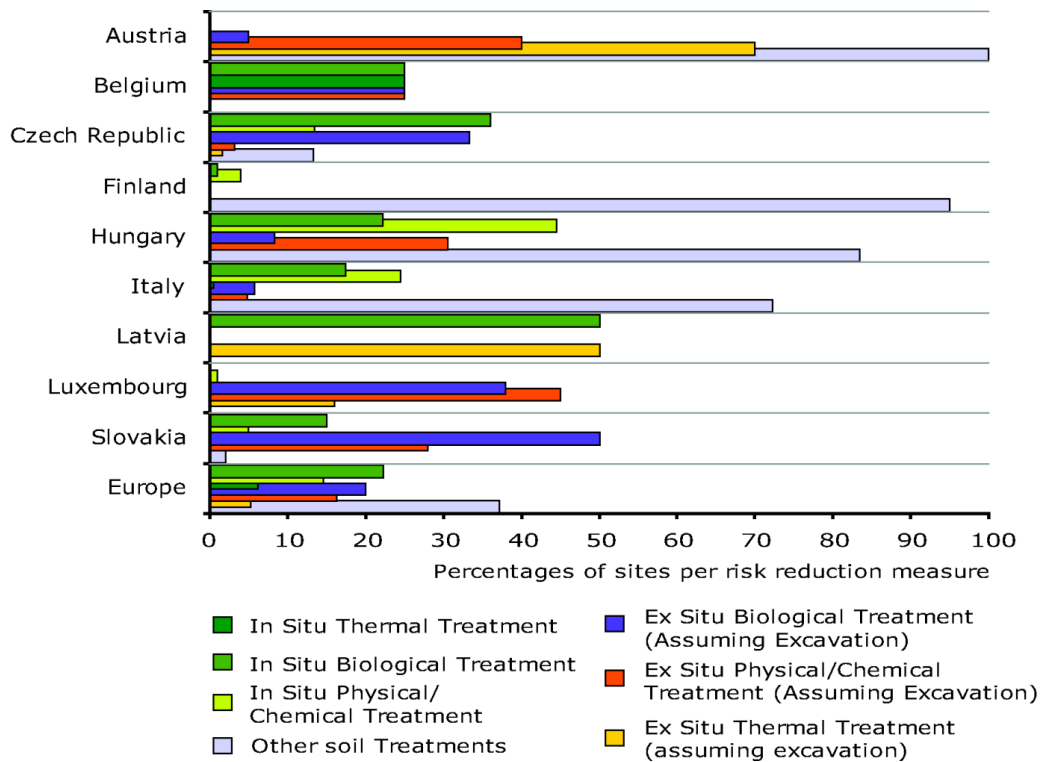
Figure 2.4: The application of several soil treatment technologies in surveyed countries expressed as percentages of sites per type of treatment (EEA, 2009). Note: 'Other soil treatment' refers to the 'traditional' soil remediation techniques such as: dig-and-dump and containment/sealing

2.4   The international Hombre project

2.4.1   Hombre description and objectives

Hombre is an European research project, with at its base the concept of circular land use. The idea is that through proper management, after the cessation of making use of an area for a certain purpose, the area can be used for a new life-cycle by taking into account the social, economic and environmental aspects. The project aims at sustainable recovery of brownfield regions by identifying the services needed for the redevelopment of the BF and its surroundings and attempts to combine them in a single approach while taking maximal opportunity of the available resources. This may also reduce the costs and time needed to complete the project. Currently, in most EU countries, the redevelopment of BF occurs in a non-sustainable way. After demolishing buildings and other structures, or after excavation of the contaminated soil, the waste material is transported off-site and generally it becomes landfilled (except for some countries where reuse occurs). There are multiple reasons possible for the lack of material recycling: due to legislative issues (the material cannot be used due to contamination to some extent), stringent time objectives (deadline in delivering the project),

the financially higher costs of recycling, or just due to a lack of communication, it is not known what the objectives of the overall project are, and recycling options for on-site reuse are not considered (Grotenhuis et al., 2013; HOMBRE, 2010; HOMBRE, n.d.).

The project is focusing on 4 fields being; water (treatment) technologies, material (recycling) technologies, soil (cleaning) technologies and (renewable) energy. HOMBRE sets as a goal to use Holistic technology trains (HTT) instead of the use of simple TT's or even integrated TT's. In a simple TT, individual technologies developed to treat one specific problem by a single approach, are combined into an overcoupling approach. With an integrated TT however, one TT can be applied to several problems of a kind or in different situations. Under a Holistic technology train, there are multiple TTs that can be applied to different situations and can also provide multiple services (Grotenhuis et al., 2013). Traditionally, a site is redeveloped according to a bottom-up approach, first considering the site-specific needs and the associated best individual technologies to fulfil the objectives. In HOMBRE, this bottom-up approach is coupled with a top-down approach, to first identify the services (needs, opportunities, outputs) and then select the technologies which are best suited to treat multiple problems at once, or are more widely applicable.

The aim of the project for redevelopment of degraded sites is not limited to the reclamation of ground for redevelopment. Besides this, another important incentive for clean-up is protection of groundwater resources, to limit the contamination of drinking water and thus human exposure (EEA, 2007). It is of large importance that the BF area after remediation satisfies all environmental constraints so that the future developments are not limited as a consequence of contamination. This is especially of crucial importance when the planned use is residential or agricultural.

2.4.2 Technology trains

The concept of technology trains (TTs) implies the combination of several 'stand-alone' services and techniques, into one (or several) integrated approach that would yield better results- economically, qualitatively, and temporally- than when applied separately like in the standard approach. In other words, a TT is the sum of all procedures and treatment techniques applied to the contaminated material or waste, used to deliver the required service or product. With application of these TTs, the investments needed during the regeneration phase

(redevelopment) but also the cost-benefit ratio for the new use phase on long term are lowered. Therefore they help a BF to enroll easier into a new life-cycle, whereas initially having negative future prospects for investment and redevelopment.

The use of technology trains is necessary to create innovative synergies between different technologies and disciplines and attempts to take into account environmental, construction and accommodation issues, together with spatial planning and land use to optimally plan the redevelopment of an area, thereby creating new opportunities. The technologies and techniques needed to perform the regeneration and remediation of the site are mainly defined by the selected end uses of the BF. This is why the projected end use(s) of the BF should be known as early as possible so that it can be maximally integrated in a holistic approach that can be applied during the regeneration procedure. When developing these TTs, the state of the current degraded brownfield area and its resources should be assessed and their applicability to the required services.

HOMBRE makes use of three specific technology combinations to test the principle of the technology trains. It should be taken into account that each BF is unique and may need another -specific- TT, developed to match the site-specific conditions. The three technology trains that are tested in the project are the following:

1. Energy-water: This TT combines the reuse of energy and contaminated soil- and water cleaning efforts. Emphasis is on in-situ remediation to remove contaminants present in the porous medium, while striving for a maximum reuse of water and a limited energy consumption. The exploitation and use of renewable energy resources is essential here. Thereby use is made of techniques such as Aquifer Thermal Energy Storage and several aquifer remediation approaches.

2. Building materials-soil: In this TT, the management of the contaminated matrix and resource efficiency together with material recycling and reuse are standing central. Research on this topic is done by experiments on carbonation and on granulation and Stabilization/Solidification to reach maximal reuse of the contaminated soil, possibly through the production of high-quality aggregates.

3. Soil-water: This TT assesses urban drainage, soil strengthening and remediation through in-situ carbonation of soil to improve mechanical soil properties and treat contaminated groundwater through volatile contaminant stripping. This may occur along with the

application of optimal soil and water conditions through proper management. (HOMBRE, n.d.; HOMBRE, 2012b)

These technology trains come with clear environmental and socio-economic benefits: The coupling leads to lower costs by sharing management expenses over different sectors. These TTs are composed in such a manner that joint clean-up of soil and groundwater can be achieved, which is much more effective than their separate remediation. In addition, this aids to reach environmental goals by reducing energy and external resources (raw materials, water) demands, as well as CO_2-emissions and waste generation compared to the traditional approach (Grotenhuis et al., 2012; HOMBRE, 2012a). Through this optimal use of the available resources initially present in the BF, these are transformed into services and benefits during redevelopment which lowers the costs for redevelopment (Grotenhuis et al., 2012).

2.4.3 Hombre techniques and approach

Crucial for the evaluation of finished projects according to the HOMBRE guidelines will be - next to the standard requirements of respecting the budget and time planning - whether the environmental footprint of the project was minimal in terms of energy use and GHG emissions, but also whether the use of natural resources such as water and raw materials was minimal.

2.4.3.1 Redevelopment techniques

When excavation of contaminated material takes place, this may partly be reused in multiple applications. A possible reuse option of the materials is as a filler for the construction of embankments or to elevate or stabilize roadbeds. It may also be used for aggregates production to serve construction purposes, or as a concrete component thanks to the fact that these materials (ashes and slags) may have pozzolanic properties enabling them to harden independently by hydraulic reaction to form cement-like material. (Grotenhuis et al., 2012).

In comparison to other waste materials, in special BOF and EAF slag seems to have the right physical, mechanical and environmental properties, making them appropriate for aggregate production. (Shen et al., 2009; Xue et al., 2006; Manso et al, 2006; Pasetto & Baldo, 2010). MSWI bottom ash could also serve as a cement constituent, but requires some pretreatment

(Forteza et al., 2004; Cheesemann & Virdi, 2005; Sorlini et al., 2011). Mechanical pretreatment may also be required to separate the most polluted fractions from the bulk material by differences in physical properties between the particles (e.g. magnetic properties, density). Some mechanical pretreatment methods:

- Sieving to obtain the required fraction for aggregate formation or to separate the fine fraction which most likely is more heavily contaminated;
- Crushing to obtain a more homogeneous mix if desired;
- Washing, to disintegrates aggregates and makes separation more efficient.

Chemical pretreatment methods may also be performed on the material to decrease the contaminant content. Examples of this are (Grotenhuis et al., 2012):

- Biopiles: Placing the excavated soil under controllable environmental conditions to promote biodegradation of petroleum constituents;
- Composting: Mixing the polluted soil with organic materials, micro-organisms will cause a natural bio-degradation process. The associated rise in temperature of the medium will promote the degradation of organic pollutants, such as PAH's;
- Chemical RedOx: With articifical addition of oxidants such as ozone or hydrogen peroxide, the polluted material is being oxidized,

Along with other remediation techniques listed in Table 2.1.

2.4.3.2 Stabilization techniques

Solidification/Stabilization (S/S) is an environmental engineering practice in which chemical binders are added to the contaminated material in order to form a stabilized, more solid matrix in which the contaminants are contained for long-term period (Angel et al., 2004; Antemir et al., 2010a). It thus aims at demobilizing the contaminant instead of removing it. Stabilisation is different from solidification in the fact that stabilisation refers to a chemical reaction rendering the contaminant less mobile through a lower solubility, while solidification implies the entrapment of the contaminant in a stable lattice, reducing the surface area on which dissolution may occur (EPA, 2000). Often the both processes occur simultaneously: the contaminants are isolated in a thermodynamically stable solid with a pH (decreased from the original value) that significantly reduces the contaminants (often heavy metals) solubility, leading to a reduced leaching of the targeted constituents (Conner, 1990). The most prevalent technique to perform solidification & Stabilization is through cementation of the matrix through the addition of so-called aforementioned 'pozzolan' substances. The latter are often

aluminous and/or siliceous materials which (when present in a very fine grain size) react with water and lime ($\rightarrow$CaOH) to form compounds with cementitious properties (Mehta, 1987).

The technique has been used on different types of wastes, but it was found that it is less applicable for situations where organic compounds are present. The latter seem to have an adverse effect on the cementitious properties of the material and may cause leaching even after the remediation process (Sora et al., 2002; Karamalidis & Voudrias., 2007; Antemir et al., 2010b).

An important S/S technique to immobilize the toxic components in a matrix, is accelerated carbonation in which the material is treated according to the regular S/S approach described above, but under a CO_2 atmosphere. Compared to the regular approach, 'ACT' may overcome cement hydration inhibitory effects that may be encountered in the presence of specific contaminant such as zinc or lead (CLA:RE, 2006). Since this technique is the scope of this research, it will be treated extensively in the next chapters.

Another technique to immobilize contaminants is through vitrification. This process takes place under high temperatures, turning the material into a glassy substance, in which the inorganic contaminants will be retained while organic ones are destroyed. Since these glassy materials are unreactive, they can be safely disposed or reused for other applications.

Finally, the formation of stable aggregates predominantly occurs through the process of granulation. With this technique, the material is being treated with a liquid binder substance while under agitation in a tumbler or mixing device. In this way aggregates of waste material are formed, which may be reused. However, when particle size exceeds $\o$ =125 μm, pretreatment through grinding, milling or crushing might be needed (Medici et al., 2000; Cioffi et al., 2011).

2.4.4 In-Situ carbonation and ECO-GROUT

This technique aims for the stabilization of contaminated soils who contain reactive elements prone to carbonization (e.g. calcium hydroxide, calcium silicates, portlandite). Doing so, the potential environmentally harmful substances are bound in the carbonates and the matrix becomes stabilized on a long-term basis. There are multiple techniques for remediation of contaminated soils. The advantages of in-situ remediation are that the contaminated matrix is

left in place in the subsurface during treatment, preventing the destruction of the soil structure, avoiding excessive costs and energy consumption through excavation, transport and often off-site remediation (as it is the case for ex-situ carbonation).

In the framework of HOMBRE, the discussed in-situ carbonation treatment could be realized in a more efficient and effective way through a coupling with other techniques. Currently, a sustainable alternative for grouting coupled with remediation is being developed called ECO-GROUT. This technique is based on the formation of carbonates (calcite) through the reaction of Ca^{2+} and HCO_3^- in saturated conditions, which process is being accelerated through the addition of chemical mixtures ($CaCl_2$ and $NaHCO_3$) (Deltares internal communication). These substances may be introduced into the subsurface through injection wells at the location of a contamination hotspot. When this contamination contains soluble or mobile compounds, a contamination plume may be formed which slowly moves along with the groundwater flow. One way of limiting the further expansion of this plume, is by demobilisation or stabilisation of the contaminant source. In ECO-GROUT, this could be done by the injection of HCO_3^- and Ca^{2+}, which react to form solid calcium carbonate and release CO_2 according to this simplified chemical reaction:

$$Ca^{2+} + 2\ HCO_3^- = CaCO_3 + CO_2 + H_2O \hspace{3cm} (2.1)$$

The formed carbonates may contain the contamination in a solid and stable matrix, limiting the further dispersal and spread of the contaminant plume. Experimental data (Deltares internal communication) has shown that significant amounts of CO_2 are released during this process which could be used for in-situ carbonation of alkaline wastes in the unsaturated zone above. The coupling of both techniques would lead to the possibility of in-situ carbonation of overlying contaminated soils with for example steel slags, even in the absence of nearby CO_2 point-sources (Figure 2.5). Thus, this could provide an integrated solution for the remediation of contamination present in the unsaturated as well as saturated soils.
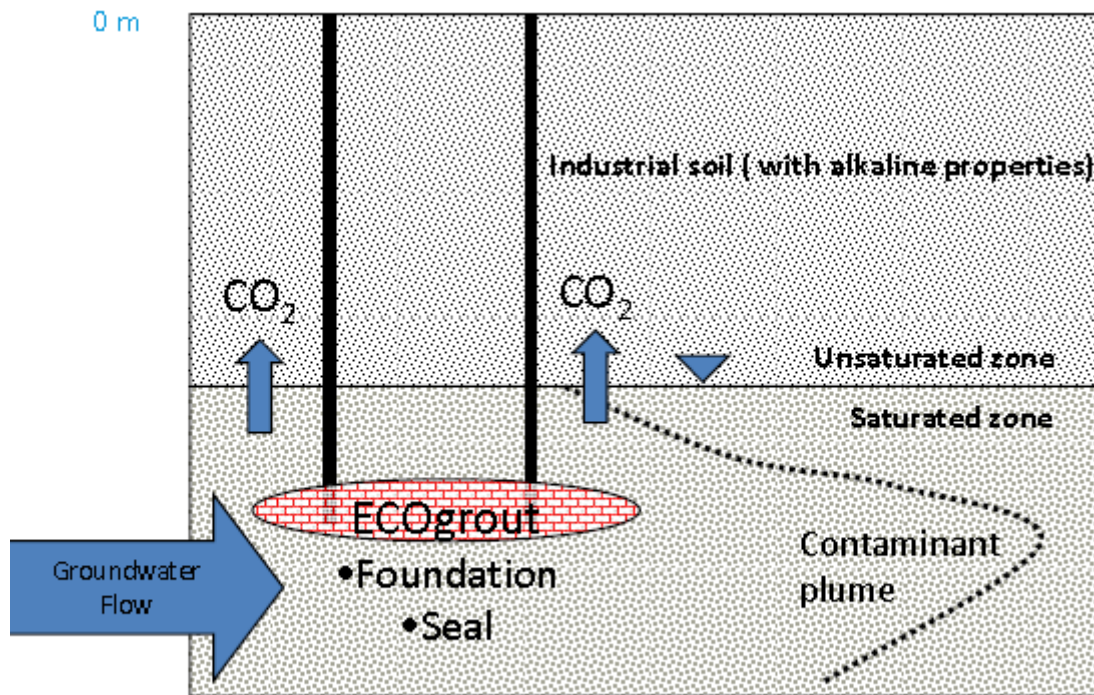
Figure 2.5: Integrated Holistic Technology Train: ECO-GROUT and ACT project principle.

2.5 Positive Side-effects: The greenhouse effect and CO_2 storage

2.5.1 Global warming

Currently, about 80–85% of the world's energy demand is being satisfied through the combustion of non-renewable fossil resources (Sanna et al., 2012). Their combustion results in the emission of greenhouse gases such as CO_2, CH_4, NO_2, CFC's. It is generally known that these anthropogenic GHG's cause a rise in the mean annual global surface temperature through their mechanism of trapping long-wave infrared radiation in the atmosphere, and re-radiating it back to the Earth's surface. Research by NASA's Goddard Institute for Space Studies (GISS) has shown that the since 1880, the average surface air temperature on Earth has increased by about 0.8 °C, very likely this majority of this rise is explained through the accumulation of these gases in the atmosphere. The majority (2/3) of this increase occurred after 1975, with a rate of approximately 0.15-0.20 °C/decade (NASA, n.d.). This warming trend is reflected in Figure 2.6 and Figure 2.7.

35

The last 10 years are listed in Table 2.2 and are all within the top 13 of the years with the largest positive temperature anomaly (NOAA, 2012). It is generally thought that this trend is due to the growing rate in the annually emitted volume of greenhouse gases.
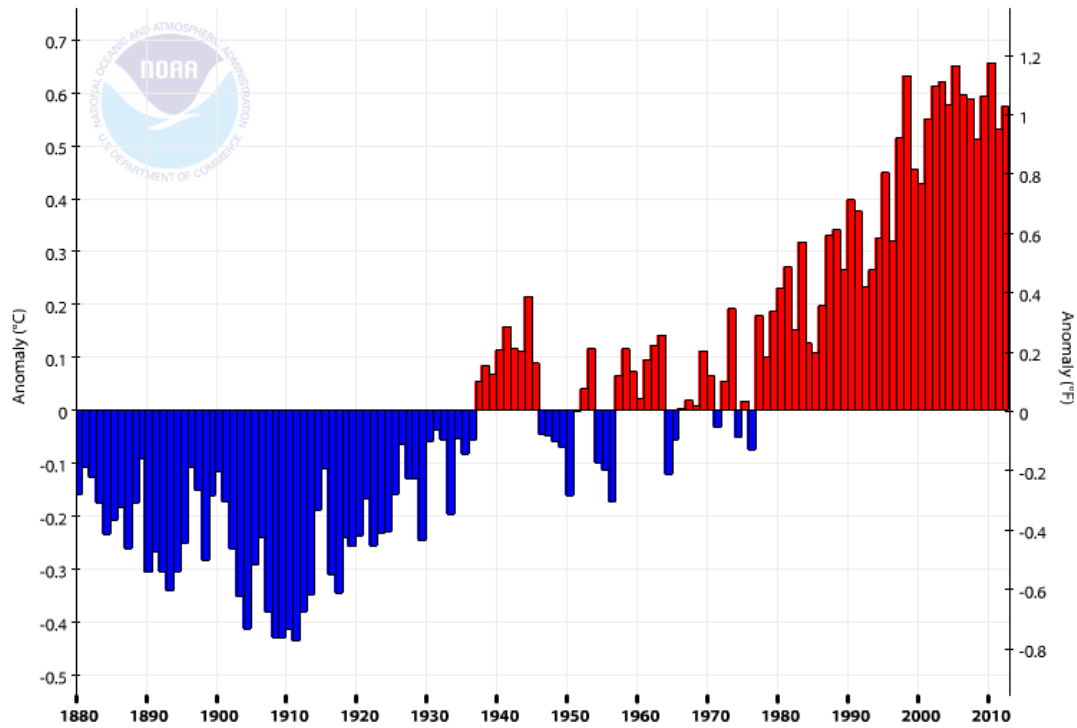
Figure 2.6: Annual Global Land and Ocean Temperature anomalies with respect to the reference period 1951-1980 (NOAA, 2012)
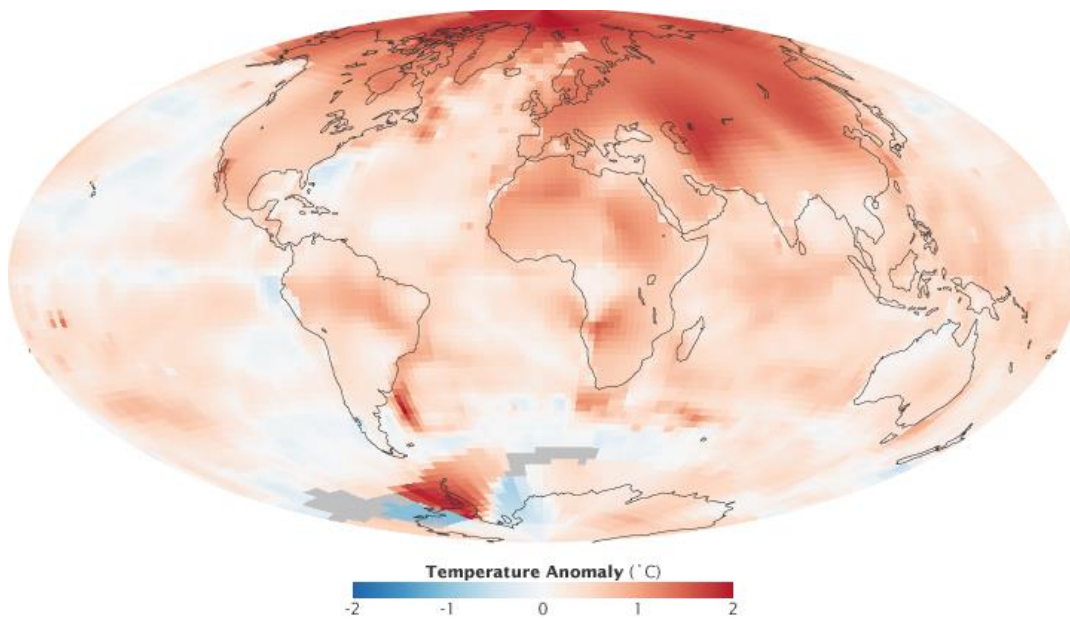
Figure 2.7: Temperature anomalies for the period 2000-2009 with respect to the reference period 1951-1980 (NASA, n.d.)

Table 2.2: List with the 10 hottest years in terms of annual global mean temperature (NOAA, 2012)

Rank	Year	Anomaly (°C)
1	2010	+0.66
2	2005	+0.65
3	1998	+0.63
4	2003	+0.62
5	2002	+0.61
6	2006	+0.60
7	2007	+0.59
8	2009	+0.59
9	2004	+0.58
10	2012	+0.58

A breakdown showing the fractional contribution of each sector to the total global emission of the CO_2-greenhouse gas is shown in Figure 2.8: The contribution of several sectors to the emission of CO2 (2010 data) (IEA, 2012). *Other= commercial/public services, agriculture/forestry, fishing, energy industries other than electricity and heat generation, and other emissions not specified elsewhere.. From this it may be noted that the main emitters are the electricity and heat sector (mainly urban supply), transport, and industry.
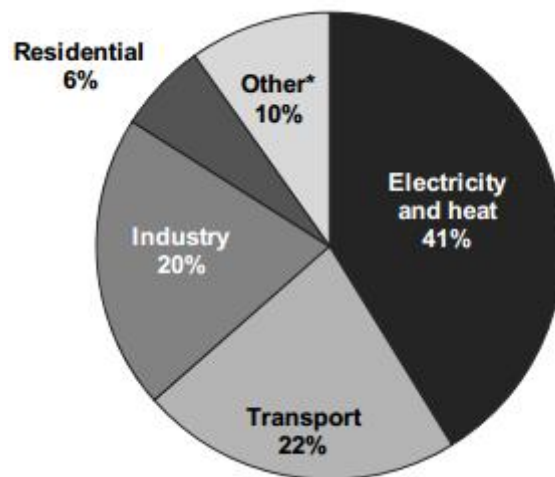
Figure 2.8: The contribution of several sectors to the emission of CO_2 (2010 data) (IEA, 2012). *Other= commercial/public services, agriculture/forestry, fishing, energy industries other than electricity and heat generation, and other emissions not specified elsewhere.

The outcomes of different AOGCM's with different non-mitigating scenarios B1, A1B, A2 (only include anthropogenic forcing) are consistent and all project further increases in the global mean surface temperature during the rest of the 21st century. The main cause of this are the increases in anthropogenic GHG concentrations, as a result of the current and forecasted anthropogenic activities. The different models forecast a temperature increase of +0.64°C to +0.69°C for the period of 2011-2030 compared to 1980-1999. For the period 2046-2065 this increase amounts to values of +1.3°C to +1.8°C and for the end of the century (2090-2099) increases of +1.8°C to +4.0°C are expected, for the aforementioned scenarios plus the scenarios B2, A1T, A1FI, A1B which are different scenarios to incorporate the impact of variations in economic development, the use of renewable or non-renewable energy sources and population growth in the model forecasts. It worth noting that only about one third of the warming for 2046-2065 and one fifth of the warming expected for 2090-2099 is inevitable since it has already been committed through our past GHG emissions or other activities (Meehl et al., 2007). In addition to this, it was shown that the temperature increase is greatest over land (about double the global average increase) and over high latitudes in the Northern Hemisphere.

In line with these projections, world's climate is facing profound changes in the future, next to the already occurring and past changes (Salukdar et al., 2012). A vast array of changes to the global environmental and climatological system may be expected such as (Own elaboration from Meehl et al., 2007):

- Increases in temperature extremes [Very likely] leading to more intense, frequent and longer heat waves;
- Increases in mean precipitation over tropic regions, decreases in subtropics;
- Increases in the precipitation extremes, droughts and the intensity of precipitation events;
- Decreases in the global average snow and sea ice extent, permafrost thawing;
- Reduced carbon sinks leading to a positive feedback (adding 20-220 ppm at the end of the century);
- Ocean acidification with drops in pH up to -0.35 units, resulting in regions becoming under-saturated in $CaCO_3$ with negative impacts on calcified sea life;
- Sea level rise with an expected +0.18 to +0.59m by the end of the century;

- Increased climate variability on a regional scale for example affecting monsoon intensity;

- Increases in the intensity of tropical cyclones [likely] leading to damage to properties, social disruption and loss of human life, as well as environmental degradation (Salukdar et al., 2012).

These consequences may separately and also combined generate significant adverse socio-economic and environmental impacts. At all cost, it should be attempted to cut back the emission of anthropogenic GHG's as much as possible over an as-small-as-possible timespan in order to reduce the impacts. As described above, only one third and one fifth of the warming projected for the middle and the end of the century is irreversible through our past activities. Since the global energy production currently relies extensively on the use of fossil fuels, a radical change in the field of technology, policy-making and conscience will be needed to evade the worst-case scenario foreseen by the models.

2.5.2 Carbon capture and Storage

In order to keep the effects of climate change under control, it would be preferable to introduce a 'stabilization level', which is a ceiling-value below which the absolute CO_2 concentration should stay to prevent dangerous interference with the climate system (UNFCCC, 1992). This stabilization value could correspond to a CO_2-concentration, below which the detrimental effects on the functioning of the Earth system should be relatively limited and beyond which a critical point or tipping point of the systems resilience could be surpassed. Keeping the natural functioning of the system in balance is indispensable with the eye on food security, protection of ecosystems and sustainable economic development (IPCC, 2007). The worldwide introduction of and compliance with such a stabilization level, would imply that the emission of CO_2 and possibly other GHG's needs to be cut back, so that over time –past the moment of attaining the stabilization level- a gradual decrease takes place in the absolute atmospheric GHG concentration.

Especially in the most 'safe' scenario with lower stabilization levels (which thus would need to be implemented sooner), emphasis is on low-carbon energy sources such as renewables and nuclear power and the use of CO_2 capture and storage (CCS) (IPCC, 2007). In this sense, CCS may be seen as a transitional technique between the current situation and a situation with low GHG emissions in the future. It may enable us to temporarily limit the GHG emissions and their impacts while optimizing techniques to evolve to GHG-extensive economy and

society. However, the storage capacity is limited and thus not suitable as a long-term approach.
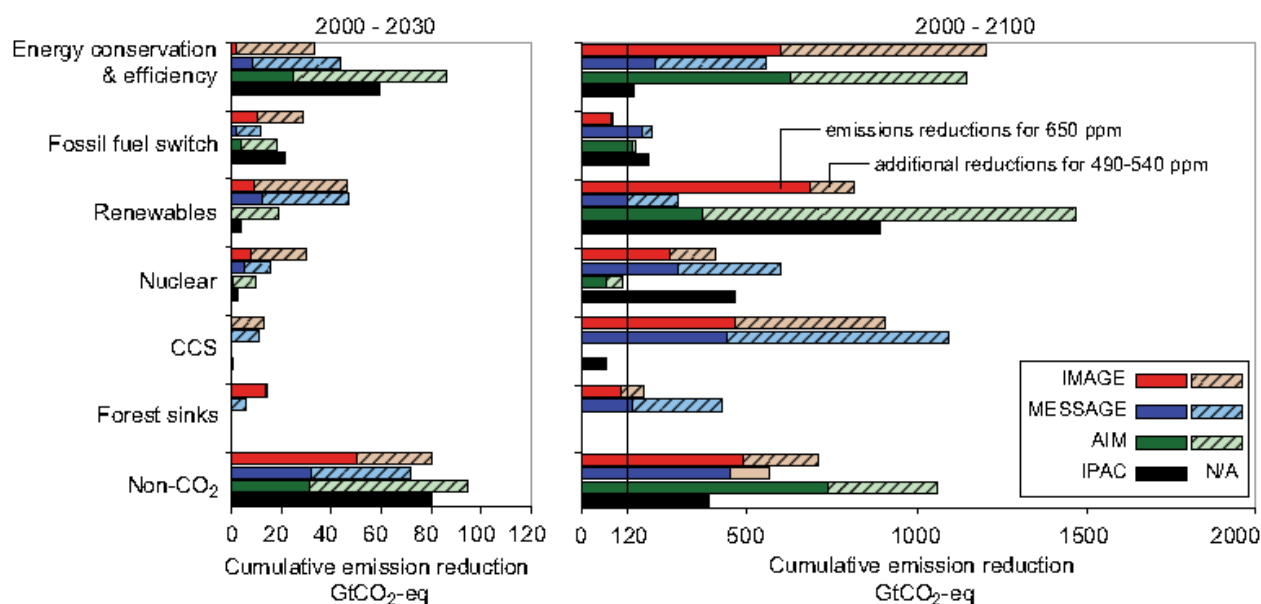
Figure 2.9: Cumulative emissions reductions by the use of alternative mitigation measures for different scenarios for the period of 2000-2030 (left) and 2000-2100 (right). Note: The cumulative reductions in GtCO$_2$-eq. per measure are shown for stabilization at 490-540 ppm CO$_2$-eq (solid and semi-solid bar) as well for stabilization at 650 ppm CO$_2$-eq (solid bar) (IPCC, 2007).

It can be seen from Figure 2.9 that CCS may play a significant role as a mitigation approach to reach and respect a stabilization level. Especially through policy-regulation and/or increasing carbon taxes (the cost for emitting a ton of CO$_2$), the use of CCS could become more widely implemented. The fact that fossil fuels still account for 80-85% of the total global energy production makes that vast amounts of anthropogenic CO$_2$ are being emitted by the energy-, industrial-, and transport sectors (Sanna et al., 2012). This illustrates the large potential for the application of 'Carbon Capture and Storage' (CCS) in heavy industry and power generation sectors.

The first step of the process is to capture the CO$_2$, which may occur pre- or post-combustion through the use of several techniques –depending on the process conditions- such as physical or chemical solvents, membranes, solid sorbents, or by cryogenic separation (different gases liquefy at different temperature-pressure domains) (IPCC, 2005). Following the capture of the carbon dioxide, there are several possibilities for storage such as in underground geological formations, in the deep ocean, in biomass, or by industrial fixation as inorganic

carbonates. Storage in subsurface geological formations (e.g. empty oil fields, salt brine caverns, fractured rocks may form a semi-permanent solution to keep the gases away from the atmosphere. This technique is already being applied in a number of commercial projects. The feasibility of storage in the deep ocean is currently still being investigated, but most likely would only be effective on a middle to long-term basis due to the tendency of re-equilibration between the ocean and the atmosphere (IPCC, 2007; Sanna et al., 2012). Regarding the option of storage through industrial fixation, this process seems to be very energy-intensive and thus costly. In any case, many of these solutions are under heavy debate concerning their safety, economic feasibility, environmental impacts (such as ocean acidification due to deep ocean storage), and are far from being accepted by society. To guarantee the safety of such projects and thus get social approval, full long-scale integrated demonstration projects and numerical simulations are required (Sanna et al., 2012, Jiang, 2011). The storage of large quantities of CO_2 in gaseous form always carries along the danger of an accidentally and sudden release of large volumes of the gas which may have fatal consequences due to its suffocative effect on humans and animals. The latter is also due to the fact that CO_2 is more dense than ambient air, and would create a suffocating layer near the surface (Lackner et al., 1997). Regarding safety-, environmental-, and economic concerns, a compromising outcome would be CO_2-storage in oxide-containing minerals or in alkaline waste materials such as industrial slags. This technique appears to be fairly safe, economically very profitable, and provides a long-term solution for CO_2 storage, although further research on the subject is needed.

3 ACCELERATED SLAG CARBONATION- LITERATURE STUDY

In theory, carbonation is the formation of a certain species of carbonates (XCO_3) following the dissolution of carbon dioxide in an aqueous solution, forming bicarbonate and subsequent reaction of it with primary alkaline earth minerals (X) from an alkaline mineral (XO), according to the simplified reaction:

$$H_2O + CO_2 \rightarrow H_2CO_3 \rightarrow H^+ + HCO_3^- \qquad (3.1)$$

$$HCO_3^- + XO + H^+ \rightarrow XCO_3 + H_2O \qquad (3.2)$$

Thus the overall reaction is:

$$CO_2 + XO \rightarrow XCO_3 \qquad (3.3)$$

Examples of alkaline earth minerals suited for CCS and carbonation are Mg –and Ca silicates (e.g. olivine, serpentine, talc) or alkaline (earth metal) oxides and hydroxides (Costa et al., 2007). Especially ultramafic rocks are a good source of Mg-silicates while wollastonite is abundant in CaO (Huijgen & Comans, 2003). The ores containing these minerals are naturally available in large quantities (especially what concerns the Ca -and Mg silicates) and it has been estimated that their total volume would suffice to bind all anthropogenic CO_2-emissions originating from fossil fuel burning. More specifically, their absolute storage capacity could amount up to about 8,000 Gt of CO_2 (Ziock et al., 2000). In addition to this, these reactions are exothermic (energy is released when recombination of CO_2 and the oxides takes place) and thus proceed spontaneously. Therefore this makes the process even more appealing as no additional energy consumption would be required in the carbonation process (Lackner et al., 1997). A large drawback however, is that the reaction proceeds very slowly (similar to the process of rock weathering) over nearly-geological time scales, too slow to be applied for the point of interest (storing CO_2 over a reasonable time span, to mitigate climate change effects). Therefore, the technique of 'accelerated carbonation' seems to fit these prerequisites better as it makes the reaction proceed significantly faster. The process is accompanied by modified conditions however, -such as a higher water content and temperature- increasing energy consumption and associated costs.
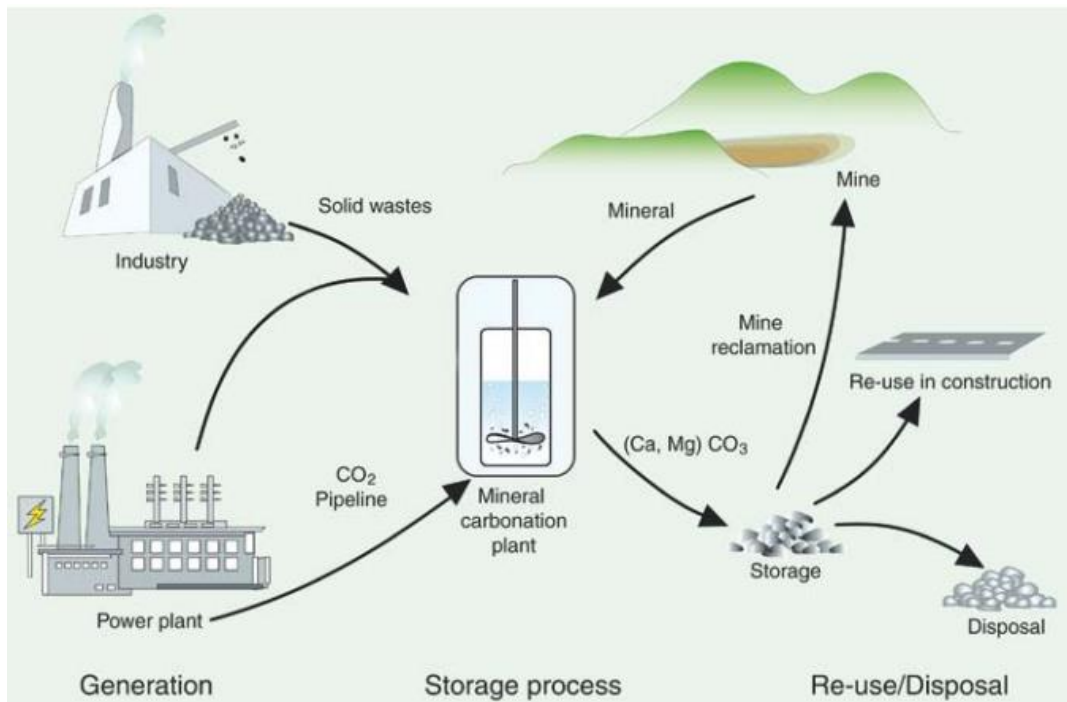
Figure 3.1: Overview of the processes needed to achieve mineral carbonation (Energy Research Centre of the Netherlands) (IPCC, 2005)

3.1 Accelerated Carbonation

Accelerated Carbonation Technology (ACT) is a patented S/S process (Hills, 1997), differing from the most prevalent S/S techniques in the fact that it occurs under a carbon dioxide atmosphere instead of under ambient air. Next to the immobilization of present contaminants, it may also improve the engineering properties of soils or materials. In contrary to the regular cementation techniques, ACT remediation is often able to overcome cement hydration inhibitory effects normally attributable to certain contaminants, such as zinc and lead (CLA:RE, 2006).

As was mentioned in the previous chapter, accelerated carbonation takes place under a (often pressurized) CO_2 atmosphere, and enhanced reaction conditions. The factors that may have a potential influence on the reaction kinetics are among others: material composition, grain size, moisture content (L/S), temperature, CO_2-pressure, reaction time, gas flow rate. Several studies have focussed on identifying the most crucial factors to reach high values of carbonation, in order to identify 'ideal operating conditions' for accelerated carbonation of certain mineral species.

Lackner et al. (1997) remarked that the rate of initial CO_2-uptake increased drastically for higher temperatures. It also seemed to enhance the maximum carbonation extent. In addition to this, higher CO_2-uptake rates were observed for small increases in CO_2-pressure of about 0.2 bar. However there are constraints on the enhancing effect of these operating condition, as it was found by Lackner et al. (1995) that for temperatures exceeding 170-410°C, 410°C and 890°C respectively for most minerals suitable to ACT, Mg-oxides, and Ca-Oxides (all under 1 bar CO_2), the equilibrium shifts towards CO_2-release instead of uptake.

An often disregarded disadvantage of mineral CO_2-sequestration however, is that a relatively large amount of Ca/Mg minerals is required to take up an amount of CO_2 (Lackner et al., 1995). Consequently, storing significant amounts of carbon dioxide in this way would require huge amounts of the raw minerals. Not only this would result in the generation of excessive amounts of waste to be disposed of, moreover this would require disproportionate amounts of energy and its associated CO_2-emissions (except for the unlikely case that solely renewable energy would be used) due to mining, transport and pre-treatment of the minerals needed which altogether will significantly reduce the CO_2-capturing efficiency of the process (Huntzinger et al., 2009). Estimates of this are provided by the Special IPCC report on Carbon capture and storage, in which it is claimed that 1.6 to 3.7 tonnes of silicates would be needed per tonne of CO_2 to be stored, finally resulting in the disposal of 2.6 to 4.7 tonnes of carbonates/tCO_2. The cost would be about 50–100 US\$/tCO_2 + the cost of capture and transport (23-53 US\$/tCO_2). As can be seen from Table 3.1, these costs are high in comparison to other techniques.

Table 3.1: Final costs for CO_2-capture and storage (2002 data) (IPCC, 2005).

CCS system components	Cost range	Remarks
Capture from a coal- or gas-fired power plant	15-75 US$/t$CO_2$ net captured	Net costs of captured CO_2, compared to the same plant without capture.
Capture from hydrogen and ammonia production or gas processing	5-55 US$/t$CO_2$ net captured	Applies to high-purity sources requiring simple drying and compression.
Capture from other industrial sources	25-115 US$/t$CO_2$ net captured	Range reflects use of a number of different technologies and fuels.
Transportation	1-8 US$/t$CO_2$ transported	Per 250 km pipeline or shipping for mass flow rates of 5 (high end) to 40 (low end) MtCO_2 yr^{-1}.
Geological storage[a]	0.5-8 US$/t$CO_2$ net injected	Excluding potential revenues from EOR or ECBM.
Geological storage: monitoring and verification	0.1-0.3 US$/t$CO_2$ injected	This covers pre-injection, injection, and post-injection monitoring, and depends on the regulatory requirements.
Ocean storage	5-30 US$/t$CO_2$ net injected	Including offshore transportation of 100-500 km, excluding monitoring and verification.
Mineral carbonation	50-100 US$/t$CO_2$ net mineralized	Range for the best case studied. Includes additional energy use for carbonation.

An alternative to the use of these raw Ca or Mg- oxide bearing minerals, could be the use of alkaline industrial wastes, containing these reactive oxides as well. The ACT treatment and subsequent reuse of these wastes would diminish the size of waste tailings, and also superfluous energy consumption due to mining and transport –as in the case of utilization of raw minerals- is avoided. Moreover, these materials are chemically relatively unstable in comparison to natural minerals, making them more reactive and further decreasing the amount of pre-treatment needed (Huijgen et al., 2005; Lackner et al., 1997). It has been found that this reactivity is not only caused by their chemical instability, but also by the large reactive surface area these slags possess as a consequence of being milled along the production process (Huijgen & Comans, 2003; Bertos et al., 2004a). Another advantage here would be that this slag material is often produced in the vicinity of an industrial CO_2-source (for example the steel manufacturing plant itself), whereas the iron and steel industry worldwide generates high CO_2-flows of about 646 Mt/yr (Table 3.2), equivalent to 4-7 % of the total CO_2-emissions (IPCC, 2005; Kim & Worrel, 2002). However, the quantity of these wastes being generated is fairly limited, leading to the fact that the potential CO_2-uptake by steel slags or other steel plant wastes is limited to about 100 Mt/yr (Zevenhoven et al., 2006).

Table 3.2: Different sectors and their absolute annual CO$_2$-emissions (IPCC, 2005)

Process	Number of sources	Emissions (MtCO$_2$ yr^{-1})
Fossil fuels		
Power	4,942	10,539
Cement production	1,175	932
Refineries	638	798
Iron and steel industry	269	646
Petrochemical industry	470	379
Oil and gas processing	N/A	50
Other sources	90	33
Biomass		
Bioethanol and bioenergy	303	91
Total	**7,887**	**13,466**

On the other hand, it must be remarked that alkaline slags have a lower absolute uptake capacity compared to oxide minerals -although the uptake capacity of steel slag is still relatively high compared to other alkaline waste materials (Huijgen et al., 2005).

These reactive alkaline wastes are: incineration ashes, incinerator sewage sludge ash, pulverised fuel ash, paper sludge ash, clinical waste ash, oil shale pulverised ash, biomass ash, sewage sludge ash, wood ash, pulverized fuel ash, steel slag (SS), blast furnace slag (BF), basic oxygen furnace slag (BOF), secondary steel slags such as argon oxygen decarburisation slag (AOD), desulphurisation slag, ladle slag, cement kiln dusts (CKD), paper wastewater sludge, recycled concrete aggregate, air pollution control residue (APC) and quarry waste and fines. The full list is very extended, since many other wastes with cementitious phases may be considered for use (Lackner et al., 1997; Sanna et al., 2012). Accelerated carbonation has already been applied to different types of alkaline wastes like slags from coal-fired power stations under which: pulverized fly ash (PFA) (Johnson, 2000), spent shale (Reddy et al., 1994) and clean coal technology (CCT) ash (Tawfic et al., 1995) (overview from Costa et al., 2007).

It was acknowledged by the U.S. Department of Energy and the National Energy and Technology Laboratory that alkaline solid wastes are a promising resource for CO$_2$ sequestration and that further research on alkaline wastes and applicable techniques will be performed.

3.1.1 ACT Methods

Multiple ACT techniques have been developed in order to study the possibilities in the field of CO_2-storage through carbonation, treatment and reuse of minerals. Most of these studies utilizing different procedures were performed on raw minerals and less on alkaline wastes. However, virtually all results have been obtained through lab-scale experiments. The efficiency of the carbonation depends on multiple factors such as: the use of direct or indirect carbonation methods (which will be described further on), the mineralogy, chemistry and physical properties of the used material, and the carbonation conditions (pressure, temperature, L/S ratio, particle size) (Costa et al., 2007; Bobicki et al. 2012). The carbonation techniques can be subdivided in 2 subcategories: indirect (also called multi-step) -and direct (or single-step) carbonation. As the name might suggest, single-step carbonation occurs through direct contact between CO_2 and the material, often inside of a reactor with adjustable temperature and pressure. Pre-treatment by means of grinding, heat treatment or chemical activation is commonly used to further speed up the carbonation process (Sanna et al., 2012). It should be kept in mind that these pre-treatments are very energy-intensive and in the end decrease the net carbon uptake of the treatment.

Indirect carbonation is generally based on the extraction of Ca-or Mg oxides from the slags with the use of chemical solvents to produce carbonate end-products of high purity and significant market-value (Teir et al., 2005). This higher purity is realizable through extraction of the reactive substances (e.g. (hydr)oxides) with use of these solvents in a first (or multiple) step(s) and subsequent carbonation (Sanna et al., 2012). However, the use of acidic solvents may lead to dissolution of elements (such as heavy metals) which have to be removed from the solution through separation steps to obtain a pure end-product. Direct carbonation on the other hand does not require this and is thus less complex and less expensive, although the resulting end-product has a lower quality.

The main effects of the carbonation reaction on the (alkaline) medium are: a decrease in pH, an altered buffering capacity, the formation of calcite, or possibly the formation of metal carbonates and other phases (Costa et al., 2007; Huijgen & Comans, 2005). Crucial is that the change in these properties leads to improved leaching properties after carbonation compared to the starting material.

3.1.1.1 Indirect Carbonation tests

Indirect carbonation processes consist of multiple steps including: dissolution of the matrix and extraction of the reactive fraction (earth alkaline metal), pH adjustment and precipitation of impurities, carbonation and regeneration of solvents (Dri et al., 2013). Metal dissolution is the rate-controlling step during the first stage and therefore acids or other solvents are often used to speed up this dissolution for the process to be applicable as an industrial carbonation technique (Costa et al., 2007; O'Connor et al., 2005). Examples of these chemical solvents are hydrochloric acid, nitric acid, sulphuric acid, carboxylic acids: acetic or succinic acid, sodium hydroxide, ammonium chloride (Park et al., 2003; Baldiga et al., 2010; Bobicki et al., 2012). However, in a later phase, an increase in pH is required in order to let the dissolved metals precipitate as carbonates. This can be achieved by the addition of other chemical agents such as for example NH_4OH (Park & Fan, 2004).

Experiments, using acetic acid in the carbonation process, were performed and described by Eloneva et al. (2008b); Kakizawa et al. (2001); Teir et al., (2005;2007a). In the first step, acetic acid is applied for the dissolution of the reactive phases (*e.g.* Ca) from the matrix (*e.g.* calcium silicates). After extraction of these reactive phases, the formed residue of silicate and other impurities is removed, and the formation of carbonate is promoted. This may occur according to several methods: one possibility is to form high-purity $CaCO_3$ (precipitated calcium carbonate; PCC) through the addition of CO_2 and calcium acetate (a weakly basic salt). Another explored option is to increase the solution's pH by addition of NaOH, increasing temperature (to 30-70°C) and raising CO_2 pressure (1 to 30 bar). According to Teir et al. (2007b), the addition of NaOH resulted in larger precipitation yield, while raising temperature and pressure had minor effect. Using the latter method, solid $CaCO_3$ is produced with a purity differing from 63-99.8% between different experiments. A drawback of this technique is that regeneration of the NaOH agent is very energy-intensive, rendering the process too expensive for CO_2-sequestration on a large scale.

Instead of using (raw) earth alkaline minerals, also slags can be used with these techniques, but this results in the dissolution of many other elements and thus often multiple separation steps are needed to lead to a high-quality end product. An example of this is the study by Kunzler et al. (2011) where hydrochloric acid was used for extraction and NaOH for subsequent precipitation of the undesired metals. Carbonation took place in an alkaline solution through the bubbling of CO_2 through the solution, yielding a product with a purity up

to 98%. Doucet (2010) remarked that the initial presence of significant amounts of calcite in the untreated material may lead to its dissolution and the production (and escape) of gaseous CO_2. This may lead to a lower overall carbonation efficiency.

3.1.1.2 Direct carbonation

Direct carbonation may occur in the two-phase system by gas-solid reaction (dry), or in the three-phase system by aqueous reaction (with water, gas and solid phases present; wet) (Dri et al., 2013). Most research has been done on the latter method. This is mainly due to the fact that reaction rates for the aqueous system are significantly higher (Costa et al., 2007). Wet one-step carbonation may occur in slurry-phase (L/S>1 w/w), most often under high temperatures (100-200°C) and significantly elevated CO_2 pressure (10-30bar), especially for materials having their reactive species (e.g. CaO, MgO) in less-soluble silicates (Huijgen & Comans, 2006; Baciocchi et al., 2009; Kodama et al., 2006). Direct carbonation in aqueous solution (wet, L/S<1) on the other hand occurs according to the following steps: material disintegration and subsequent dissolution of the earth alkali metals into solution, along with dissolution of CO_2 in the solution and the formation of HCO_3^-, and finally the formation of carbonates through recombination of the bicarbonate and earth alkali metal ions (Huijgen et al., 2006). Most often this occurs under lower temperature (30-50°C) and 1-10 bar CO_2 pressure (Baciocchi et al., 2009) Just as with indirect carbonation, the rate-limiting step is the formation of the positive (earth alkali) metal ions (O'Connor et al., 2005). However, a difference with indirect carbonation is that the above-mentioned phases do not happen as separate steps in the process but can occur more gradually, temporally overlapping. Also here, solvents may be used to speed up the reaction rate by increasing the dissolution rate of metal ions, but this is not required. It should be noted that direct carbonation is less expensive due to lower energy requirements and the unnecessity of solvents (and their regeneration). As may be expected, the experiment conditions (temperature, CO_2 pressure, L/S, grain size, reaction time) play a role next to the kind of material used. The next chapters will further elaborate on the importance of these factors since the direct carbonation technique (wet) has been used for the experimental study of this thesis (Chapter 4 and 5).

The reaction steps for the process of aqueous carbonation of calcium oxides is as follows (Huijgen et al. 2005):

$$CO_2(g) + H_2O(l) \rightarrow 2H^+(aq) + CO_3^{2-}(aq)$$

$$CaSiO_3(s) + 2H^+(aq) \rightarrow Ca^{2+}(aq) + SiO_2(s) + H_2O(l)$$

$$Ca^{2+}(aq) + CO_3^{2-}(aq) \rightarrow CaCO_3(s) \qquad (3.4)$$
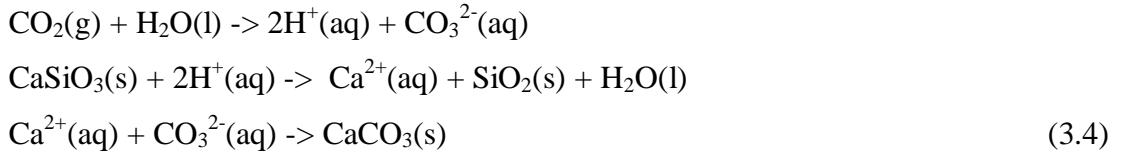
The reactions for carbonation of slags are based on the same principle of reaction steps.

Huijgen et al. (2005) found that the rate of carbonation diminishes with time, finally approaching a maximum value (even though not all reactive phases may be converted) due to the formation of a calcite crust at the surface of the reactive material and the presence of a calcium-depleted layer below. Both layers act as a barrier, limiting the diffusion of CO_2 inwards and the diffusion of water (and the associated dissolved elements) outwards of the grains.

3.1.2   Carbonation extent

The theoretical maximum possible CO_2-uptake (wt.%) for a specific material can be calculated from the total Ca- and Mg concentration in the elemental composition, using a modified Steinour formula (Steinour, 1959; Huntzinger et al., 2009):

$$\%ThCO_2 = 0.785 * (\%CaO - 0.56 * \%CaCO_3 - 0.7 * \%SO_3) +$$
$$1.091 * \%MgO + 0.71 * \%Na_2O + 0.468 * (\%K_2O - 0.632 * \%KCl) \qquad (3.5)$$

This is based on the assumption that the full Ca and Mg content can be carbonated and the fractions are expressed as a percentage of dry mass.

In contrary, the effective CO_2-uptake capacity is often estimated from the concentrations of Ca and Mg in the leachate of the treated material or by Thermal Gravimetric Analysis and is always lower than the 'theoretical' capacity (Doucet, 2010; Santos et al., 2013). Therefore, it is more reasonable to consider the effective CO_2-uptake when evaluating carbonation techniques or when considering the applicability of a certain type of material in order to meet the proposed objectives. According to Doucet (2010), the effective uptake was up to 25% lower than the theoretical uptake for BOF and EAF slags in a specific experiment. This is thought to be due to limited dissolution of the material, and in addition due to an incomplete conversion of the dissolved reactive phases to carbonates. Therefore, the theoretical uptake

may better be used as an indicator to assess the suitability or applicability of a materials for carbonation (Doucet, 2010).

The carbonation extent of a material depends especially on its fraction of highly reactive species. Especially phases such as CaO, MgO and portlandite are rapidly converted to carbonates because when introduced into an aqueous solution, they easily leach their Ca and Mg ions which may then react to form carbonates. However, other phases containing Ca and Mg such as silicates or aluminates are often more abundant and generally are less prone to dissolve fast (Lekakh et al., 2008). However, the ease of leaching is also determined by grain structural features, as the inclusion of more soluble species inside less soluble (e.g. silicates will impede their dissolution (Doucet, 2010).

3.2 Crude Steel slags

3.2.1 What are steel slags- the production

The steel manufacturing process starts with the input of beginning material such as raw iron ore, coal, and lime into the blast furnace, producing pig iron and the waste product BF slag. This pig iron is used as input for the basic oxygen furnace together with input of recycled metal, producing steel (which is afterwards refined and coated) and the waste product steel furnace slag or BOF slag. The input of the electric arc furnace is mainly recycled scrap steel and produces steel and the waste product EAF slag (EPA, 2006). Into each of these furnaces, the starting materials of iron ore (or pig iron in the case of the BOF), or scrap metal are introduced together with fluxing agents (e.g. lime) and are heated beyond the melting point of about 1600°C. After being completely fused, two or more liquids will have formed, floating on top of one another due to their different specific density. The liquid on top, having a lower specific density, forms the waste product and is skimmed off to form the slag upon solidification. Slags are thus composed of impurities such as complex metallic and non-metallic oxides (e.g. Ca-, Fe-, Si-, Al-, Mg-, Mn-oxides) present in complexes of calcium silicates, alumino-silicates and alumino-ferite (National Slag Association, 1998). Next to the chemical composition, the physical properties (e.g. density, grain size, structure) are determined by the cooling process as will be further elaborated upon under paragraph 3.2.5.

Thanks to the high Ca-content and the alkaline properties, many types of steel slags are suited for ACT and CO_2-sequestration.

Since official data is not always available, it is estimated that annually, the global iron and steel industry generates 220-420 million tonnes of iron and steel slags (Miklos, 2000; Eloneva et al., 2008a; Doucet, 2010; World Steel Association, 2010). However, according to a rapport of the U.S. Geological Survey (2013), annual global iron slag and steel slag output are respectively 260-310 and 130-210 million tonnes. They account for about 15wt% of the total steel output (Das et al., 2007). In 2010, in the E.U. alone, 21.8 million tonnes of steel slags were produced while worldwide this figure amounted to approximately 170 million tonnes (U.S. Geological Survey, 2012). These steel slags consist mainly of the following categories (Figure 3.2): Basic Oxygen Furnace slag (BOF) (accounting for 62%), Electric Arc Furnace slag (EAF) (29%) and finally of secondary metallurgical slag such as ladle slag (9%) (Gahan et al., 2009).
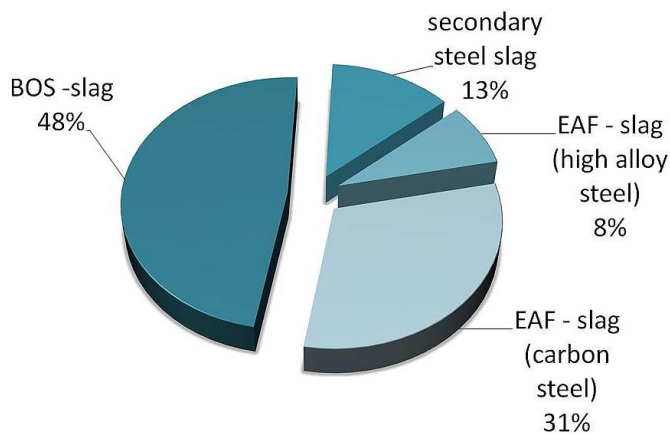
Figure 3.2: Fraction of different types of steel slags produced in the E.U. (2010) (Euroslag, 2010). Note: BOS = Blast Oxygen Furnace slag = BOF

It should be mentioned that steel manufacturing waste is composed of both steel slag waste and steel dust wastes (often steel slag is used as an expression for both). In some cases the quantity of steel dust even exceeds the volume of (coarser fraction) slags, accounting for up to 1-2 wt% of the initially used steel ores (Zhang & Hong, 2011; Lopez et al., 1997; Zunkel, 1996). These fine wastes show to be less suitable for reuse; therefore steel slag waste intended for reuse is most often sieved, after which the fine fraction is discarded of, or its grain size is increased through sintering. Steel slag waste is generally considered to be non-hazardous due to the low concentrations of trace elements in the slag's leachates (Proctor et al., 2000). Stainless steel slags on the other hand (para.3.3), often have a relatively high concentration of

Cr or other trace elements in their leachates and may be classified as hazardous (Shen & Forssberg, 2003), depending on the national or regional guidelines. Therefore, remediation of the last-called type of slags is more common before reuse or introduction into the environment. In any case, the advantages of using steel slags over raw minerals for CO_2-sequestration are versatile: slags are cheap, may be available near large point sources of CO_2, their chemical instability leads to a relatively short reaction time, it limits the consumption of raw materials and the need for additional mining activities, and reduces waste volumes along with the associated negative environmental impacts (Huijgen & Comans, 2003; Huijgen & Comans, 2005; Huijgen et al., 2007).

In addition, these alkaline steel slag wastes generally still contain high concentrations of valuable (heavy) metals which could be recovered through proper management and recycling (para. 3.2.4).
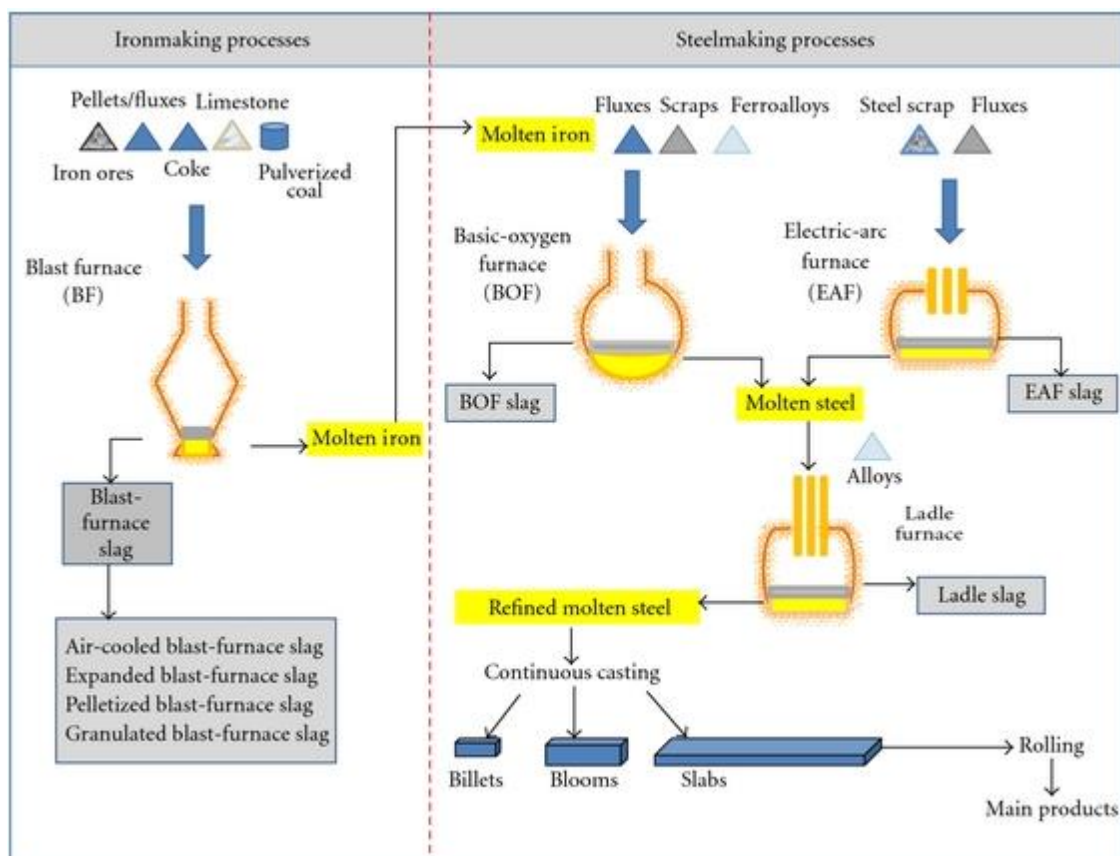
Figure 3.3: Schematic representation of the iron –and steelmaking process and the origin of its waste slags (Yildirim & Prezzi, 2011)

3.2.2 Steel slag characterisation

3.2.2.1 Composition

The wastes originating from steel making processes are generally a complex mix of multiple materials and potential harmful substances. The slags are composed of stable oxides such as CaO or MgO, SiO_2, Al_2O_3, as well as of less stable oxides such as Fe, Cr-,Ni-, and Mn-oxides and may in addition also contain volatile organics such as fossil fuel derivatives, PAH's, VOC's (Motz & Geiseler, 2001; Ye et al., 2003).

The reason for the abundance of Ca in the material is to the use of limestone as fluxing agent to remove impurities from the steel (e.g. Si and P) (Huijgen et al. 2005). The mineralogical composition of the steel slags is most often dominated by dicalcium and tricalcium silicates, calciumaluminium silicates, calcium oxides and periclase (MgO) (Shen & Forssberg, 2003). More specific, mineral speciations are present such as: merwinite ($3CaO \cdot MgO \cdot 2SiO_2$), olivine ($2MgO \cdot 2FeO \cdot SiO_2$), C2S ($2CaO \cdot SiO_2$), C_4AF ($4CaO \cdot Al_2O_3 \cdot FeO_3$), C2F ($2CaO \cdot Fe_2O_3$), CaO (free lime), MgO, FeO and C3S ($3CaO \cdot SiO_2$) (Qian et al., 2002a &2002b; Shen et al., 2004). Whereas the mineralogy of BOF and EAF is according to Doucet (2010) composed of: Larnite (β-Ca_2SiO_4), brownmillerite ($Ca_2Fe_{1.4}Mg_{0.3}Si_{0.3}O_5$), wuestite (Fe), calcite, magnetite (Fe_3O_4), lime, portlandite ($Ca(OH)_2$), Ca-silicate (α-Ca_2SiO_4), Akermanite ($Ca_2Mg(Si_2O_7)$), Katoite ($Ca_3Al_2(OH)_{12}$), Gypsum ($CaSO_{4.2}H_2O$) and quartz ($Si(OH)_2$).

Obviously, the exact composition is different for each type of slag (e.g. BOF, EAF, BF, AOD) and the exact procedure followed during the production process. According to a publication of the US Department of Transportation (1998), the average calcium oxide content of steel slags is 34-52%. In line with this, in Sanna et al. (2012) it is claimed that all steel slags, CKD, biomass ash, oil shale ash, AOD slag, APC residue and paper incineration ash contain 40-70% of CaO.

3.2.2.2 Leaching properties

Steel slag waste is generally considered to be non-hazardous due to the low concentrations of trace elements in the slag's leachates (Proctor et al., 2000). Therefore, under normal condition, the amount of heavy metals leaved from the material is limited and generally does not exceed the imposed limits, although this may depend on the exact nature of the material.

3.2.3 Direct-Carbonation

This section elaborates upon the practical side of direct-carbonation, providing an overview of the different techniques used in several studies performed. Since the objective of the current work is to assess the feasibility of in-situ carbonation of alkaline wastes, the emphasis will be on research performed upon the latter type of waste.

Up to now, the most common technique to perform accelerated direct-carbonation tests on alkaline solid wastes has been through the aqueous route with three-phase reactions (e.g. Bertos et al., 2004b; Van Gerven et al., 2005; Huijgen & Comans, 2006; Baciocchi, 2010) and less through gas-solid reaction. The reason for the use of furnace slags has been their high Ca content (34–55%) and alkaline (pH 11.3–12.4) properties, making them suitable for ACT.

3.2.3.1 Effect on leaching behaviour

Research presented in multiple papers has shown that carbonation of alkaline solid wastes affects the leaching behaviour of certain elements. For several kinds of wastes, the leaching of potentially harmful elements decreased after being carbonated. This decrease may be due to several reasons such as: co-precipitation of these substances in carbonates, the formation of other minerals, changing (decreasing) pH altering their solubility, or through sorption onto freshly precipitated surfaces (Huijgen et al., 2006). In line with this, Meima et al. (2002) found that carbonation of municipal solid waste incineration (MSWI) bottom ash reduced the leaching of Cu and Mo. Reddy et al. (1994) obtained results showing that carbonation of fly ash from coal fired power plants reduced the leaching of the elements Cd, Cu, Ni, Pb, Se, and Zn. Also the carbonation of coal effluent ashes (air pollution control ash) led to a lower concentration of As, Cd, Cr, Pb, and Se in the leachates according to Tawfic et al. (1995).

According to research of Huijgen & Comans (2006), ACT reduces the leaching rate of alkaline earth metals (except for Mg) through the transformation of Ca-phases (portlandite, ettringite, Ca-(Fe)-silicates) into calcite. Also part of the earth alkali metals may be carbonated (e.g. Ba, Sr) thus decreasing their concentration in the eluate. Opposite to this, the leaching of vanadium was found to increase upon carbonation, probably due to the dissolution of Ca-vanadate. Carbonation also reduces the leachate concentration of trace elements such as oxyanions (*e.g.* ClO^-, SiO_3^{2-}) and heavy metals through sorption on metal (hydr)oxides (their

reactive surface area increases upon carbonation, with exception of Mn) (Apul et al., 2005; Fällman et al., 2000).

3.2.3.2 Example Column tests

A column test was performed on cement kiln dust slag (CKD) by Huntzinger et al. (2009). In this study the influence of a varying concentration of the incoming CO_2 gas, its relative humidity and flow rates (45-60ml/min), and the material's initial moisture content on the extent of carbon sequestration was investigated. Total experiment duration was 3.5–12 days, until full breakthrough of CO_2 concentration was observed. It was found that full CO_2-uptake continued longer in the case when the gas was humidified, probably explained by an increased aqueous absorption of CO_2. However, the overall sequestration extent seemed to be decreased due to a higher water content, likely due to its slowing or hindering effect on the CO_2 transport to the reaction sites. On the other hand, for the dry slag the overall carbonation appeared to be higher due to the greater pore gas volume in the medium and lower diffusion limitations. A higher concentration of the incoming CO_2 gas resulted in faster carbonation rates ánd a greater overall carbonation extent at the end of the experiment. However, it was acknowledged that sample homogeneity could have had an effect on the results, as the samples were left undisturbed from the sample site. The final result were carbonation extents up to 70% of the theoretical extent.

3.2.3.3 Example Reactor tests

A publication by Huijgen et al. (2005), studied direct carbonation of BOF slurry in a reactor set-up. It was found that particle size (tested over the range 38 um - 2 mm) and temperature (25-225 °C) were the two most important parameters determining the rate of the steel slag carbonation process. The relevant Ca-containing phases were identified to be: $Ca(OH)_2$, Ca-silicates and Ca-Fe-O. The former 2 are generally known as easily soluble phases that can be readily carbonated, while the latter seemed virtually insoluble. Studying the carbonation of Ca/Mg silicate particles on a microscopic scale, the exact procedure of reaction was identified. First calcium from the material dissolves and migrates into solution, subsequently calcite precipitates on the exterior of the particles. The reaction rate seemed to be limited by the rate of Ca migration out of the grains. Next to the formation of a calcite crust, also a Ca-depleted silica zone formed under the grain surface.

The reaction occurred relatively fast, with 40% of the calcium being carbonated after 2 minutes, and with only an additional 13% reacting for times up to 30 min. In addition, the paper states that the conversion-particle size relation (IEA, 2000) is determined to be:

$$\text{Conversion} = (D)^{-0.7 \text{ to } -0.4} \tag{3.6}$$

Making particle size the most important factor in determining carbonation extent. Temperature seemed to be the second-most influential parameter: carbonation increases with temperature between 25 and 175 °C. Below this temperature, Ca-leaching is rate-limiting and above it CO_2 solubility becomes minimal and limiting. The effect of varying CO_2-pressure was marginal. Carbonation resulted in the partial consumption of Ca-Fe-O and calcium silicate (party non-dissolved) to form $CaCO_3$ and a SiO_2 phase. Next to this, the pH of the medium dropped to more neutral values. In line with this, it was pointed out that the reaction temperature had an effect on the mineralogy of the formed species: a lower carbonation temperature promotes the formation of amorphous over crystalline Fe-(hydr)oxides, with the former having a larger specific surface area, promoting adsorption of several types of cations.

3.2.3.4 Example of a field study

Up to present, in-situ field scale experiments or treatments have been barely applied. The first field-scale application of ACT took place in 2000 in Kent (UK). A former fireworks production site was heavily contaminated with copper, zinc, lead and nickel with concentration of about 96,000, 81,000, 750 and 600 mg/kg respectively. The study compared S/S and ACT treatments, by comparing 4 pilot cells containing soil: one treated with binders and subjected to ACT (20 min reaction time), one only treated with different binders, and a reference cell with untreated soil. The results from the leachate tests indicated a pH between 7.5-10.2 for the ACT treated material in contrary to 10.5-14 for the S/S treatment alone. In addition to this, metal leaching was significantly reduced, even to levels below drinking water limits. Also the engineering properties of the originally cohesive clay-rich soil were clearly improved (C8s, n.d.; CLA:RE, 2006). In addition, the formed carbonated material seemed to be stable, since monitoring in 2003 showed that the material was still stable, and no changes in leaching had occurred.

An example of another field scale treatment with ACT and S/S is the CL:AIRE Technology Demonstration Project (TDP8). The field experiment was performed in 2001 to treat a wide

range of contaminants, occurring at high concentration, at a site near Chesterfield (CLA:RE, 2006). The presence of multiple contaminants is interesting because of the fact that in many brownfields, not just alkaline waste slags occur, but also multiple other contaminants. The site was extensively contaminated with coal tars, lime sludge, acids, phenols, PAH's, VOC's, spent oxide, heavy metals and so on. Low but significant concentrations of arsenic, cadmium, chromium, lead, mercury, selenium, copper, nickel, boron and zinc were measured. The different kinds of material were separated according to the pollutants they contained (the former waste tip –with a mix of contaminated material-, the plant area, -mainly organic pollutants: phenols, petroleum hydrocarbons and aromatic hydrocarbons-, and spent oxide deposits, mainly composed of metallic cyanides).

After excavation, binders were added to the material under mixing for 5 minutes and subsequent AC took place by exposing the material to CO_2 during 10 minutes at 20 °C. The temperature increased during the treatment from 20 to 40°C (S/S), reaching up to 65°C during ACT, what increased the release of certain volatile organic compounds. 28 Days after treatment, leaching tests were performed showing that ACT treatment of the waste tip material yielded low heavy metal concentrations (below screening values) while for only-S/S treatment, this was not the fact. Results with respect to leaching of cyanide, petroleum hydrocarbon and PAH were less favourable, indicating an increased leaching after treatment, which gradually decreased with time. However, ACT treatment produced solid granules of the material (only-S/S treatment didn't), rendering the material suitable as a filler for engineering purposes, according to the values set by the Specification for Highways Manual (Highways Agency, UK).

3.2.4 Plant Internal Recycling of Slags

The increasing demand for metals and their rising prices on the international markets have as a consequence that the search for recycling methods of slags is being promoted, rather than the previously more common practice of disposal and landfilling (or tailing) (Majuste & Mansur, 2008). Proper reuse of the metals in the waste is important to reduce the use of raw materials and in addition to limit contamination of the environment with waste materials. Currently, in most steel plants, the produced slags –with their generally high content of entrained valuable metals- are re-fed into the blast and steel furnaces (U.S. Geological Survey, 2013). This recycling is especially targeting the recovery of *e.g.* chromium, iron, lead, nickel, zinc, and cadmium. Especially slags with a high fluxing capacity (those rich in

CaO or MgO) are often re-fed into the blast furnace (about 30 wt.% in E.U.) (Das et al., 2007). Numerous treatment procedures exist: based on physical separation methods (e.g. magnetic and gravity separation), pyrometallurgical methods involving the use of heat (e.g. calcining, roasting, smelting), and hydrometallurgical methods occurring in aqueous solution (e.g. leaching, solution concentration and purification, recovery through electrolysis or precipitation) (Geldenhuis, 2002; Laforest & Duchesne, 2006; Youcai & Stanforth, 2000). Specific technologies used for recovery were described by Chen et al. (2011). Some of the technologies frequently applied (to the still liquid slag) are hot splashing technology, water quenching, or wind quenching. After the application of one of the aforementioned techniques, often crushing and magnetic separation is performed on the solidified slag to recover iron and return it to the blast furnace. On the other hand, recovery of other valuable metals (Pb, Zn, Cr) may occur through the use of specific solvents (often acids), depending on the element targeted for extraction (Das et al., 2007).

In addition, many sludge and dust wastes are recycled through sinter making. In this process, the material is heated to a high temperature, making the fine particles to fuse together forming larger particles. Following this also the already mentioned techniques such as quenching may take place to make the particles suitable for reuse as a furnace input (Das et al., 2007).

At the end of the stainless steel production process, the steel is pickled in strong acids such as HNO_3 and HF, in order to obtain the characteristic smooth and corrosion-resistant surface (Li et al., 2005; Rögener et al., 2012). This process however causes enrichment of the acid solution with metal salts containing valuable metals such as Cr and Ni. Regeneration of both the acid and the metals it contains may be achieved by applying pyrometallurgical processes, whereas partial regeneration (e.g. nanofiltration), results in recovery of the acid only. Recovery of only the metals is possible through the energy-intensive process of membrane electrolysis, yielding a metal precipitate on the electrode (Rögener et al., 2012). In many cases, the quality of the recovered precipitate was sufficient for reuse in the BOF.
Alternative recycling, not by recovery of the present valuable elements, but through reuse of the material in constructional applications may also occur, as will be discussed later on in para. 3.2.5.
An example of a study on recovery of heavy metals from waste slags or sludge was performed by Ye et al. (2003) in which stainless steel production side products were treated through a

pyrometallurgic procedure with a DC furnace with a hollow electrode reactor in which slags and dusts could simultaneously be treated. This was done with EAF slag, AOD slag, EAF dust, oily millscale and hydroxide sludge. Treatment resulted in Cr- and Ni- recovery up to 90% and 100% respectively, producing slags whose Cr-leachate concentration was 10–100 times lower than originally for the untreated material.

3.2.5   Reuse of untreated or carbonated slag

Unfortunately, disposal of slag waste in landfills is still a common practice in many developing countries such as for example India and China (Mukherjee, 2011; Halliday, 2012; Teng, 2012). Currently, the use of steel slag in China is only about 22% (Yi et al., 2012). Reasons for the material being landfilled most often are that it is unclear how to properly treat it, when the treatment-processes are too expensive or when it is preferred to wait until a better managing technique is found. Doing so is a non-sustainable and non-profitable way of dealing with steel slag wastes. However, together with raw stock prices, also the price of scrap metal is rising (Rögener et al., 2012), promoting better recycling and reuse of the generated waste flows.
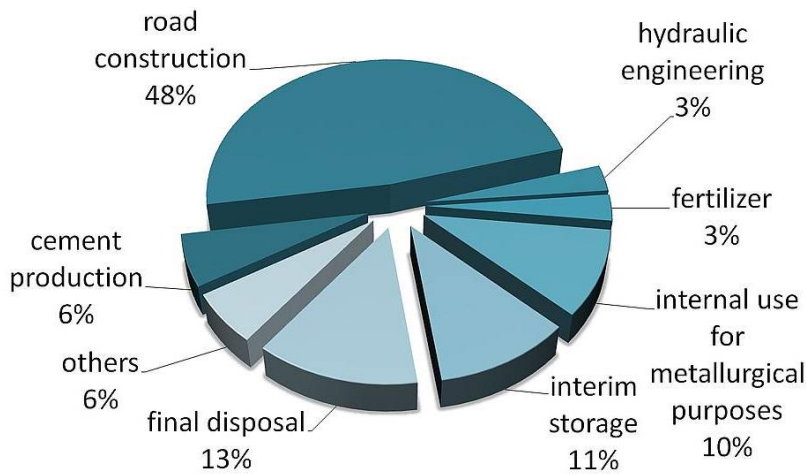
Figure 3.4: The use of steelmaking slags in E.U (Euroslag, 2010).

As already discussed in section 3.2.4, internal recycling is a profitable act but next to this, the material may also be sold for reuse in external applications.

The potential for reuse of the slags is essentially dependent upon both its chemical and physical properties. What concerns the chemical status, crucial is that the slags should comply with national guidelines (if existent) with respect to leaching concentrations. The physical

status is of importance to be sure they are suited for the technical purposes they are intended to be used for. Their specific density, grain size and porosity are determined by the applied cooling or treatment process during solidification of the slags. BF slag may be air-cooled, granulated or expanded, whereas EAF and BOF slags typically are air-cooled. The U.S. Geological Survey ("USGS") 1997 Annual Review (USGS, 1998) explained the various cooling processes as follows:

Air-cooled slags develop through gradual cooling by air of the material in an open pit. Because the material is allowed to cool down slowly, the gradual escape of gases results in the formation of porous aggregates with a low density. In contrary, rapid cooling through air quenching creates dense non-porous aggregates, more suitable for constructional applications. Using water-quenching, molten slag is converted into a glassy substance, resulting in granulated slag. Expanded slag is produced by subjecting the material to a rapid (but controlled) cooling by means of water, possibly with a combination of steam and compressed air to increase the porosity of the slag. In this way, low-density aggregates suitable for use in concrete are formed.

Steel slags are mainly sold to the construction industry, where they are used for construction purposes in the public sector, of which half is granulated (mainly) iron (BF) slag (U.S. Geological Survey, 2013). For instance, the average reuse of carbon steel making slags in the E.U. is about 70%, serving as aggregates for road-filling or in cement production. By contrary, stainless steel slags are less commonly reused because of the high concentrations of Cr or V they often feature (frequently exceeding limits) and their poor physical properties due to large amounts of Ca-and Mg oxides (Ye et al., 2003).

An abundance of the latter substances may result in hydration of the material, causing a significant decrease in the material strength, yielding it unsuitable for construction purposes (Motz & Geiseler, 2001). This may be explained by the fact that phases such as free lime (CaO), hydrate when they come into contact with water to form portlandite ($Ca(OH)_2$). Since the latter has a lower density, the hydration thus causes volumetric expansion. Also other phases such as MgO or C2S may hydrate but less readily (Yildirim & Prezzi, 2011). It has been demonstrated (Johnson et al., 2003; Chen et al., 2007) that accelerated carbonation of this material can not only improve the environmental behaviour of the slags, but also their mechanical strength, through conversion of the hydratable phases, so that they become suitable to be reused for constructional purposes. On the other hand the elimination of these

phases can also take place by applying a 'curation' process to induce controlled hydration of the phases until they are stable enough for reuse (National Slag Association, 1998). This may occur through: weathering in pits (slow and inefficient), steam hydration, or the addition of SiO_2 and O_2 to the molten slag to free lime in silicates with a lower solubility (Motz et al., 2001; Toshiyuki & Akio, 1994).

There are numerous applications for steel-making slags, as indicated in
Table 3.3. Obviously the potential destination of a specific type of slag depends on its specific physical and chemical properties.

Table 3.3: The potential use of steel slag wastes and the involved properties (Own elaboration from: Yi et al., 2012 and Nippon Slag Association, 2003).

Potential use of steel slags	Property
Road and hydraulic construction	High strength and durability
Civil engineering, backfill material	Large angle of internal friction, permeable
Cement and concrete production	Cementitious properties: C3S, C2S, C4AF
Glass/ ceramics	Hydraulic properties
Rock wool	Insulating properties when turned into fibers
Waste water treatment	Porous structure, large surface area
Fertilizer	Fertilizer components: CaO, SiO_2, MgO, FeO, P_2O_5
Acid Mine Drainage	Highly alkaline properties
Snow and Ice control	Grain-like properties

Note: C3S= $3CaO \cdot SiO_2$, C2S= $2CaO \cdot SiO_2$, C4AF= $4CaO \cdot Al_2O_3Fe_2O_3$

3.2.5.1 CO_2-uptake or CO_2-emissions evaded

The reuse of untreated slag as well as slag carbonation and subsequent reuse both imply the abatement of CO_2-emissions, for the former this is due the evading of new CO_2-emissions, that would be released due to the mining, processing and production efforts of the material that may be 'saved' through reuse. Whereas for the latter aspect it is very complex to make estimates on this volume of CO_2-emission evaded, the CO_2-uptake may more readily be estimated.

Generally, the maximum TCO_2 uptake of the material is about 25-52 wt.% (Sanna et al., 2012; Lekakh et al., 2008). In line with this, Huijgen & Comans (2005), calculated the TCO_2-uptake capacity of steel slags to be between 205 and 509 gCO_2/kg slag carbonated. Similarly, Lekakh et al. (2008) estimated that BOF and EAF slags have the potential to sequester respectively 35–45% and 6–11% of the CO_2-emissions generated in their associated production process. However, the effective uptake is always lower than the theoretical uptake. Based on the modified Steinour formula of Huntzinger et al. (2009) (para. 3.1.2), and the annual production of the waste, in Sanna et al. (2012) the theoretical annual maximum CO_2 storage potential of a certain waste was calculated (Mt CO_2/year) as follows:

$$ThCO_{2\ Storage}(P) = Waste\ available(P) * ThCO_2(P) \qquad (3.7)$$

Where P stands for the Potential waste resources and 'Waste available' stands for the waste which is currently sent to landfills. In this way, the (total) carbon dioxide storage capacity of a certain type of waste can be more effectively assessed. An estimate on the potential storage of CO_2 in iron –, steel-, and stainless steel slags will be elaborated upon in para. 3.3.5.1.

Carbonated slags can be used as substitutes for raw materials in industrial production processes *e.g.* PCC through carbonation of slaked lime, and may serve as a substitute for synthetic PCC originating from limestone, which is widespread used in paper industry (Teir, 2005). Conventional PCC production, using oil combustion for the carbonation of calcinated lime (CaO), is estimated to emit 0.21 kg CO_2/kg PCC (Teir et al., 2007a) against a net fixation of 0.34 kg CO_2/kg PCC that could be achieved through indirect carbonation (acetic acid route) of wollastonite (too expensive) or alternatively slags (with a similar CaO content) (Kakizawa et al., 2001; Eloneva et al., 2008b). About half of the Ca present in wollastonite and about the entire Ca content for BF slag could be extracted. The PCC produced through this process by Teir et al. (2007b) was found not to be sufficiently pure. Eloneva et al (2008b) however, promoted the precipitation process through use of NaOH and reached conversion rates of 31-86% of the dissolved Ca into precipitated PCC having a purity of 99.5-99.8%. In 2003, global PCC production was 7 Mt; producing high-quality PCC from slags could cause a tenfold increase in their value (Roskill Information Services, 2005; Teir et al., 2007b). This learns us that annually 3.85 Mt of CO_2 –emissions could be evaded when traditional PCC production processes would be replaced by the process of the carbonation of

alternative minerals or slags. On the other hand, also magnesium carbonates with a sufficiently high quality could be used in various production processes such as for rubber, cosmetics or medicines (U.S. Department Of The Interior, 2005).

These are only a few examples, whereas in many other applications carbonated slag (if the $CaCO_3$ or $MgCO_3$ content is sufficient) could be used as a filler (replacing clay) in for example the rubber, plastic, or paint industries (Eloneva et al., 2008b; Teir, 2007b).

Following this reasoning, the vast amounts of steel yearly being produced may be seen as an untapped resource to store current CO_2-emissions, in a safe end-product, and may generate additional economic benefits. In addition, part of the slags stored in tailings or dumps may still be reactive, because a major part of the reactive Ca/Mg silicates is fairly insoluble and thus unreactive under ambient environmental conditions (van Oss, 2003). Therefore, mining of old slag piles is already occurring and will more likely increase to do so in the future under rising raw ore prices.

3.3 Stainless steel slag

3.3.1 What is stainless steel slag

Stainless steel is the name for alloys which are iron-based, but have a larger content of heavy metals such as chromium, nickel or manganese and is produced during the secondary steel-making process (Rögener et al., 2012). The process takes place through the input of lime, molten steel from the EAF and addition of alloy materials. Through changing the Cr-content and adding other alloying elements like Ni, Mo, Mn, Cu, Ti, Nb, many different types of stainless steel may be obtained. In the AOD vessel, the content of carbon (and of other impurities such as sulphur) is strongly reduced by blowing oxygen and argon through the molten steel. The addition of argon ensures the reaction of oxygen with carbon, and not with the alloys. The slag resulting from this treatment is called AOD slag. and has a much lower FeO and a higher Al_2O_3 content than regular steel slags. Nowadays, 68.7% of the stainless steel is produced through the use of AOD units with vessel stirring systems for refinement of the aforementioned steel mix (Steelworld, 2008). Alternatively, a Ladle Heating System may be used. In a later stage, after cutting and rolling, the material may be sent through pickling

and annealing to optimize the surface properties (Colombus Stainless, 2013; Sanna et al., 2012; Shi, 2002; Steelworld, 2008).

There are diverse advantages for the use of stainless steel over carbon steel, the most important being its higher resistance to corrosion and its higher fire-resistancy through a better strength retention at high temperatures (200-1200°C) (Baddoo, 2007). Due to these properties, demand is high, making the stainless steel industry one of the most rapidly growing industrial manufacturing sectors despite the rising prices (Rögener et al., 2012). With this, also the associated waste production is increasing: for each tonne of end product approximately 330 kg of slag is generated (Zhang & Hong, 2011; Ma & Garberscraig, 2006; Shen et al., 2004; Huiting & Forsberg, 2003). In any case, the amount of stainless steel slags is relatively small in comparison to the quantities of iron and steel slags (Proctor et al., 2000) with its annual global production amounting to about 9 million tonnes (NineSigma, 2011). The slags produced by the process originate both from the EAF (somewhat different composition than the EAF slag from regular steel production) and the AOD vessel (AOD slag) and are considered potentially toxic and environmentally harmful due to their significant content of heavy metals (Cr, Ni) (Stefanova et al., 2012).

In spite of the prevalence of the EAF and AOD slag, the application of other stainless steel-making techniques, leads to the existence of different kinds of secondary metallurgical slags such as dusts, sludges, millscale (Adolfsson, 2011).

3.3.2 Stainless steel slag characterisation

3.3.2.1 Composition

Stainless steel is composted of stainless steel slag (SSS) which has a grain size of d>100um and stainless steel dust with d<100um, with 70-90% being smaller than 5um and a large fraction even below 1um (Li & Tsai, 1993; Wu & Themelis, 1993; Nolasco-Sobrinho et al., 2003). In comparison to regular steel slag, stainless steel slag (SSS) in general has a much lower Fe content, a lower content of MgO, more SiO_2, high contents of Cr (2-5%) and some Ni (0.02-0.55%) (Shen & Forssberg, 2003; NineSigma, 2011).

The main components of stainless steel slags seem to be especially constituents of the form: CaO, SiO_2, MgO, Al_2O_3, FeO, MnO (Shen et al., 2004; Huaiwei & Xi, 2011; Lopez et al., 2004). The very fine fractions on the other hand (EAF and AOD dust, (oily) millscale) are relatively enriched with phases like: Fe_2O_3, Cr_2O_8, $FeCr_2O_4$, MnO and NiO (Shen et al., 2004;

Majuste & Mansure, 2008). An overview of the major components in EAF and AOD slag found in several studies is presented in Table 3.4 and Table 3.5. While Cr and Fe occur mainly in the form of oxides, Mo and Ni are mostly present in the form of metals (Majuste & Mansur, 2009). The main mineralogical composition is similar to that of regular slag: dicalcium and tricalcium silicates, calcium aluminium silicates, calcium oxides and periclase (MgO), however SSS in addition contains Mg and Ni chromites (Shen & Forssberg, 2003). (Shen et al., 2004) listed the dominant mineral speciation of AOD and EAF slag as being composed of Ca–Mg–Al silicates, Ca–Mg oxides, Fe–(Cr–)Ni alloys and Fe–Cr oxides, or more specifically described by Adolfsson (2011) to contain the mineral phases: Ca_2SiO_4, merwinite ($Ca_3Mg(SiO_4)_2$), melilite ($(Ca,Na)_2(Al,Mg,Fe^{2+})[(Al,Si)SiO_7]$), Ca_3SiO_5, CaO, MgO, $Ca_2Fe_2O_7$ and $2(Ca_2AlFeO_5)$. From the above it can already be concluded that the composition of these stainless steel slags is very complex, with the many different mineral species being indicated by XRD analysis (Lopez et al., 1997; Shen et al., 2004). The exact composition depends on the steel grade (kind of steel), the raw input materials, the exact production process (different techniques are in use as described in 3.3.1), the cooling conditions of the slag, and the fraction considered (Rao, 2006).

The frequent presence of magnetite (Fe_3O_4) and iron disilicate ($FeSi_2$), may be explained by their use as reducing agents in the AOD-L converter for the refinement process (Majuste & Mansur, 2009).

It appears that AOD contains approximately double the amount of Ni present in EAF while for Cr this is the other way around (Shen & Forssberg, 2004). Moreover, it was found by Shen et al. (2004), that the content of Ni and Cr for very fine fractions (20um) of AOD dust was lower than for the coarser dust fractions (300um) whereas for EAF the distribution was equal from 20 to 300 um (Shen & Forssberg, 2004). In general, fine slag fractions are relatively richer in heavy metals compared to the coarser slag fractions. However, recovery of the valuable elements from these fractions is complex. In line with this, Stefanova et al. (2012) found that the highest Zn content was present in the finest fraction. Valuable metals such as Fe, Cr and Ni are mainly contained in phases such as magnetite, chromite, Fe–(Cr–)Ni alloys and in stainless steel ($Cr_{0.19}Fe_{0.7}Ni_{0.11}$) residue (Shen et al., 2004). The metals from these alloys seem to be the most easy to be recovered.

Table 3.4: Main components in EAF slag according to various authors (Own elaboration)

Phase	EAF Slag			EAF dust
	Shen&Forssberg (2003)	Ye et al. (2003)	Adolfsson (2011)	Shen et al. (2004)
1	CaO	CaO	$Ca_3Mg(SiO_4)_2$	Fe_2O_3
2	SiO_2	SiO_2	$(Fe,Mg)_2SiO_4$	Cr_2O_8
3	MgO	MgO	Ca_3SiO_5	MnO
4	Cr	Cr_2O_3	$Ca_2Fe_2O_7$	NiO
5	MnO	MnO	$2(Ca_2AlFeO_5)$	Zn (volatile)
6	Al_2O_3	Al_2O_3	Ca_2SiO_4	

Note: Shen et al. (2004) found a similar composition for EAF dust and other secondary metallurgical dusts.

Table 3.5: Main components in AOD according to various authors (Own elaboration)

Phase	AOD slag				AOD dust	
	Shen& Forssberg (2003)	Adolfsson (2011)	Lopez et al. (1997)	Ye et al. (2003)	Stefanova et al. (2012)	Majuste&Mansur (2008; 2012)
1	CaO	Ca_2SiO_4	CaO	CaO	$FeCr_2O_4$	$FeCr_2O_4$
2	SiO_2	$Ca_3Mg(SiO_4)_2$	SiO_2	SiO_2	$MgFe_2O_4$	Fe_3O_4
3	MgO	Ca_3SiO_5	MgO	MgO	Fe_3O_4	$CaCO_3$
4	Al_2O_3	CaO	Al_2O_3	Al_2O_3	ZnO	$FeSi_2$
5	Fe	MgO	Cr	F	CaO	FeO
6	Cr		Fe	Cr_2O_3	$CaCO_3$	Fe

The composition of stainless steel slag may vary substantially. In order to give an indication on the range of values which may be expected (focussing on AOD and EAF), Table 3.6 was developed, which gives a composite image of the mineralogical composition (wt%) from Ye et al. (2003); Sanna et al. (2012); Zhang & Hong (2011); Lopez et al. (1997); Shen & Forssberg (2003) and Shen et al. (2003). For some relevant metals, also their total concentration (of all phases they are present in) was displayed. It should be kept in mind that this are reference values which may differ significantly per slag. In addition these values are representative for the whole bulk volume, not a certain fraction.

Table 3.6: Range of values (wt%) common for the different phases in stainless steel slag (Own elaboration).

CaO	SiO$_2$	Al$_2$O$_3$	MgO	MnO	Cr$_2$O$_3$	FeO	F	V$_2$O$_5$
40-61	26-34	1.7-9.7	3.7-7.3	1-2.6	0.8-2.9	1-1.2	0.6-2.6	0.1-1.3

Fe$_2$O$_3$	Na$_2$O	K$_2$O	TiO$_2$	P$_2$O$_5$	NiO	MoO$_3$	Fe$_{Tot}$	Cr$_{Tot}$
0.21	0.05-0.2	0.05-0.15	0.16-1	0.01-0.02	$\leq$0.01	<0.01	1.7-2	1.7-4.5

Ti	Cu	Ni$_{Tot}$	Mo$_{Tot}$	Zn	Pb	Cd		
0.1-0.7	0.05-0.1	0.2-0.5	0.01-0.04	0.01-0.03	0.005-0.05	<0.005		

The presence of a generally high fraction of reactive species such as free lime, periclase and other oxides, makes the material particularly suitable for carbonation. This is also reflected by its high specific surface area with a value of about 4.29 m²/g (Shen et al., 2004).

3.3.2.2 Leaching behavior

Due to the fact that the concentration of heavy metals is higher in stainless steel slags than in regular slags, it is sometimes classified as a potentially toxic waste. This is caused by the fact that part of these hazardous compounds may end up in the environment, polluting soils and/or water resources through leaching. The most toxic component prone to leaching is chromium (ICDA, 2007). An assessment of the leaching properties of the material is therefore necessary, of which 2 examples are shown in Table 3.7 and Table 3.8. These were performed according to the TCLP (Toxicity Characteristic Leaching Procedure). A leaching test, performed on SSS from a Canadian plant however revealed much higher concentrations in the leachate for Cr, Zn and Ni (Table 3.9).

Table 3.7: Leachate (mg/l) of AOD slag against the detection limits (Lopez et al., 1997).

	Element						
	Cr$_{Tot}$	**Pb**	**Cd**	**Zn**	**Ni**	**Cu**	**Hg**
Content	**1.0**	**<0.5**	**<0.1**	**-**	**<0.5**	**<0.5**	**-**
Standard	**<5**	**<5**	**<1**	**<10**	**<10**	**<10**	**<0.2**

Table 3.8: Leachate (mg/l) of AOD and EAF slag (Zhang et al., 2008; ICDA, 2007)

	Element						
	Cr$_{Tot}$	**Pb**	**Cd**	**Zn**	**Ni**	**Cu**	**Hg**
EAF	**0.098±0.011**	-	-	-	-	-	**<0.001**
AOD	**0.170±0.009**	-	-	-	-	-	**<0.001**
Standard	**<5**	**<5**	**<1**	**<10**	**<10**	**<10**	**<0.2**

Table 3.9: Leachate results (mg/l) of SSS dust (Laforest & Duchesne, 2006).

	Element						
	Cr_{Tot}	Pb	Cd	Zn	Ni	Cu	Hg
Content	9.7	0.4	-	93.9	2.3	-	-
Standard	<5	<5	<1	<10	<10	<10	<0.2

It can be seen from these tables that the standard values often were not exceeded and thus the leaching of hazardous elements was considered to be minimal (the values indicated by '-' were below the detection limit). The stainless steel dust in contrary (Table 3.9), has higher concentrations of some heavy metals; even exceeding the 'Toxicity Characteristic Regulatory Level' values. Applying the TCLP test, even higher values were found for Cr (14%) by Majuste & Mansur (2008) (Similar results were found according to research of Proctor et al., 2000; Laforest and Duchesne, 2006; Tang et al., 2008). This implies that stainless steel dust should be classified as being potentially hazardous whereas risks associated with the coarser slag fractions are lower (Zhang & Hong, 2011).

Generally, the formed leachate will have alkaline pH values when performed with ultrapure water alone (or increased pH values when acid was added prior to the test), due to dissolution and the release of *e.g.* Ca. Under the former conditions only small amounts of slag dissolve (<1%) whereas under more acidic conditions this amount can significantly be increased (adding 1M HCl led to the dissolution up to 31% for fine slag dust) (Shen et al., 2004). This increased dissolution (due to HCl addition) led to an increased concentration of Ca, Mg, Mn, Si, Na, Ni, K, (Fe) (high to low) but reduced concentrations of Al and Cr.

3.3.3 SSS Carbonisation experiments

As discussed in the previous paragraph, stainless steel slag contains a significant fraction of reactive phases, depending on the exact type of slag. This makes the material a good candidate for ACT, especially considering that leaching of the material may in some cases cause heavy metal concentration beyond the allowed limits. According to Johnson (2000), stainless steel slags may be among the most effectively carbonated waste materials. ACT has been claimed to be an effective remedy for reducing the metal concentrations in the leachate, rendering the material non-hazardous after treatment. Despite the fact that the amount of research studying carbonation of SSS is limited, some examples of carbonation experiments on stainless steel slag using different methods are described further on.

3.3.3.1 Batch

Baciocchi et al. (2009; 2010;2011) studied the process of stainless steel slag carbonation in a temperature-controlled batch system for the reaction of EAF slag, an AOD-EAF mix and pure AOD. While the AOD seemed to have a fairly homogeneous size distribution, the mix had a rather heterogeneous distribution. Therefore the latter was sieved and divided in distinct size classes. All materials were relatively Ca-rich (>40 % wt.), as agreed upon by e.g. Ye et al. (2003); Sanna et al. (2012); Johnson et al. (2003) (see para. 3.3.2.1) due to the presence of Ca-phases such as $CaSiO_4$ and CaF_2. For the EAF-AOD mix the Ca and Mg content decreased but Fe, Cr, Al, Mn and V content increased with particle size. The AOD slag displayed lower concentrations for all just-mentioned elements except Ca (Table 3.10). Dominant in the material composition was the presence of crystalline oxides and silicate phases. The accelerated carbonation tests were carried out on the <0.105mm fraction in a pressurised stainless steel reactor inside of a (temperature-controlled) water bath. The conditions resulting in the highest CO_2-uptakes were: 50°C, 3bar and 10bar CO_2 pressure for EAF and AOD respectively, and a L/S of 0.4. Resulting uptakes were 130 and 300 g CO_2/kg slag respectively for the AOD-EAF mix (finest fraction) and the AOD slag, whilst the uptake for EAF was intermediate with 180 g CO_2/kg (up to 50% Ca-conversion). The most influential parameters for the carbonation process seemed to be temperature (increases in carbonation-extent with temperature from 30-50°C) and grain size (larger uptake for finer fraction).

Applying the slurry-phase process to EAF carbonation, even when adopting more energy-intensive operating conditions, did not improve the CO_2-uptake kinetics and conversion yield in comparison to the wet treatment. The results matched very closely to findings from Huijgen et al. (2005) where applying the direct slurry-phase route, resulted in uptake values up to 180 g/kg, or a Ca-conversion of 74% (30 min reaction time, 19 bar CO_2, 100°C, finely milled). The same uptake of 180g/kg (after 1h) was found by Johnson et al. (2003), where the carbonation of SSS was assessed. The best operating conditions in the latter research were reported to be achieved under ambient temperature, 3 bar CO_2, and L/S= 0.125.

Carbonation resulted in a decrease of the amount of Ca- and Mg oxides, a decrease in silicate phases (Ca_2SiO_4) and an increase in the amount of $CaCO_3$. The effect of carbonation on the leaching behaviour was inspected by comparing the results of the untreated and treated material (AOD-EAF mix) leaching tests. It was found that for the untreated material leachate,

the Ca, Mg and Cr concentrations were significantly higher for finer size fractions. Treatment caused the leachate concentrations of Ca and Cr to respectively decrease and increase.

Element	Mix class A	Mix class B	Mix class C	Mix class D	AOD
Al	26.0400	22.0800	17.9867	16.8400	6.8533
As	0.0035	0.0031	0.0041	0.0062	0.0174
Ca	432.3333	402.0000	445.3333	500.3333	403.3333
Cd	0.0517	0.0018	0.0143	0.0035	0.0200
Cr	42.4667	34.0667	29.9333	30.4667	0.3987
Cu	0.2280	0.2347	0.1453	0.1667	0.5280
Fe	59.7333	53.0000	43.6000	43.2667	0.6160
K	0.3107	0.3347	0.3133	0.3560	0.1133
Mg	22.1667	26.4667	29.9000	44.6000	14.3867
Mn	10.4533	8.7733	7.8667	7.6000	0.3293
Mo	0.2307	0.1867	0.1680	0.2253	<0.002
Na	1.9600	1.8933	1.7387	1.5413	0.7267
Ni	0.3760	0.7507	0.4587	0.4613	0.0587
Pb	0.0760	0.0773	0.0580	0.1200	0.0679
Sb	0.0015	0.0015	0.0012	0.0013	0.0017
V	1.5200	1.1333	0.8133	0.9200	0.0016
Zn	0.1121	0.1008	0.1284	0.1441	0.1184

Table 3.10: Elemental composition (g/kg dry weight) of 4 classes of EAF-AOD mix and AOD slag (Baciocchi et al., 2010b).

Note: 2-0.425 mm (class A); 0.425-0.177 mm (class B); 0.177-0.105 mm (class C); < 0.105 mm (class D).

3.3.3.2 Column

No study on SSS carbonation was found with use of a (non-pressurized) column set-up. This will be performed in the current study however (Chapter 4).

3.3.3.3 In-situ

Generally, the potential threat stainless steel slags may pose for the environment is due to dissolution and subsequent leaching of toxic heavy metals from the solid material into the underlying or surrounding soil. There, the presence of OM may temporarily cause adsorption of these contaminants, but when the retention capacity is exceeded, it may eventually end up in the groundwater (which is potential drinking water or used for agriculture) (ICDA, 2007). Despite the lab research that has been performed, it is be essential to execute these tests on a large field-scale, preferentially in-situ, to assess whether techniques yield the same results as would be expected from the theoretical point of view.

There are no reports yet of research done on in-situ carbonation of stainless steel slags. The only field works that have been performed took place by excavation and subsequent treatment of the material on pilot scale, thus ex-situ (see para. 3.2.3.4).

3.3.4 Recycling of stainless steel slag

Because of the high content of valuable metals present in these SSS, they are generally reprocessed. The coarser fractions (mean diameter 100 um; 40 wt%) are easily reusable as input for the steelmaking process, following compaction in brickettes (Majuste, 2007). The finer fraction (dusts, mean diameter 1 um; 60 wt%) in contrary, is less readily reusable since it does not easily form aggregates. Therefore the latter are often landfilled, or are processed in separate treatment plants to increase the grain size before being suitable for internal recycling (Palencia et al., 1999; Majuste, 2007). This treatment can proceed through pyrometallurgical (most common), hydrometallurgical, or combined processes as explained in para. 3.3.4 (Orhan, 2005; Rao, 2006). However, this recovery is very energy-intensive and complicated due to the fact that the metals are bound in complexes (mostly oxides) (Xia & Pickles, 1999; Ma & GarbersCraig, 2006).

As discussed in para. 3.3.2.1, SSS contains a relatively low content of heavy metals such as Cr and Ni, albeit higher than in regular slags. However, this needs to be seen in perspective: data from DNPM (2007), claims a Ni-concentration of about 1-2% (wt/wt) Ni in raw mined brazilian Ni ores while the values in SSS generally are in the order of 0.5 wt% or higher. In the case of Fe, the content in steel slag dust may be even higher than for certain iron ores (Zhang & Hong, 2011). However, not only the absolute metal content of the slag is of importance; the possibilities of recovery strongly depend upon the structure of composite grains. When for example alloy particles are present in a silicate matrix, the former may be recovered through the application of processing techniques like crushing, prior to recovery. However recovery often becomes less profitable as the grains contain more impurities and have a more heterogeneous composition (Shen et al., 2004). An example of this is the study by Huiting & Forssberg (2004), where alloy particles appeared to be present inside the grains of AOD slag, with the concentration of Cr and Ni being highest for the finest fractions (dust). In these alloy particles, Fe; Cr; and Ni were present in an almost pure phase which seemed to be easily recoverable by crushing and gravimetric separation. On the other hand, Majuste & Mansur (2009) examined the possibility to achieve Ni- and Cr recovery from AOD sludge

using H_2SO_4 and HCl in a 2-step process through: a leaching step to recover Fe and leave the solid enriched in Ni and Cr, followed by a high-pressure-leaching step for Ni- and Cr recovery. Use of HCl resulted in the largest selectivity for Fe (70 °C, HCl 12% (v/v)), leaching 50% (w/w) of the initial Fe-content and causing Cr to become more concentrated in the solid phase (to 110%, w/w). Unfortunately, also 40% (w/w) Ni leached during the first step, making the process less interesting (even more separation steps would be needed).

In line with this, recovery of Zn or other valuable metals from AOD dust through the use of NaOH as a solvent was examined in Stefanova et al. (2012; 2013). Results indicated that leaching was dependent upon the amount of NaOH added, temperature, stirring rate, and L/S. The maximum Zn-extraction achieved was 50-80%, after 2 hours at high temperature (95°C) and stirring rate, applying a strong (8M) NaOH solution and a low L/S ratio. Also significant amounts of Mo leached but no other metals, indicating that NaOH is a strongly selective solvent, suitable for use in the recovery process.

3.3.5   Reuse of stainless steel slag

AOD slag is prone to fall apart into a powder upon cooling, and aside from internal recycling, there are barely options known for reuse. However, the addition of boron to the slag before solidification may promote the formation of a crystalline solid, transforming the slag into aggregate-like material and making it a possible candidate for reuse in the applications listed in para. 3.3.5 (Bullock, n.d.). The other kinds of SSS may be used for these applications as well regarding their similar physical properties. What concerns the fine SSS powders, next to internal recycling (which is limited due to their poor capability to aggregate), in most cases they are being landfilled because there are currently no further practical applications (Domínguez et al., 2010).

3.3.5.1 CO_2-uptake by iron, steel and stainless steel slags

The effective maximum CO_2-uptakes for direct carbonation of stainless steel slag (values obtained through direct-carbonation experiments) are estimated to be in the order of 160-300g/kg for AOD slag (Sanna et al., 2012; Santos et al., 2013;2013; Baciocchi et al., 2010a) and in the order of 150-180 g/kg for EAF slag (Baciocchi et al., 2010a; 2012, Johnson, 2000;2003). For the non-stainless slags uptakes are in the order of 70-230 g/kg (mean is 150

g/kg) (Eloneva et al., 2008a) for BF slag (value obtained through indirect carbonation experiment) and about 150 to 210 g/kg for respectively EAF and BOF slag (Sanna et al., 2012).

The annual global iron slag output is estimated at about 260-310 million tonnes (mean is 285 Mt), and steel slag output at 130-210 million tonnes (mean is 170 Mt) (U.S. Geological Survey 2012). The stainless steel slag production is estimated at about 9 million tonnes (NineSigma, 2011). Assuming that the fraction of slag being carbonated at present is minimal and that all this material could be treated using accelerated in-situ carbonation before the reuse or landfilling; the potential slag CO_2-storage capacity can be calculated as follows:

Potential effective CO_2-uptake of iron and steelmaking slags=
$(285*10^9 \text{ kg} * 150 \text{ g/kg}) + (170*10^9 \text{ kg} *0.3*150 \text{ g/kg}) +$
$(170*10^9 \text{ kg} *0.7*210 \text{ g/kg}) + (9*10^9 \text{ kg} * 210 \text{g/kg}) =$
$7.728 * 10^{13} \text{ g} = 77.3 \text{ MtCO}_2/\text{yr}.$ (3.8)

In the calculation following values for CO_2-uptake were used (composite of the values mentioned before): 230 g/kg for BF slag, 190 g/kg for steel slag, and 210 g/kg for stainless steel slag. Note that the value for steel slag uptake was calculated assuming that the output of BOF and EAF slag respectively are about 70% and 30% of the total steel slag output according to data from the BIR (2013).

This value of 77.3 $MtCO_2$ uptake/yr is significant, but purely hypothetical since the implementation of worldwide CCS (to deliver the CO_2), as well as the implementation of large-scale ACT of iron and steelmaking slags presently is too costly to be performed.

4 MATERIALS AND METHODS

4.1 Materials

4.1.1 AOD slag

4.1.1.1 Site description and sampling method

The slag examined in this study was collected at an Italian steel production plant. The material was collected by the steel-making plant staff, and was taken directly out of the ladle cattle at the outlet of the argon decarburization unit and was thus claimed to be AOD slag. The complete test sample had a weight of 5.88 kg and was stored in an air-tight plastic container from the time of sampling until the characterisation of the material a few months later. The material had a significant fraction of loose aggregates, which easily disintegrated upon disturbance. The colour of the material was dark greyish and became light grey upon drying.

4.2 Methods

4.2.1 Characterization

4.2.1.1 Sample moisture

The initial moisture of the sample was determined by oven-drying a known amount of material at 105°C for 24 hours. The material was put in 4 aluminium cups of which the tare and brut weight (cup + moist material) was recorded. After 24 hours, the material was taken out of the oven, allowed to cool down in the desiccator and weighted. From this the initial moisture of the field sample was calculated. This was done by the formula:

$$\text{Moisture}_i\ (\%) = \frac{w_i - w_f}{w_f} * 100 \tag{4.1}$$

in which w_i and w_f respectively are the initial (moist) and the final weight (dry).

4.2.1.2 **Particle size distribution**

To determine the particle size distribution of the material, first a portion of it was selected applying the "quartering method" (Sampling Method MD2, n.d.). by which a portion is taken from the original sample. This was done by spreading and homogenizing the whole test sample on a flat surface with a shovel in an oval shape and taking one quarter of it. This procedure was repeated until the required sample size was obtained, and care was taken not too lose dust from the sample. This material was air-dried for 48 hours until dry, *i.e.* when a portion was put in the oven, the net weight of the material was unchanged.

Subsequently, the material was sieved according to the "ASTM D422" method using several sieves with mesh sizes of: 10, 4, 2, 1.18, 1, 0.84; 0.425; 0.177; 0.125; 0.105 and 0.075 mm. Special attention was paid to the finest fractions, in line with the Italian legislation that states that most contamination in slags and hazardous materials is contained in the fractions below 2 mm (Capobianco, 2013). The sieving took place using a Retsch automatic sieve device type "AS 200" setting the operation interval at 15seconds shaking and 5seconds rest, an amplitude of 0.4-1 mm/g and total duration of 2-5minutes for respectively coarse and fine fractions. The material was divided into size classes with the class upper bound being the mesh size it passed and the class lower bound being the mesh size it did not pass. Finally, the particle size distribution curve was formed by plotting on the vertical axis the material passing (cumulative) (%) and on the horizontal axis the sieve size (mm). Three fractions were chosen to do the characterisation upon: a coarse (0.84-2mm), an intermediate (0.177-0.84mm) and a fine (<0.177mm) fraction.

4.2.1.3 **Material composition**

4.2.1.3.1 Alkaline fusion- Elemental composition

To understand the environmental behaviour of the examined material, it is essential to determine its elemental composition. The elemental composition of the solid material can be determined by alkaline fusion and subsequent 'Inductively Coupled Plasma Optical Emission Spectrometry' (ICP-OES) analysis of the obtained solution. Alkaline fusion is a technique that converts the solid material at very high temperatures into a glassy inorganic substance, which can subsequently be dissolved by acid to bring all elements in solution. The advantage of this technique is that the resulting glassy matrix is very homogeneous, concentrated and

does not require the use of large amounts of acid. The alkaline fusion was performed for the different fractions of interest and for each one, the experiment was performed in triplicate.

Each platinum crucible (cup) was filled with 0.5 g of AOD, 3 g of lithium tetraborate ($B_4Li_2O_7$) and was thoroughly mixed with a glass stick. Then another 0.5 g of lithium tetraborate was added on top without mixing, spread and slightly compacted until it had a smooth surface, covering the underlying mixture. After this the crucibles were put in a pre-heated stove at 500°C and the temperature was raised to 1050°C. From the moment when the latter temperature was reached, the experiment started and from then on the samples remained in the stove for 2 hours. This high temperature is needed to ensure to dissolution of the silicates present in the material. When the heating phase ended, the crucibles were removed from the stove with a pair of tongs, cooled down in a bucket of cold water and the exterior of the crucible was washed with an HNO_3 acid solution (1:10). Subsequently each crucible was put in a separate beaker filled with HNO_3 and a magnetic stir was inserted to dissolve the glassy matrix. The system was heated from below to a temperature of 50-70°C to speed up the dissolution process of the matrix and if needed, the acid was replaced to further promote dissolution. After complete dissolution of the material, the obtained solution inside of each beaker was filtrated with paper filters of the type 'rapido Whatman no. 41' (d = 20 µm) and brought to a volume of 200 ml by rinsing the beaker and crucibles several times with acid in order to dissolve all present glassy material. After cooling down, some more HNO_3 was added to adjust for volume reduction. The obtained acidic solution was subsequently analysed by ICP analysis, pure and as 1:100 dilution.

In order to calculate the effective concentration of analysed elements in the starting material from the ICP-OES results, the dilutions with acid during alkaline fusion (solution 1) and later with UP for ICP analysis (solution 2) had to be taken into account. The concentrations are calculated as mg element 'X' per kg of AOD as:

$$C_X \text{ (mg/kg)} = \frac{\frac{m_X (mg)}{V_{sol\ ICP\ (l)}} * Dilution\ ICP}{\frac{m_{AOD}\ (mg)}{V_{sol\ Alk\ F\ (l)}}} * 1000000 \tag{4.2}$$

In which X is a certain element. The numerator of the above-mentioned equation takes account for the dilutions made for ICP analysis by multiplying the obtained values (mg/l) with the dilution factor: 1:1 and 1:100. The denumerator is the ratio of the average mass of AOD used (for the triplicate samples) (mg) over the volume of the alkaline fusion solution (l), which was equal to 0,2 l.

4.2.1.3.2 XRD- Mineralogical composition

The mineralogical composition of the untreated as well as carbonated material was determined through powder X-ray diffraction analysis with Cu Kα- radiation. The apparatus used was a Philips Expert Pro diffractometer equipped with a copper tube operated at 40 kV and 40 mA, with an angular step of 0.02 held for 2 s with 2θ spanning from 5 to 85°. The material was milled to d<0.125 mm prior to analysis.

The technique of powder XRD makes it possible to analyse crystallographic structures, to estimate the quantity of different phases present in multi-phase mixtures.

The incoming X-rays are scattered by the atoms making up the crystal lattice of a mineral: the part not being scattered may pass to the next layer of the lattice and so on. When the refracted rays from multiple layers are in phase, constructive interference will create an intensity peak (Connolly, 2007) As the angle of the incident X-rays is varied, the interaction of X-rays with crystalline material creates a diffraction pattern in which the intensity of the signal is plotted against the angle of the detector (2θ). This pattern is unique for each mineral and therefore acts like some kind of fingerprint. In addition it may provide a quantitative indication, as the area under the diffractogram peak is related to the amount of a phase (Connolly, 2007).

As can be seen in Figure 4.1, the X-ray source sends out the X-rays to the sample at a certain angle θ, the sample scatters the rays in a certain pattern and intensity according to the mineralogy of the sample, and is finally read by the detector which is positioned 2θ above the path of the incident rays.
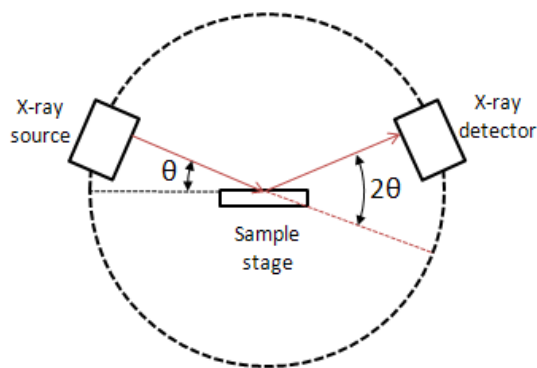
Figure 4.1: Simplified XRD setup (US Davis, n.d.)

4.2.1.3.3 ICP-OES

Elemental analysis of acidified eluates or aqueous solutions was done by 'inductively coupled plasma optical emission spectroscopy' (ICP-OES). The apparatus used was a VARIAN 710-ES device. A wide range of elements can be detected with this technique, except for H,C,O,N, and halogens (F, Cl, Br, I, At).

This technique was developed to analyze inorganic (trace) elements present in aqueous solutions. As the argon gas flows through a quartz torch, embedded in an energized radio frequency coil, the electrons are stripped from the energized argon atoms and result in plasma formation. As can be seen from Figure 4.2, the sample solution is sprayed as a very fine mist (aerosol) into the inductively coupled argon plasma (up to 10,000°C) what causes the sample to become gaseous, to atomize, and become thermally excited. Further excitation converts part of the atoms to excited ions, both of which may emit photons to return to their ground state. The wavelength of these photons is element-specific and the total number of photons emitted is a measure for the element's concentration. Therefore the elemental composition of the sample and their concentration may be identified by the emission spectrometer (EAG, 2013; Hou & Jones, 2000).

As illustrated by Figure 4.2, part of the emitted photons are collected and focussed by an optical lens, and internally this image is send (through use of multiple mirrors) to a grating (wavelength selection) device, the exiting wavelength(s) are send to a photodetector and is processed, converted to an electrical signal, and finally displayed (Hou & Jones, 2000).

Figure 4.2: Basic ICP-OES concept (Colorado Mountain College, 2013)

4.2.1.3.4 Solid Inorganic carbon

The solid inorganic carbon content (SICC) of the AOD slag was determined prior to carbonation for the 3 fractions (<0.177mm: fine, 0.177-0.84mm: intermediate, and 0.84-2mm: coarse) selected of the untreated material, as well as for the original, heterogeneous field sample to indicate the $CaCO_3$ content before carbonation. Doing so makes it possible to calculate the absolute amount of carbonation that occurred through the carbonation experiments.
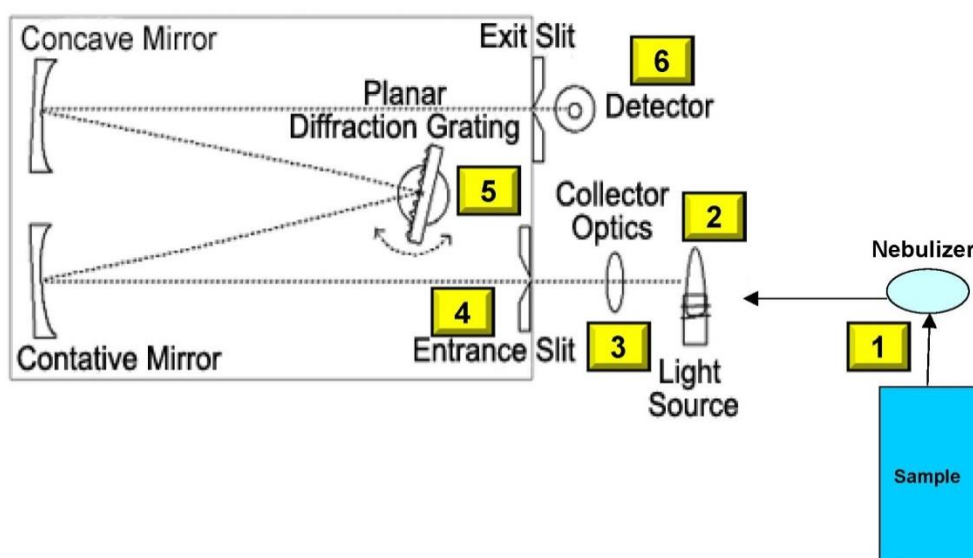
The SICC material was determined through use of the Solid Sample Module 'SSM-5000A' from a 'TOC-V CPH' analyser device of Shimadzu. Before analysis, the material of the intermediate or coarse fractions was milled for 1minute in a steel grinding mill using an electronic milling device (RS200 of Retsch) at 700 rpm for 1 minute. After this, the grinded material was removed from the mill with the use of a small brush, sieved manually through a sieve with mesh size of 0.177mm and temporarily stored in polyethylene bottles of 20 ml. Only material with a grain size below 0.177 mm could be analysed in the TIC (total inorganic carbon) device. The mass of material retained by the 0.177mm sieve was however negligible. Subsequently the TIC analysis (according to standard EN 13137) was performed with 190-200mg of material contained in a porcelain sample boat, inserting the sample in the device and after waiting 3 minutes, 0.7-0.9 ml of orthophosphoric acid (acid:UP= 1:2) was injected into the sample boat just prior to insertion in the stove at 200°C until the measurement was complete. This process was repeated 2-3 times per sample (depending on the deviation between the values) to reduce the measurement error in the value.

The addition of the orthophosphoric acid to the material, together with the high temperature (200°C) in the combustion furnace which is supplied with purified air, leads to the transformation of inorganic carbon into gaseous CO_2 (and other evolving gases). The escaping gas is cooled, dehumidified and subsequently analysed with the non-dispersive infrared detector. Through the unique infrared absorption properties of each gas, the amount of CO_2 released may be identified. In this way, and through use of the calibration formula (that is created when the instrument is calibrated with a substance –sodium carbonate- with known IC-content) the IC content is calculated (Shimadzu, n.d. a).

From the obtained IC value, the initial CO_2-content of the material can be calculated by:

$$CO_2\text{-content} = \frac{IC}{M_C} * M_{CO_2} \qquad\qquad (4.3)$$

in which IC is the inorganic mass fraction (%), M_C and M_{CO2} are respectively the molecular weight of carbon and CO_2. The effective CO_2-uptake of the AOD sample during the carbonation experiment can be calculated by taking account of the initial $CaCO_3$ content as:

$$CO_2\text{-uptake (\%)} = \frac{(CO_{2f} - CO_{2i})}{100 - CO_{2f}} * 100 \tag{4.4}$$

with CO_{2i} and CO_{2f} being respectively the initial CO_2 content of the sample prior to reaction and the final CO_2 content of the carbonated sample after reaction.

Moreover, the $CaCO_3$ content was calculated from the CO_2-content given in eq. 4.3 by:

$$CaCO_3(\%) = \left(\frac{IC\ (\%)}{12}\right) * 100 \tag{4.5}$$

4.2.2 Environmental behaviour

4.2.2.1 Standard leaching test (EN 12457-2)

The leaching behaviour of a material is crucial to understand in what degree it is environmentally hazardous. Assessment of the leaching behaviour of solid wastes is required before one can proceed to landfilling or reuse, and the obtained values should comply with the national guidelines for allowed leaching concentrations. If a material leaches excessive quantities of toxic elements (with respect to the guideline values) then reuse or landfilling is not allowed, and special care should be taken to avoid contamination of groundwater and soil. The release of contaminants from the solid matrix at neutral pH was examined by subjecting the material (d<4mm) to a leaching test during 24 hours to reach the state of thermodynamic equilibrium with the solute, according to standard procedure EN 12457-2.

A new test sample was taken by the quarter-division method and the fraction with d>4mm was crushed according to the standard procedure. The test was performed in quadruple in high-density polyethylene (plastic) bottles at a L/S ratio of 10; each containing about 8g of AOD and 80ml of distilled water. The bottles were carefully sealed with parafilm tape and then locked in cylinders and placed on a bench top roller device (Wheaton) for 24h-during agitation. After this period, the samples were taken out and left to rest for 1hour in order to let suspended sediments settle down. After this, pH and temperature of the aqueous solution was measured by a 'Microprocessor pH Meter 213' of Hanna Instruments, and the leachate was filtrated manually through a 450 µm filter with use of a syringe and separated in 2 parts. One

part was acidified with a few drops of HNO_3 solution (1:10) for subsequent ICP-OES analysis while the other part was not, for subsequent determination of the concentration of soluble chlorides concentration (para. 4.2.2.1.1).

4.2.2.1.1 Soluble Chlorides determination

The concentration of soluble chlorides in the material was determined through a silver nitrate titration of the non-acidified leachate according to the standard method UNI 8520. The test proceeded as follows: the leachate was diluted with distilled water to a specific ratio (1:10 to 1:2) in which the volume of the initial leachate was accurately known and 2drops of the chemical indicator potassium chromate (K_2CrO_4) was added per 10ml of solution. Then the titration slowly took place, adding $AgNO_3$ to the solution while being mixed with a mechanical stir. The principle of this method is that the silver nitrate reacts with the dissolved chloride ions to form AgCl until all dissolved chloride is depleted. So at the moment when all the dissolved Cl^- has reacted, the excess silver nitrate added will react with the indicator to form silver chromate (Ag_2CrO_4) which has a brownish red colour and this reaction suddenly changes the solutions colour. At this point the titration is ceased, and the added volume of silver nitrate is recorded. The silver nitrate solution had a concentration of approximately 0.04629mol/l. The Cl-concentration ($\frac{mg}{l}$) of the original leachate was calculated with use of the formula:

$$C_{Cl^-} = \frac{V_{AGNO_3} * c_{AgNO_3} * M_{Cl}}{V_{sample}} * 1000 \qquad (4.6)$$

In which V_{AGNO3} is the volume of silver nitrate added, c_{AGNO3} is the molar concentration of the silver nitrate solution added, M_{Cl} is the molecular weight of Cl and V_{sample} is the volume of the tested sample.

4.2.2.1.2 Other elements determination

The acidified leachate was analysed pure as well as diluted with ultrapure (UP) water to the dilutions 1:1; 1:10; 1:100. The mentioned dilutions were made because some measured values (mg/l) were above the upper constraint of the used standards. However, when a measured value was less than 10% exceeding the highest standard value or less than 10% below the lowest standard value, it was accepted. Measurements below the detection limit of the ICP-OES analysis device (Table) were excluded in any case.

In order to calculate the concentration of analysed elements in the leachate from the ICP-OES results, dilutions (if made) have to be accounted for. The concentrations are calculated as mg element 'X' per litre of leachate as:

$$\rho_{leach} = \rho_{ICP} * dilution\ factor \tag{4.7}$$

in which $\rho_{leach}\ and\ \rho_{ICP}$ are respectively: the mass concentration of a specific element 'X' in the leachate (mg/l), and the mass concentration of element 'X' as detected by ICP-OES.

4.2.2.2 Acid neutralization capacity

Acid neutralization capacity (ANC) is a measure of a substances ability to neutralize acidic inputs. The European Union has set landfilling restrictions (EU Landfill Directive 1999/31/EC) that require information on the characterization of waste, such as its (long-term) environmental behavior. One part of this is to assess the acid neutralization capacity (ANC) of waste: it reveals the behavior of the material and its potential effect on (or interaction with) other materials present. According to the guidelines set, the overall landfill waste body needs to attain and maintain a near-neutral or slightly alkaline pH (7-9) (the solubility of most heavy metals is at minimum in this pH range) to evade adverse long-term effects on the environment. The latter include: increased leaching of metals and/or organic components from the stored waste, and an increased erosion rate of the landfill lining membrane which both may occur due to very low or high pH-values in waste leachate. These effects may be prevented due to an adequate acid neutralization capacity of the stored waste (Wahlström et al., 2009).

Typically, the ANC for a sample containing buffering species (carbonate) is composed of the different carbonate species:

$$ANC = [HCO_3^-] + 2[CO_3^{-2}] + [OH^-] - [H^+] \tag{4.8}$$

However, it has been stated that waste ashes and steel slags also contain significant amounts of amorphous phases that may contribute to the buffering capacity but from which the effects are hardly monitored through short-time lab testing (Wahlström et al., 2009).

The ANC test has been performed on the intermediate fraction (0,177-0,84mm) of the AOD material. The procedure was as follows:

- 4,0 grams of AOD was put in falcon tubes;
- The required amount of UP water and HNO_3 acid was added -with the total volume equalling 40ml- and the tubes were sealed;

- The samples were placed on the rolling device for 48 hours;
- The samples were left to rest 1 hour for the suspended material to settle;
- The pH and temperature were recorded;
- The samples were filtrated using 450 um filters, the samples with a higher acid content had a slurry-like consistency and were placed in the centrifuge prior to filtration;
- The most acidified sample were filtrated through vacuum filtration with coarse filter paper;
- Subsequent ICP analysis of the samples.

The general ANC of the material was visualised by plotting the amount of acid added (in meq/g) on the x-axis versus the pH on the vertical axis. The acid volume was recalculated to meq/g by the following formula:

$$HNO_3 \left(\frac{meq}{g}\right) = \frac{V_{HNO3}}{m_{AOD}} * c_{HNO3} \tag{4.9}$$

In which V_{HNO3} is the volume of acid added (ml), m_{AOD} is the mass of slag used (g) and c_{HNO3} is the molarity of the used nitric acid, which was in this case 2 mol/l (or 2mmol/ml).

4.2.3 Carbonation experiments

4.2.3.1 Batch carbonation

The first phase of carbonation experiments were performed as preliminary batch experiments. The experimental set-up consisted of a sealed 150 ml stainless steel reactor in a water bath with temperature control ranging from 0-70°C. Initially, during cycle 1, the batch tests were performed on the fine fraction (<0.177 mm) in order to determine the maximum CO_2-uptake possible for the examined AOD slag. To reach this, carbonation was performed under conditions that were found to optimize CO_2-uptake in previous research by Baciocchi et al. (2010a) with the same experimental set-up and: a reactor temperature of 50°C, L/S ratio of 0.4 and a CO_2-pressure of 10bar.

The samples were contained in small (d=2cm) tin foil cups which were renewed after each experiment. The experiment was performed in triplicate, with each of the 3 cups being filled with approximately 1 g of AOD and then brought to the required L/S ratio by carefully dripping distilled water on the samples with a syringe while weighting on an electronic balance (accuracy 0.0001 g). Care was taken to wet the material as homogeneously possible. Swiftly after moisturizing, the samples were placed on a vertical rack one above another and

introduced into the reactor, at the bottom of which a NaCl-solution was placed in order to minimalize variations in humidity (constant at ~75%). After inserting the samples, the reactor was closed and sealed with teflon tape. The reactor was flushed thoroughly for 3 times with CO_2 to replace present ambient air, and the experiment was started after bringing the pressure to the desired value of 1 bar. Multiple experiments were performed in order to develop a kinetics curve for reaction times of 15 and 30 minutes, and 1, 2, 4, 8, 16 and 24 hours. During cycle 2, the same sequence of experiments was performed -under the same optimal conditions- but on the intermediate fraction $(0.177 - 0.84 mm)$, in a way to put the carbonation efficiency of the later column set-up (phase 2) in perspective. Finally in cycle 3, the whole reaction kinetics was determined –also for the intermediate fraction- but under more ambient conditions: 22°C, L/S ratio of 0.2 and 1 bar CO_2-pressure (the same conditions as during the column experiments: para. 4.2.3.2) to evaluate possible differences between the use of the different set-ups under identic conditions. An schematic overview of all performed experiments can be seen in Figure 4.3.

At the end of the reaction time, the CO_2-supply was stopped and the pressure inside was gradually reduced before taking the reactor out of the water to cool down. After approximately 5 minutes, the system was opened and the samples were taken out.
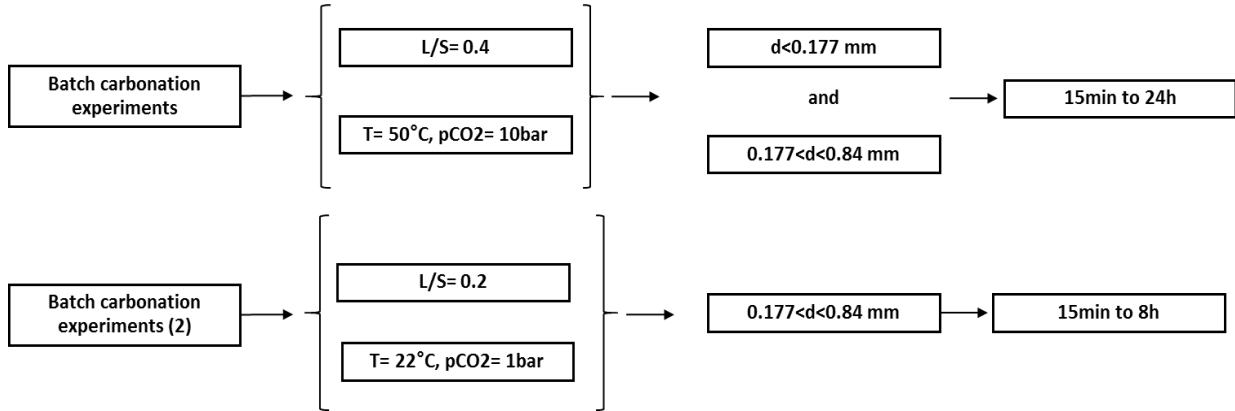
Figure 4.3: Overview of all batch experiments performed

4.2.3.2 Column carbonation

The second and main stage of the carbonation experiments was formed by column experiments to determine the extent of carbonation under conditions more suitable for application in the field: under ambient temperature (22-24°C) and 1bar of CO_2 (100%). The column tests were only carried out on the intermediate AOD fraction. This was based on the fact that the intermediate fraction constituted a relatively large mass fraction (37%) of the

total mass of the sample material. In fact, its mass fraction was significantly larger relatively to the fine and coarse fractions. In addition to this, this intermediate sized material was preferred to ensure a sufficiently large material porosity and permeability in order to sustain and maintain a good gas flow throughout the medium.

The setup of this experimental phase consisted of the following: a glass column of 16 cm height and 2 cm diameter to contain the reactive material (Figure 4.4). A flow meter was installed to control the flow rate of the injected CO_2 and was set at a value corresponding to about 10.4 ml/min. This CO_2-flow then passed through a bubbler filled with distilled water to wet the gas and promote the reactivity.
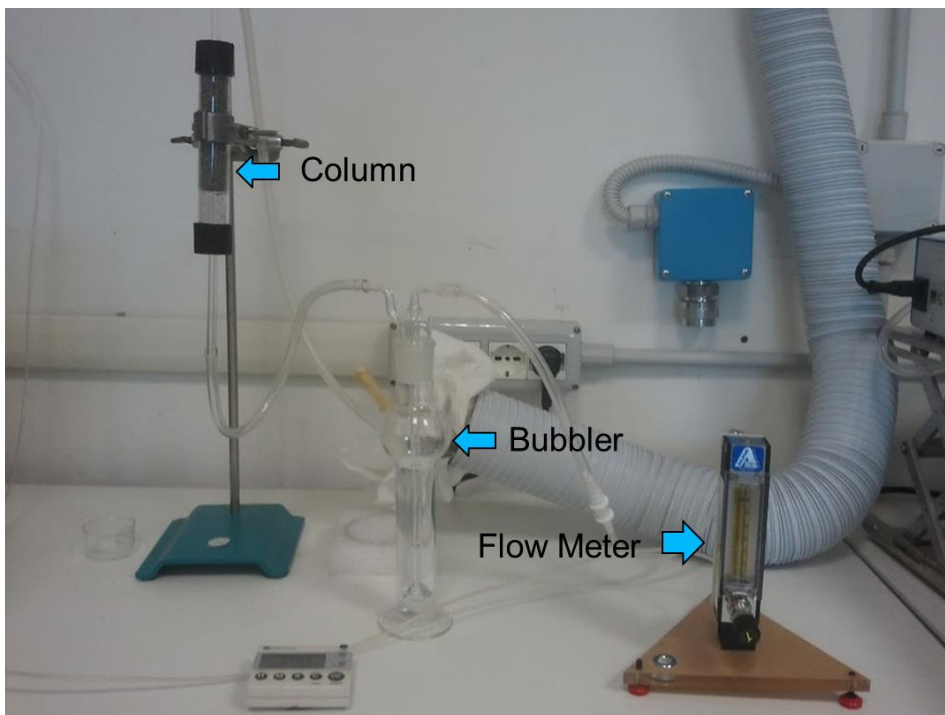
Figure 4.4: Column experiments setup.

The gas flowed from below upwards through the column with at the bottom of the column a layer of glass beads to ensure an homogeneous dispersal of the gas. On top of this, the material was inserted which was brought to a L/S ratio of 0.1 or 0.2 by mixing the dry material with the required amount of distilled water in a beaker until homogeneously wetted, and subsequently inserting it into the column (Figure 4.5). The material was slightly compacted at regular intervals (after inserting each 10 g) with a plastic tool to avoid the presence of preferential flow pathways. On the other hand, also some tests were performed - under similar conditions and with the same set-up-, but by using percolation instead of mixing

to wet the slag. In this case, water was added by dripping it on the material after it was inserted in the column (also after each addition of 10g).

Figure 4.5: Left: Beaker with approximately 40 grams of slag material being wetted with UP water up to the required L/S ratio on the digital balance, before mixing. Right: Detail of the column before the start of the experiment. With starting from below: one filter, a layer of glass beads, 2 filters, the wetted material, 1 filter.

These column experiments were performed with 20 and 40 grams of dry material, a L/S ratio of 0.1 and 0.2 each, and for a reaction time of 1, 2, 4, and 8 (only with 40g of dry material) hours each (Figure 4.6).
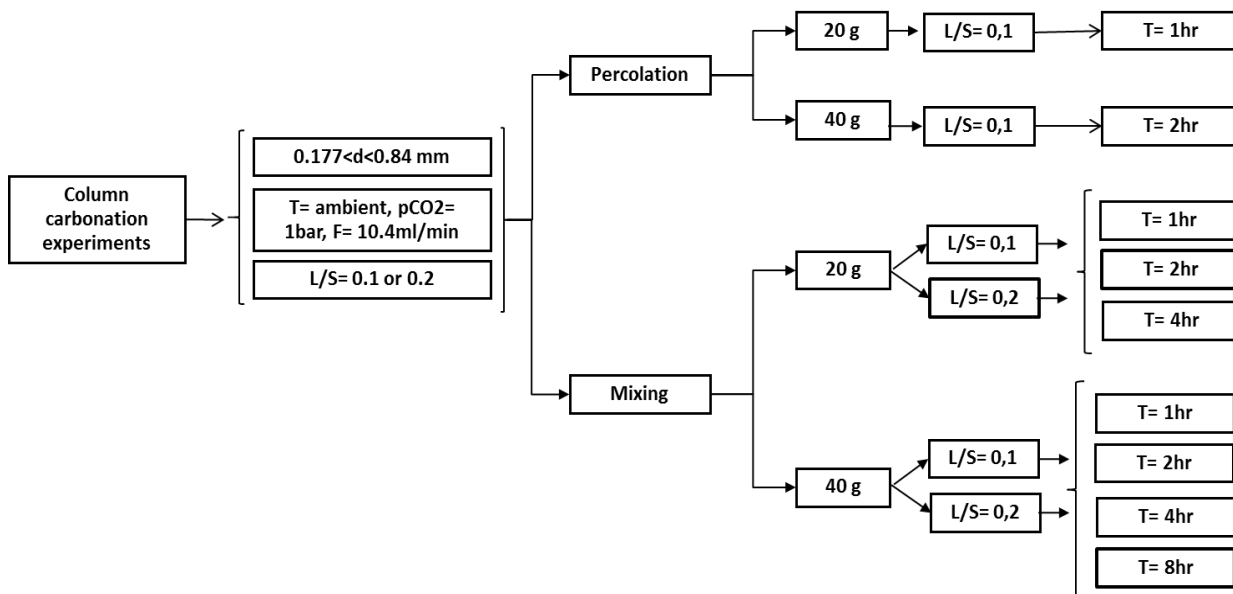
Figure 4.6: Overview of all column experiments performed.

The CO_2-supply was opened about 6 minutes before the start of the experiment, as this was the time calculated, needed to replace all ambient air in the system and its tubings. After this, the CO_2-flow rate was adjusted, and the column was attached to the system. At the end of the experiment duration, the CO_2-supply was stopped and the column was again disconnected.

4.2.3.3 Sample processing

After removing the batch samples from the reactor, they were placed in the desiccator, weighted and subsequently put in the oven for overnight drying at 105°C. After drying they were put in the desiccator for cooling and were subsequently weighted again in order to determine the mass increase. Finally the batch samples were milled all 3 together in the vibratory disk mill to d<0.177mm, and stored in sealed polyethylene bottles until TIC analysis.

What concerns the column samples, directly following the experiment, the column was weighted with all components, and then again without filters and glass beads. Then the carbonated material from the 'top', 'middle' and 'bottom' sections (Figure 4.7) was taken out of the column, put in separate glass cups and dried overnight at 105°C. For some experiments, the column with carbonated AOD slag was put in the oven in order to calculate the mass-increase (removing the material from the column resulted in the inevitable loss of some

material). However this seemed to stress the columns making them more prone to break, therefore the former procedure was preferred. The separation of the material in different layers (top-middle-bottom) was done to examine potential differences in carbonation with distance throughout the column. Afterwards, the column samples (top-middle-bottom) were milled separately and subsequently stored in sealed polyethylene bottles like for the batch samples.
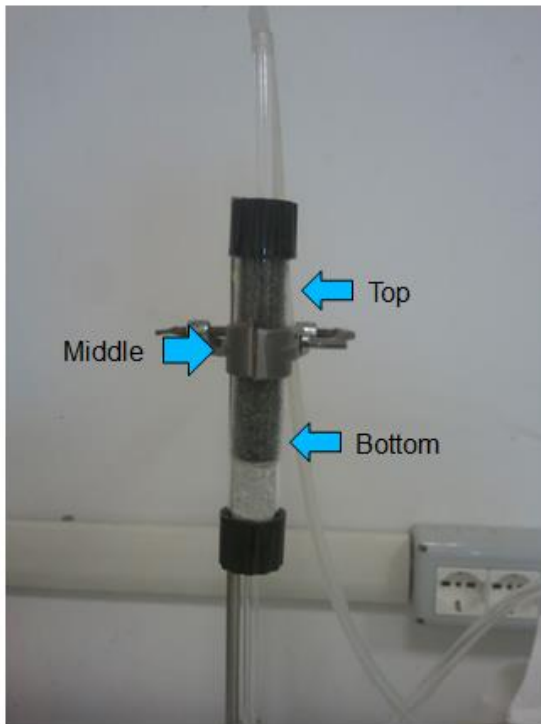
Figure 4.7: The respective layers: top-middle-bottom, in which the material was separated after carbonation.

5 RESULTS AND INTERPRETATION

5.1 Characterisation

5.1.1 Initial Moisture Content

The moisture content of the slags was determined after approximately 24 hours of drying at 105°C. The average initial moisture content of the material was determined at about 15.45% (Table 5.1). It must be noted that the material had been stored for some months in an air-tight plastic container, however this should not have influenced the moisture content.

Table 5.1: The results for the weighting of the 4 containers with the AOD slag before and after drying, and the calculated moisture content.

Sample	Tare	Total wet	Total dry	Moisture content (%)
1	147,74	1047,18	912	15,03
2	149,73	1050,86	913,8	15,21
3	145,17	1246,5	1075,8	15,50
4	146,94	1193,6	1025,4	16,07
			Average	15,45

A significant moisture content of slags may be a major obstacle for recycling in a sinter plant because of adhesive forces and aggregate forming. Also with the current material it was observed that sticking of the gains occurred up to some extent, creating agglomeration of particles, but which easily fell apart upon drying. Due to the moisture present, all material had to be dried before further characterisation could be performed.

5.1.2 Particle size distribution

The results from the sieving are displayed in Figure 5.1, from which it can be seen that the mass composition of the material is mainly dominated by fine-grained particles. In the lower part of the figure, the size classes which were selected to perform the further characterisation

and carbonation experiments upon are highlighted to indicate the degree in which they are representative for the whole sample.
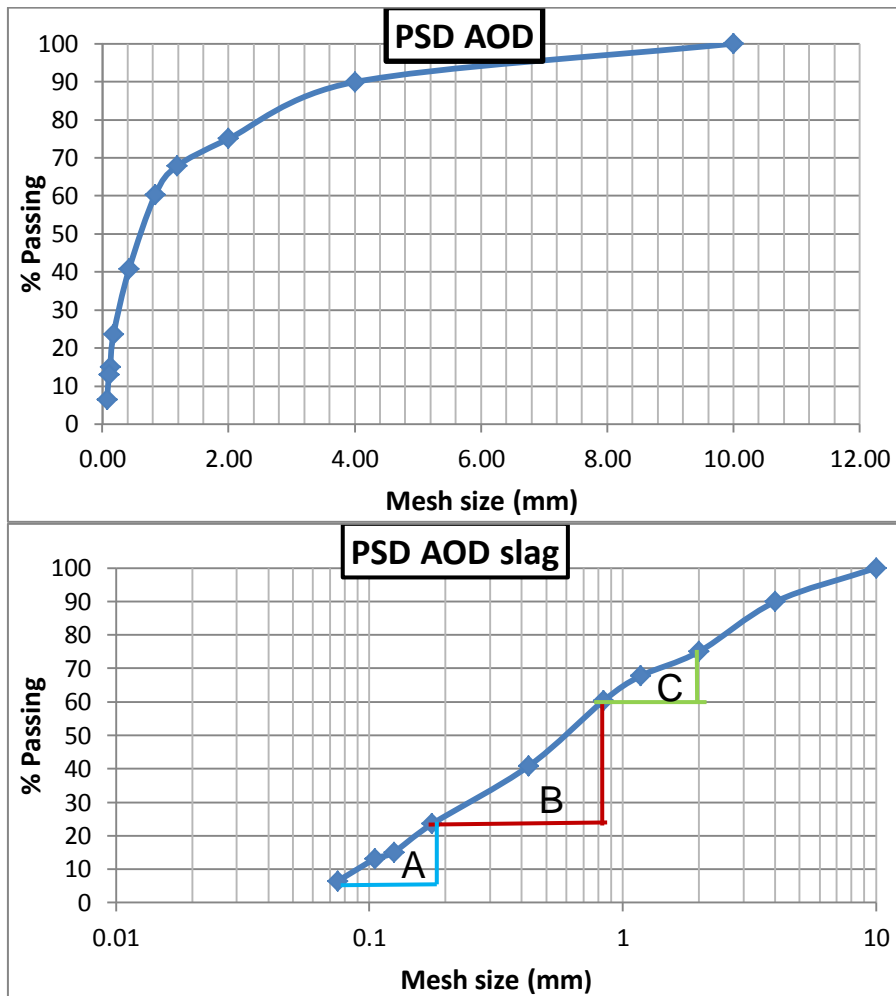

Figure 5.1: The particle size distribution curve for the entire AOD sample. Upper: Mesh size expressed on a linear scale. Lower: Expressed on a logarithmic scale with the range of the different experimental fractions (fine (A)- intermediate (B)- coarse (C)).

Table 5.2: The sieving results per size class for the entire AOD sample (PSD data).

Size Class (mm)	Mass (g)	wt% of total
>10	0	0.00
4 to 10	122.8	10.09
2 to 4	181.8	14.93
1,18 to 2	87.7	7.20
0,84 to 1,18	90.9	7.47
0,425 to 0,84	238	19.55
0,177 to 0,425	210	17.25
0,125 to 0,177	102.9	8.45
0,105 to 0,125	25.1	2.06
0,075 to 0,105	79.9	6.56
<0,075	78.2	6.42
Total	1217.3	100.00

The finest particles had a grain size below 0.075 mm (finest sieve available) and the size of the coarsest particles was between 4 and 10 mm (Table 5.2). The raw material had a relatively heterogeneous size distribution: about 90% of the slag had a grain size below 4 mm, about 75% below 2 mm, 50% below 0.84 mm and a significant amount (24%) of the material had a size below 0.177 mm and was rich in dust. Following E.U. legislation, material with a diameter below 2 mm should be handled with more care as it is more prone to contain contamination and thus needs to be examined in more detail. About 75% of the material had a size fraction below 2mm, and it is upon this fraction that the further characterisation and carbonation tests will be done. However solely the material in the range of 0.177 – 0.84 mm diameter, was used to assess the carbonation capacity during the column tests. The former material was subdivided in 3categories 'coarse', 'intermediate', and 'fine' as can be seen from Table 5.3. Since generally fine steel slags are more readily carbonated, this provided a first indication on the suitability of the material for ACT.

Table 5.3: The 3 selected experimental fractions (coarse-intermediate-fine) and their respective mass relative to the overall sample

Fraction	Size Class (mm)	Mass (g)	Wt% of total
Excluded (E)	>2.00	304.6	25.02
Coarse (C)	0.84-2.00	178.6	14.67
Intermediate (B)	0.177-0.84	448	36.80
Fine (A)	<0.177	286.1	23.50
Total		1217.3	100.00

5.1.3 Material Composition prior to carbonation

5.1.3.1 Elemental composition

Through alkaline fusion and subsequent ICP-OES analysis, the absolute elemental composition of the slag was determined. The concentration of elements in the solid AOD material were determined in mg/l of solution and recalculated to the 'real' concentration in the slag (mg/kg) by applying the formula supplied in para. 4.2.1.3.1.

The analysed values for most elements in the alkaline fusion solution were valid (i.e. their value was between the analytic standards and exceeded the elements quantification limit (LOQ)), except for Cd and Ti which both were below the LOQ. The obtained B and Li values were not accounted for because their abundance was caused by the use of lithium tetraborate in the fusion process. It should be noted that the values of As and Hg may not be reliable since the technique of ICP-OES is not suited for their accurate determination.

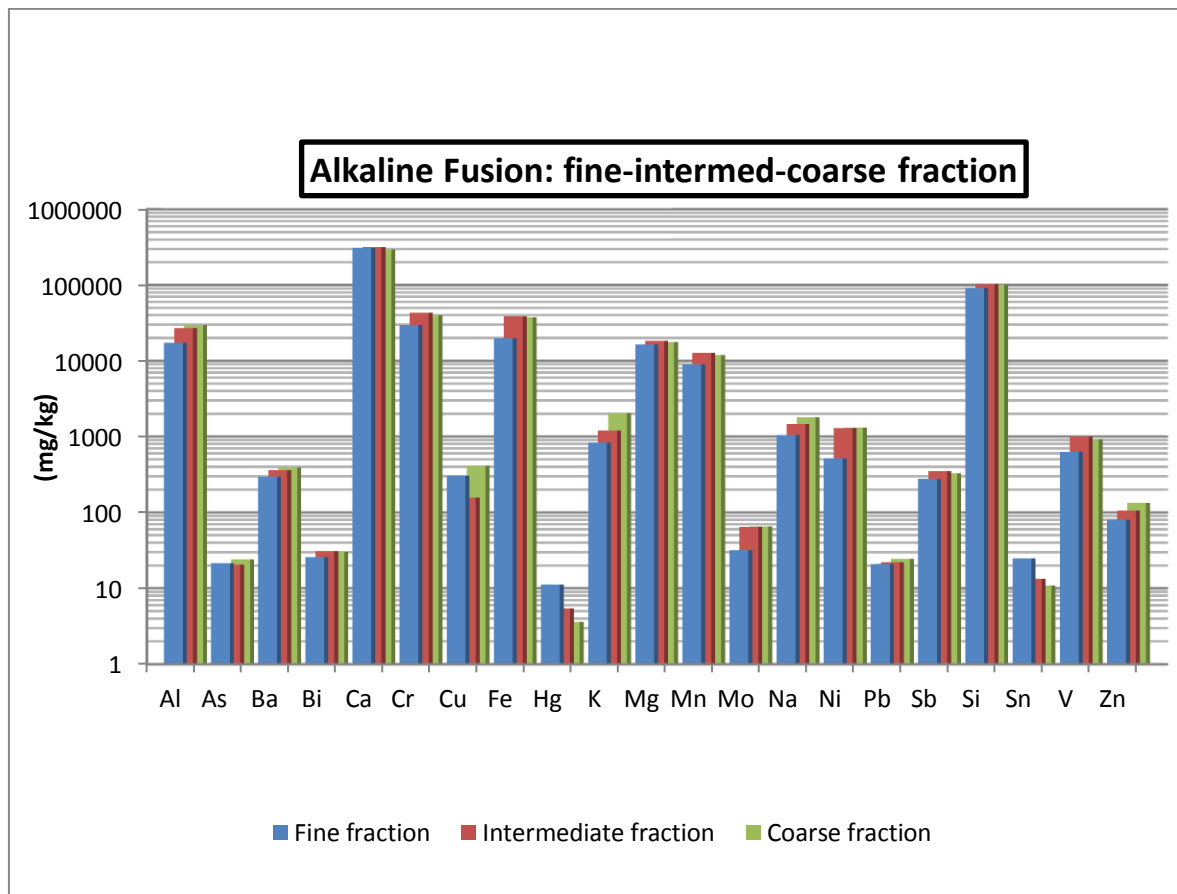The obtained values are presented and compared below in Figure 5.2 for the 3 examined fractions.

Figure 5.2: Results of the alkaline fusion showing the elemental composition of the material.

The main elemental constituents of the intermediate fraction are Ca, Si, Cr, Fe, Al, Mg and Mn (highest to lower concentration), having concentrations exceeding 10,000 mg/kg for all three fractions (except for Mn in the fine fraction), followed by Na, Ni, K, V; with concentrations of 1000-1500 mg/kg. The intermediate fraction showed to be relatively richer in Bi, Ca, Cr, Fe, Mg, Mn, Mo, Ni, Sb, Si, V compared to other fractions. The concentration of Ca was found to be about 29.6-31.6 wt% for the coarse and intermediate fraction respectively, with the value for the fine fraction being in between these values. It must be remarked that these values are comparable to the concentrations usually reported for EAF slags as will be discussed in Chapter 6, para. 6.1. The concentration of Al, Cr and Fe is significantly -and of Si and Mg is slightly,- lower for the fine fraction, with the values for the intermediate and coarse fraction laying close to each other.

Elements with a relatively low concentration were: Ba, Sb, Cu, Zn, Mo, Bi, Pb, As and Sn with the latter 5 elements being classified as trace elements since they had a relatively low concentration below 100 mg/kg. Significant amounts of Ni and V were detected from 0.05 and 0.06 wt% in the fine to 0.13 and 0.1wt% in the intermediate fraction respectively.

The data of all obtained values from the alkaline fusion for the three examined fractions is presented in the Appendix (Table B).

5.1.3.2 Mineralogical composition

The XRD analysis pointed out that the untreated SSS material contained the following phases: calcium aluminium silicate ($CaAl_2SiO_6$), portlandite ($Ca(OH)_2$), melilite $Ca_2(Mg_{0.5}Al_{0.5})(Si_{1.5}Al_{0.5}O_7)$, calcite ($CaCO_3$), iron sulphide (FeS), iron oxide ($Fe_{21.34}O_{32}$), quartz (SiO_2), calcium silicate (Ca_2SiO_4), and calcium fluoride (CaF_2). Previous characterisation and carbonation experiments (only batch experiments) had been done on a different AOD sample by Tor Vergata University as reported by Baciocchi et al. (2010). Therefore the properties of both the current ('AOD tq 2012') and previously-examined ('AOD tq 2010') could be compared.

It may be seen from Figure 5.3 that the mineralogical properties of both types of material differ significantly. Whereas the 2012 material features a wide array of mineral species and displays a complex diffractogram, this was not the case for the 2010 slag in which only the phases calcium silicate and calcium fluoride, magnetite (Fe_3O_4), chromium oxide (CrO) and periclase (MgO) were discovered; the former 2 also present in the currently investigated

material, the latter 3 were not. However, the peaks of calcium silicate and fluoride show a very similar response signal for both AOD materials. This partly confirmed the suspicion that the examined material was not pure AOD, but most likely AOD mixed with different waste products such as EAF.

The examined stainless steel slag was relatively rich in silicates (calcium- and calcium aluminium silicate) and already contained significant amounts of calcite. In the unsieved material, the most abundant phases seemed to be portlandite and calcium (aluminium) silicate. For the intermediate fraction (used for the column experiments) the major species were portlandite, calcium silicate and iron oxide. Its content in portlandite, melilite and iron oxide seemed to be significantly higher relative to the other fractions. In contrary, the fine fraction contained few portlandite and a higher concentration of calcium aluminium silicate. The amount of calcite, calcium silicate (slightly higher for fine fraction), and calcium fluoride seemed to be fairly equally distributed among all fractions for the untreated material. In addition to this, low amounts of quartz, calcium oxide and iron sulphide were detected in the material composition.
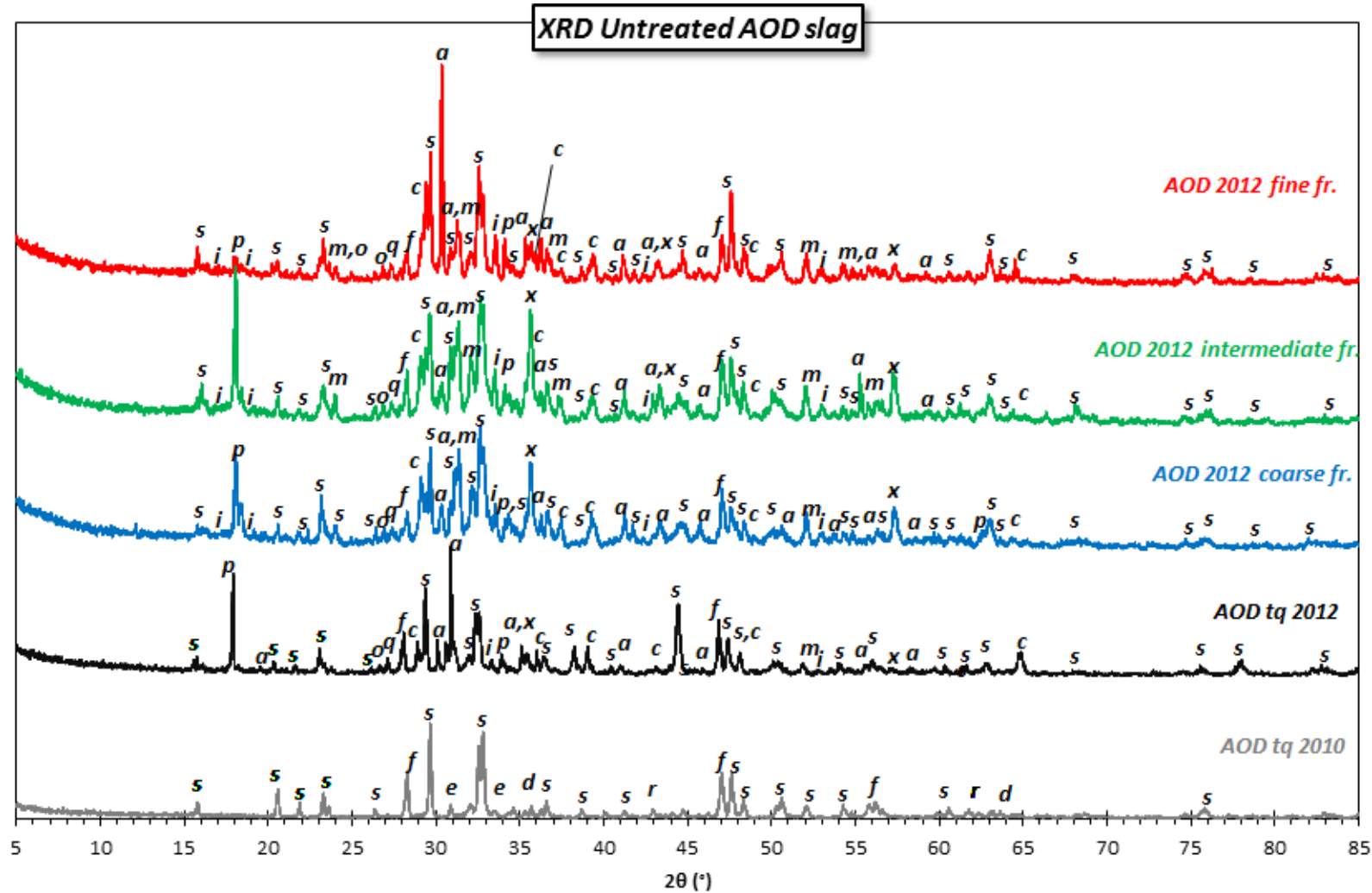
Figure 5.3: XRD Results of the untreated AOD slag (2012) and its different fractions, in comparison to the slag examined in 2010. Legend: a) Calcium Aluminum Silicate $CaAl_2SiO_6$; c) Calcite $CaCO_3$; d) Magnetite Fe_3O_4; e) Chromium oxide CrO; f) Calcium fluoride CaF_2; i) Iron Sulfide FeS; m) Melilite $Ca_2(Mg_{0.5}Al_{0.5})(Si_{1.5}Al_{0.5}O_7)$; o) Calcium Oxide CaO; p) Portlandite $Ca(OH)_2$; q) Quarz SiO_2; r) Periclase MgO; s) Calcium Silicate Ca_2SiO_4; x) Iron Oxide $Fe_{21.34}O_{32}$.

5.1.3.3 Solid Inorganic Carbon Content

The inorganic carbon (IC) content of the slag was determined for the untreated material prior to the experiments, in order to be able to determine the amount of carbonation. From this value, the initial calcite content was determined, assuming that all IC was in the form of calcite.

Table 5.4: The initial IC and CaCO₃-content of the slag.

Fraction	IC(wt%)	CaCO$_3$ (wt%)
<0.177	0.56%	4.65
0.177-0.84	0.18%	1.48

As may be seen from Table 5.4, small amounts of calcite were already present in the material before treatment.

5.2 Environmental behaviour prior to carbonation

5.2.1 Standard Leaching test

A standard leaching test was performed on the non-carbonated material: for the raw unsieved material (d<4mm), and for the fine, intermediate and coarse fractions.

5.2.1.1 pH

Figure 5.4: The pH of the leachate for the different fractions

The eluate of all samples displayed high, alkaline pH values. The leachates pH of the fine, intermediate and coarse fraction peak to values of 12.31-12.37. The eluate of the unsieved material deviates somewhat with a slightly lower value (12.15). In any case, all values are
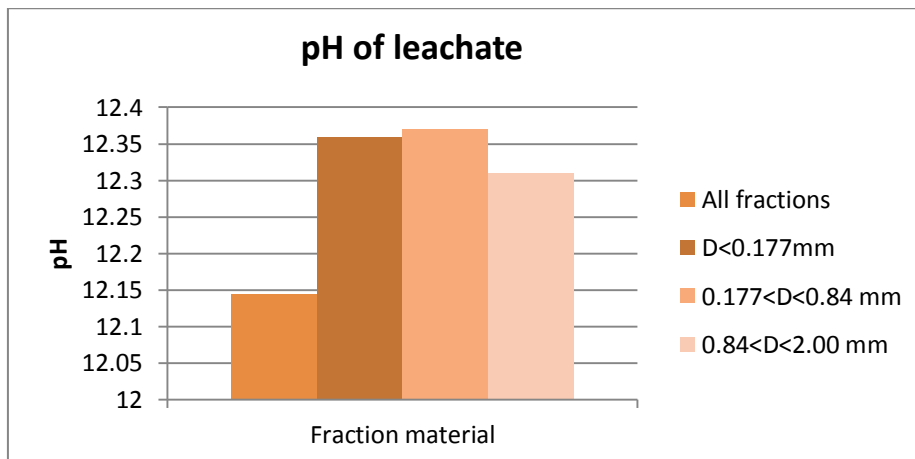
exceeding the limits prescribed by Italian legislation for material reuse (5.5<pH<12). The high pH value is mainly caused by the presence and dissolution of portlandite and calcite.

5.2.1.2 Leachate Composition

5.2.1.2.1 Chlorides determination
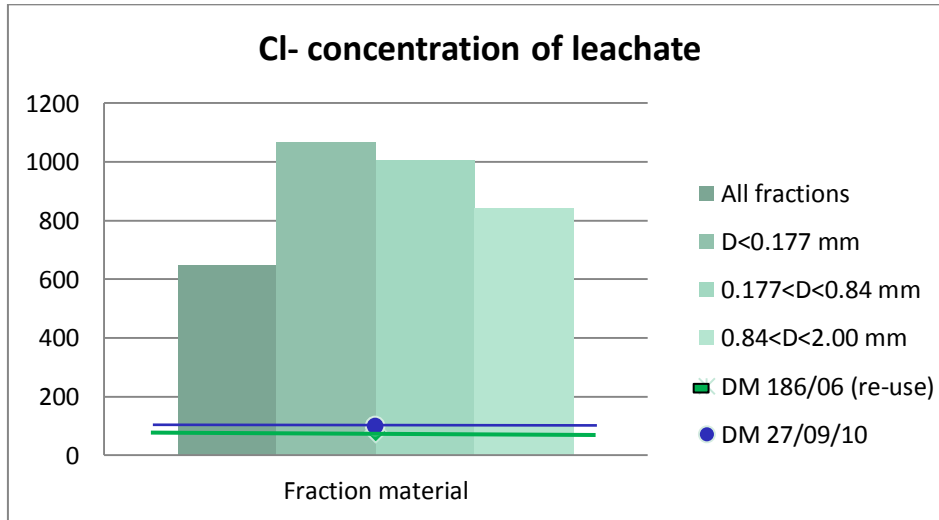
Figure 5.5: Concentration of soluble chlorides present in the eluate of the different fractions.

From Figure 5.5 it can be seen that there is a trend in the concentration of soluble chlorides. For the fine fraction the concentration is highest with about 1067 mg/l, decreasing with increasing grain size to about 842 mg/l for the coarse fraction. The lowest value was found for the heterogeneous, unsieved material which was about 648 mg/l, which is probably caused by the fact that the emitted fraction (d>2mm) possessed a low soluble chloride content. However, overall these are unexpected high values, which would normally not results from stainless steel slag leaching. The maximum allowed limits imposed by italian legislation of 80 mg/l (It. MD. 27/09/10) and 100 mg/l (It. MD. 186/06) for inert landfilling and material reuse respectively, are rigorously trespassed.

5.2.1.2.2 Other elements

The ICP-OES results for the elemental composition of the eluate (mg/l) obtained for the unsieved material, as well as the fine, intermediate and coarse fractions can be seen in Figure 5.6. The analysis of the unsieved material's eluate was performed on the pure leachate, and for dilutions 1:5, 1:10 and 1:100. For the different fractions this was on the pure leachate and the dilutions 1:10 and 1:100.
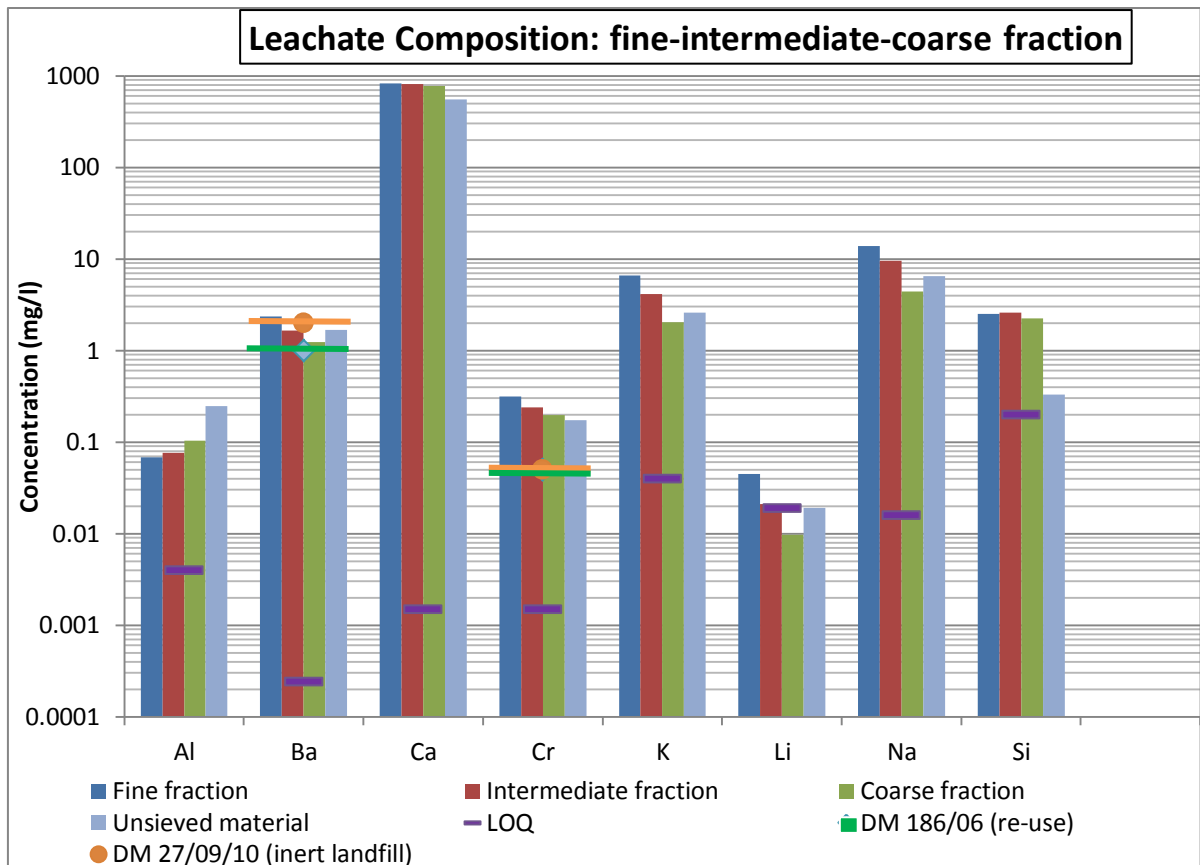
Figure 5.6: Overview of the leachate analysis results for the different fractions, with comparison to the limits of landfilling and reuse.

Multiple elements were below LOQ, even in the pure test: As, Be, Bi, Cd, Co, Cu, Fe, Mg, Mn, Mo, Ni, Pb, Sb, Se, Sn, Tl, V, Zn. The value for B exceeded the standards, but this was thought to be due to overdraft from previous analysis of the alkaline fusion leachate, since during the analysis its concentration gradually decreased.

It may be seen from the figure that the reuse limit (DM 186/06) and the inert waste landfill limit (DM 27/09/10) were exceeded for some elements: for Cr and Ba, the limits of reuse and inert landfilling were both trespassed, although for Ba the latter limit was only exceeded by the leachate of the fine fraction.

What concerns the intermediate fraction, the leaching of Mg, Mo and V was minimal. The concentration of Cr in the leachate was more significant with values up to 0.24 mg/l, which was higher than the values found in previous research (Shen et al., 2004; Baciocchi et al., 2009; 2010b).

5.2.2   Acid neutralization capacity

5.2.2.1   On untreated slags

The buffering capacity of the slag material and thus its environmental behaviour was assessed through an ANC test (Figure 5.7). This graph was obtained by plotting the amount of acid added (in meq/g) against the corresponding pH value of the eluate observed.
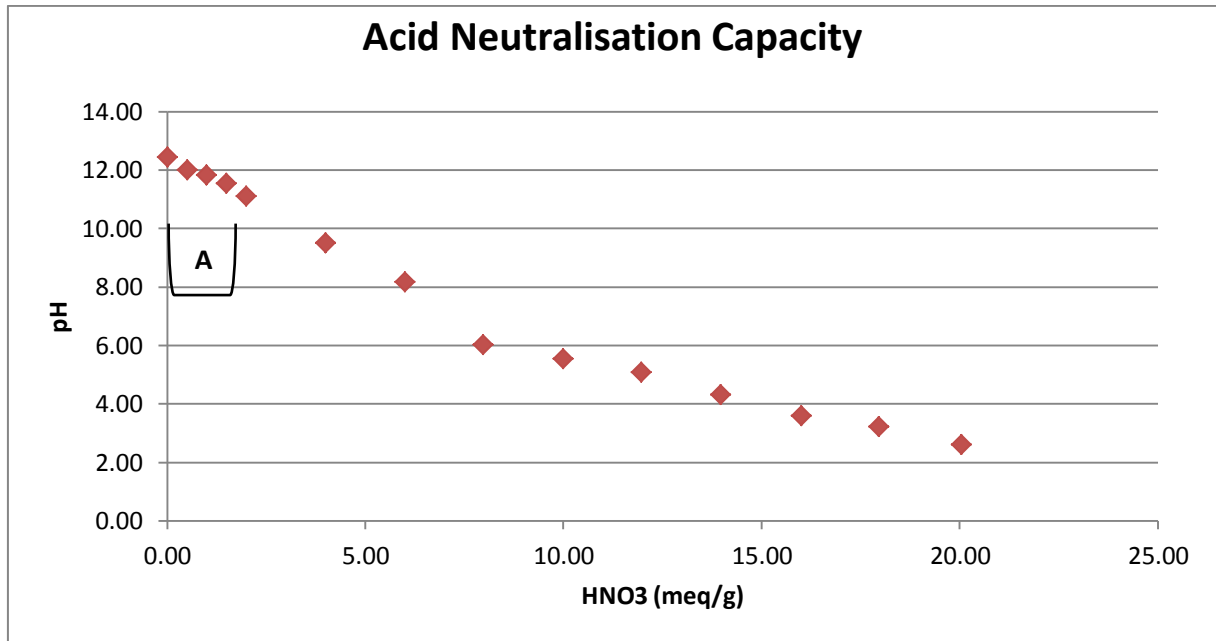
Figure 5.7: Results of the ANC test on the intermediate slag fraction.

In Figure 5.7, a region (A) in the curve may be identified, where the decrease in pH per amount of added acid is slightly lower compared to the overall slope of the part between 0 and 8 meq/g acid. This buffering occurs roughly in alkaline pH range (12.4-11.1) for addition of 0-2 meq/g HNO_3. The part indicated by 'A' is located between a pH of roughly 12.40 and 11.10 and is (most likely) caused by the buffering capacity of calcium hydroxides (portlandite). Also for HNO_3-addition of 7-12meq/g, there is a slight buffering, (probably) due to the dissolution of carbonates (calcite) and later of more resistant silicates.

The graph (Figure 5.8) show the evolution of the concentration of the measured elements with pH, and was obtained by ICP-OES analysis of the pure leachate, and for dilutions 1:10, 1:100, 1:1000 and 1:5000.
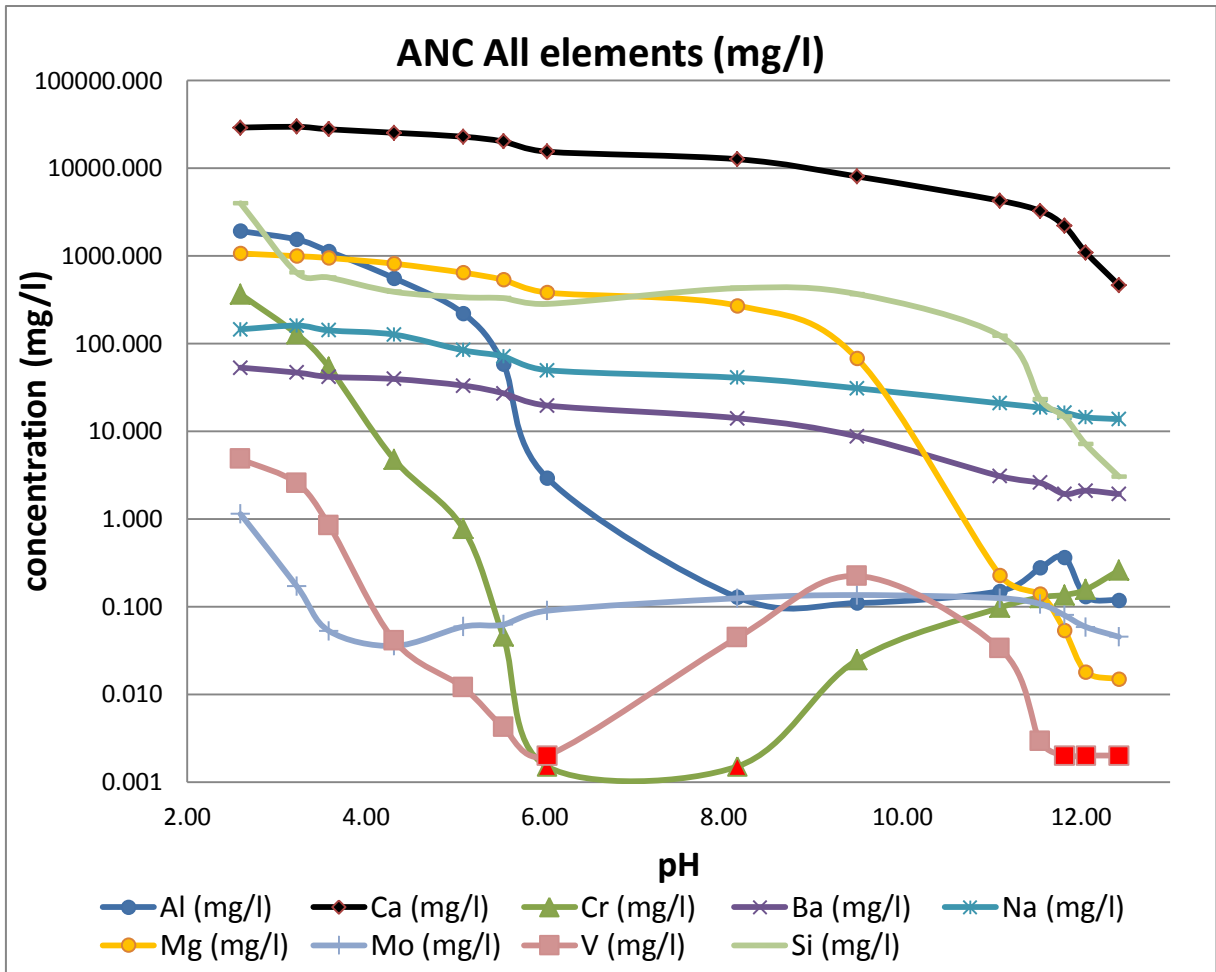
Figure 5.8: The element-specific ANC data. The most relevant elements are shown. The red points in the graphs for Cr and V indicate that the value was below LOQ.

The overall trend is that the concentration of the displayed metals is significantly higher at low pH with regard to their abundance in the leachate at an alkaline pH value.

Cr has its lowest concentration in the leachate for a near-neutral pH and significantly higher values at lower pH. For Ca, Mg, Si, Al, the behaviour is roughly similar: after an increase in their concentration going from pH 14 to 10, the rate of increase is slowed down around near-neutral pH and then further increases in the more acidic pH range. All of these elements are present in reactive species (e.g. $CaCO_3$, MgO, Ca-(Al)-silicates) which are related with carbonate formation, and thus are released along with carbonate dissolution upon acidification. The behaviour of V and Cr seems to follow the standard metal solubility pattern, with in general a lower solubility at near-neutral pH values.

5.3 Carbonation Tests- Change in solid IC-content

5.3.1 Batch tests

For the batch tests performed under the 'optimal' conditions (50°C, 10bar CO_2, L/S=0.4) on the fine slag fraction, the resulting kinetics was obtained by plotting sample CO_2-uptake against carbonation time.
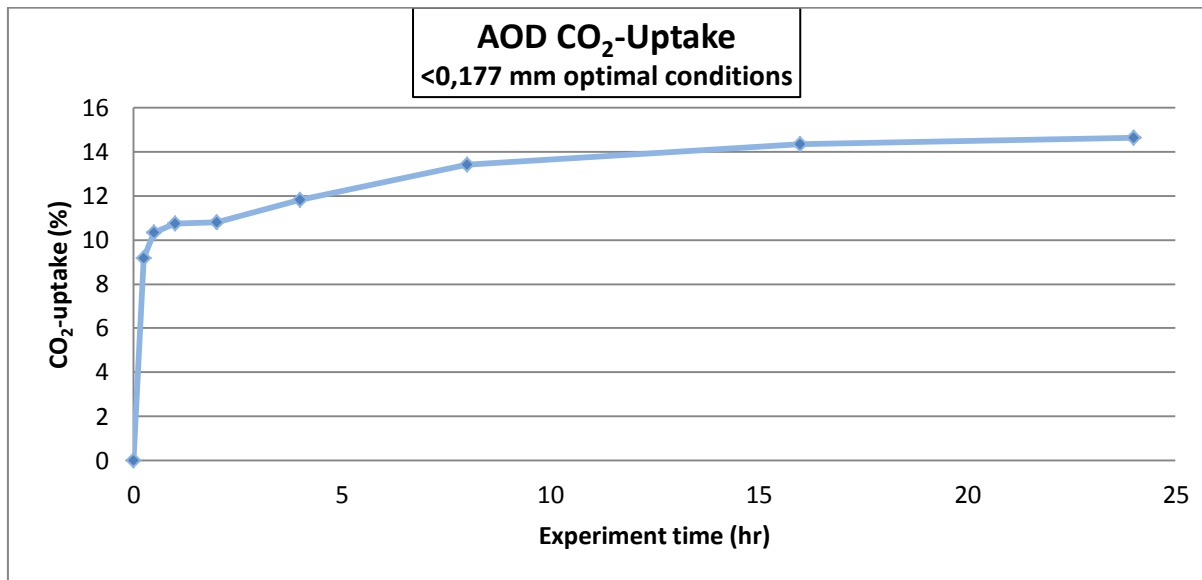
Figure 5.9: Measured CO_2-uptake kinetics for the batch test on the fine AOD fraction at 50°C, 10bar CO_2, L/S=0.4.

A fairly fast increase in CO_2-uptake is indicated by Figure 5.9 for short reaction times up to 30 minutes. After solely 15 minutes of treatment, already a CO_2-uptake exceeding 9% was reached. A first semi-plateau is reached for 0.5 up to 2h of reaction time. After this, the rate of CO_2-uptake further increases, although at a lower rate than initially until approaching a second plateau of about 14.5% CO_2-uptake and higher for 16 hours and onwards. The initial high CO_2-uptake rate is probably caused by the conversion of highly reactive phases like portlandite ($Ca(OH)_2$), iron oxide ($Fe_{21.34}O_{32}$) and calcium oxide (CaO), which dissolve rapidly and react with the dissolved CO_2 to form carbonates. The lower CO_2-uptake rate at larger experiment times is likely due to the conversion of less reactive silicate phases such as calcium aluminium silicate ($CaAl_2SiO_6$), calcium silicate (Ca_2SiO_4), quartz (SiO_2) and possibly melilite ($Ca_2(Mg_{0.5}Al_{0.5})(Si_{1.5}Al_{0.5}O_7)$) which are less soluble and will primarily form carbonates at longer carbonation times.

Subsequently, the batch experiment was repeated, but for one cycle this was done with the intermediate instead of fine fraction under enhanced conditions and for yet another cycle (up to 8h reaction time) with the intermediate fraction but under 'less favourable' conditions of 22°C, 1bar CO_2 and a L/S ratio of 0.2 (identical to the conditions prevailing during the following column experiments). The comparison between the two kinetic curves can be made from Figure 5.10.
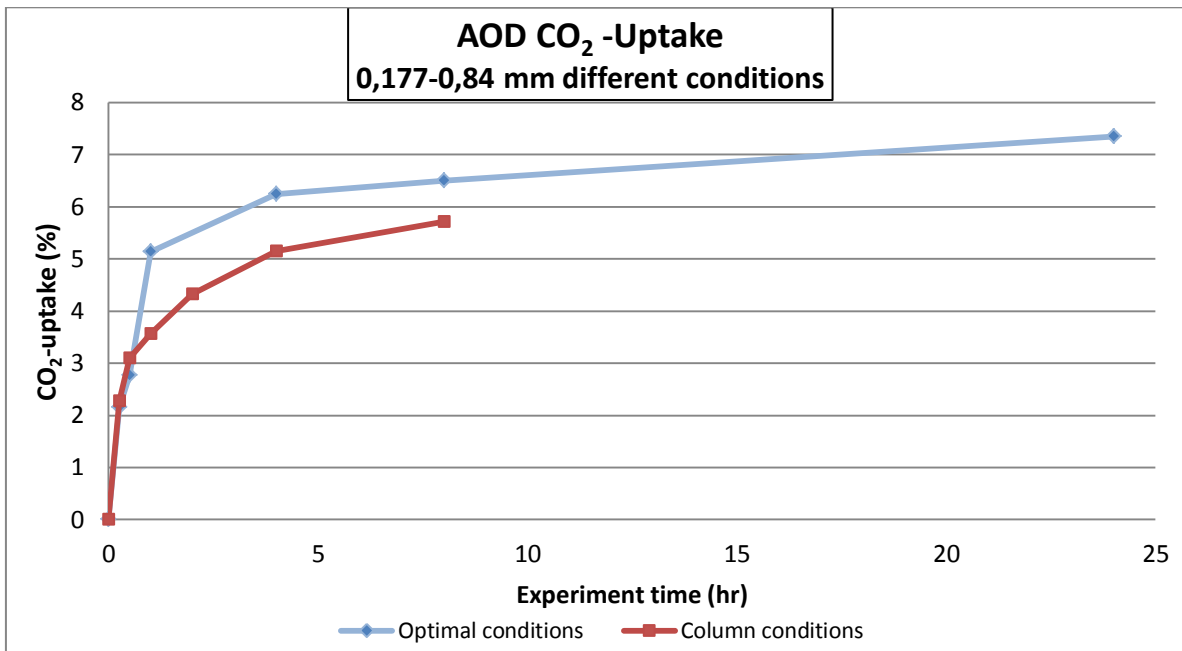
Figure 5.10: Measured CO_2-uptake kinetics for the batch test on the intermediate AOD fraction under 'enhanced' (50°C, 10bar CO_2, L/S=0.4) and under 'column' conditions (22°C, 1bar CO_2, L/S=0.2).

On one hand, comparison between the kinetic curves for the fine (Figure 5.9) and intermediate fraction (Figure 5.10) under optimal conditions points out the importance of grain size on the slags reactivity for carbonation. The rate of CO_2-uptake is clearly lower for the intermediate fraction: for t<30min, uptake is more gradual and the maximum CO_2-uptake of 7.4% reached after 24 h (the platform value) is about half the maximum value of 14.6% for the fine fraction. The absolute maximum CO_2-uptake seems not yet attained for a reaction time of 24 h. This indicates the importance of material grain size for the carbonation efficiency: the rate of carbonation decreases with increasing grain size and so does the maximum carbonation extent.

On the other hand, the effect of the experimental conditions (temperature, pressure, L/S) was assessed by comparing the aforementioned results to the ones obtained from the batch test under 'less favourable' experimental conditions: a temperature of 22°C, a CO_2-pressure of 1bar and a L/S ratio of 0.2, also on the intermediate fraction. Figure 5.10 shows a comparable

but slightly (although significant) lower CO_2-uptake (0.8% lower for 8 h) for the latter conditions. Remarkably, for short reaction times (<1h) the uptake is as high or higher than under the enhanced conditions.

From this we may conclude that –for the material tested- the effect of the grain size on carbonation is more profound than the state of the experimental conditions: CO_2-pressure, temperature and L/S.

5.3.2 Column tests

The next phase of the carbonation experiments consisted of carrying out the column tests which were performed on the intermediate fraction at ambient temperature (22-24°C), a CO_2-flow of 10.4 ml/min and a L/S ratio of 0.1 and 0.2 as described in para.4.2.3.2. The following figures display for each experiment the CO_2-uptake measured for the top, middle and bottom layer of material under the given conditions. The average uptake for the whole column is indicated by the blue line crossing the points.

Figure 5.11: Measured CO_2-uptake for the column test with 20g of the intermediate fraction under 22°C and 10.4ml/min CO_2 for a L/S=0.1 (left) and a L/S=0.2 (right).

Figure 5.11 shows that for a reaction time of about 1h, the registered CO_2-uptake for the top layer of the material was lower than for the middle or bottom layers. This was the case for both L/S ratio and is probably due to the fact that the dispersion of CO_2 through the material takes some time: therefore carbonation starts somewhat later in the upper part of the column. This effect is yet more pronounced for the tests with 40 g of material (Figure 5.12) since a larger mass of material increases the travel time for CO_2 gas through the medium as the sampling points are further apart. This thus results in a higher deviation from the average uptake for the different layers. At longer reaction times (2&4h or 4&8h for the 20g and 40g experiments respectively), the opposite trend occurs: CO_2-uptake seems to be lower at the bottom compared to the middle and upper layers. This trend is again more apparent from Figure 5.12. The reason for this is not clear but a likely explanation may be that this is due to a decrease in L/S ratio with time as will be discussed later on (Figure 6.2) in Chapter 6, para. 6.2. The average CO_2-uptake is only slightly higher for the experiment with L/S=0.2, with average uptake being 0.1-0.5% higher than in the case of L/S=0.1. In general, uptake is about 3.6% after 1h to about 5.2% after 4h.
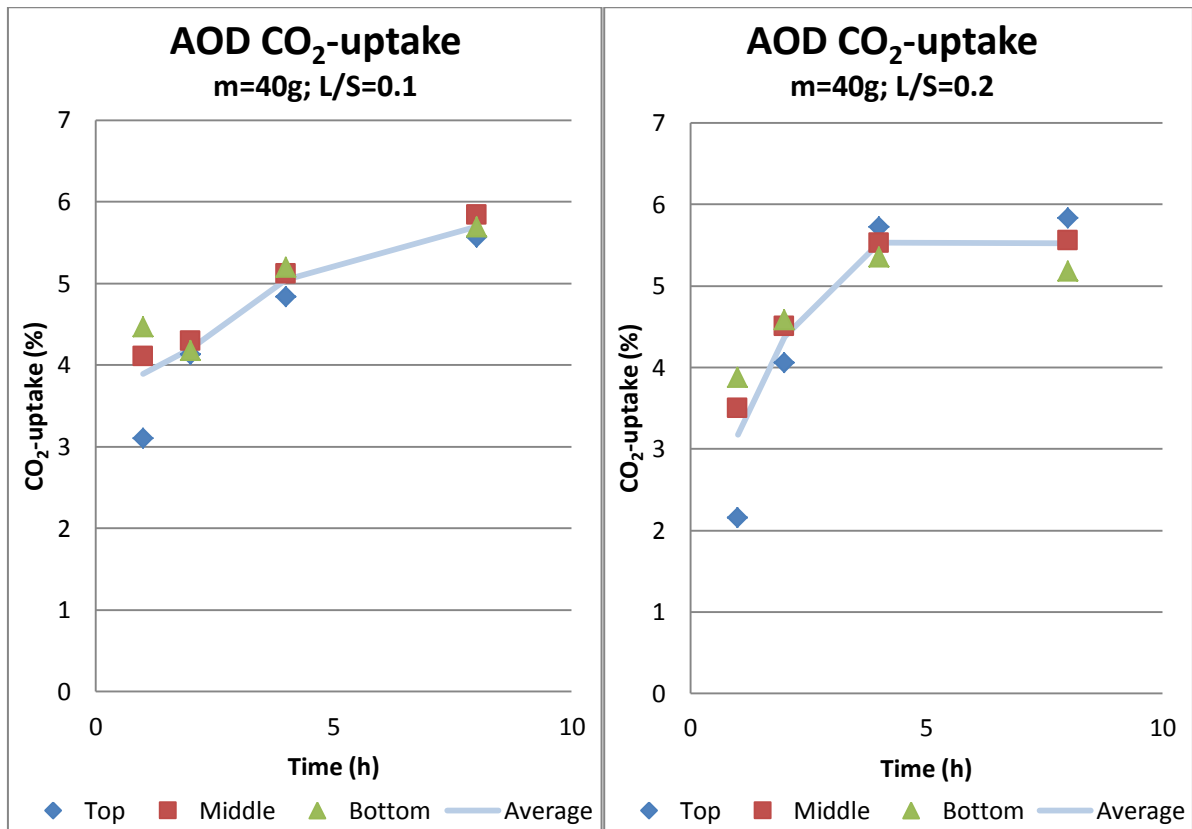
Figure 5.12: Measured CO_2-uptake for the column test with 40g AOD of the intermediate fraction under 22°C and 10.4ml/min CO_2 for a L/S=0.1 (left) and a L/S=0.2 (right).

The uptake values for the experiments using 40g of slag show average uptakes (1h) between 3.2% and 3.9% for a L/S of 0.2 and 0.1 respectively. For longer reaction times, the uptake values for both L/S ratios converge more and reach uptake values up to 5.7% after 8h (L/S=0.1). For the test with L/S of 0.2, it seems as if the maximum value was already reached after 4h, while for the lower L/S this seemed not to be the case after 8h. Further experiments would be needed to determine this.

The validity of the first obtained value (1hr) for the 40 g experiment at 0.1 L/S could be questioned however, since the CO_2-uptake measured at the top of the column is larger than the value for its uptake at a reaction time of 2h.
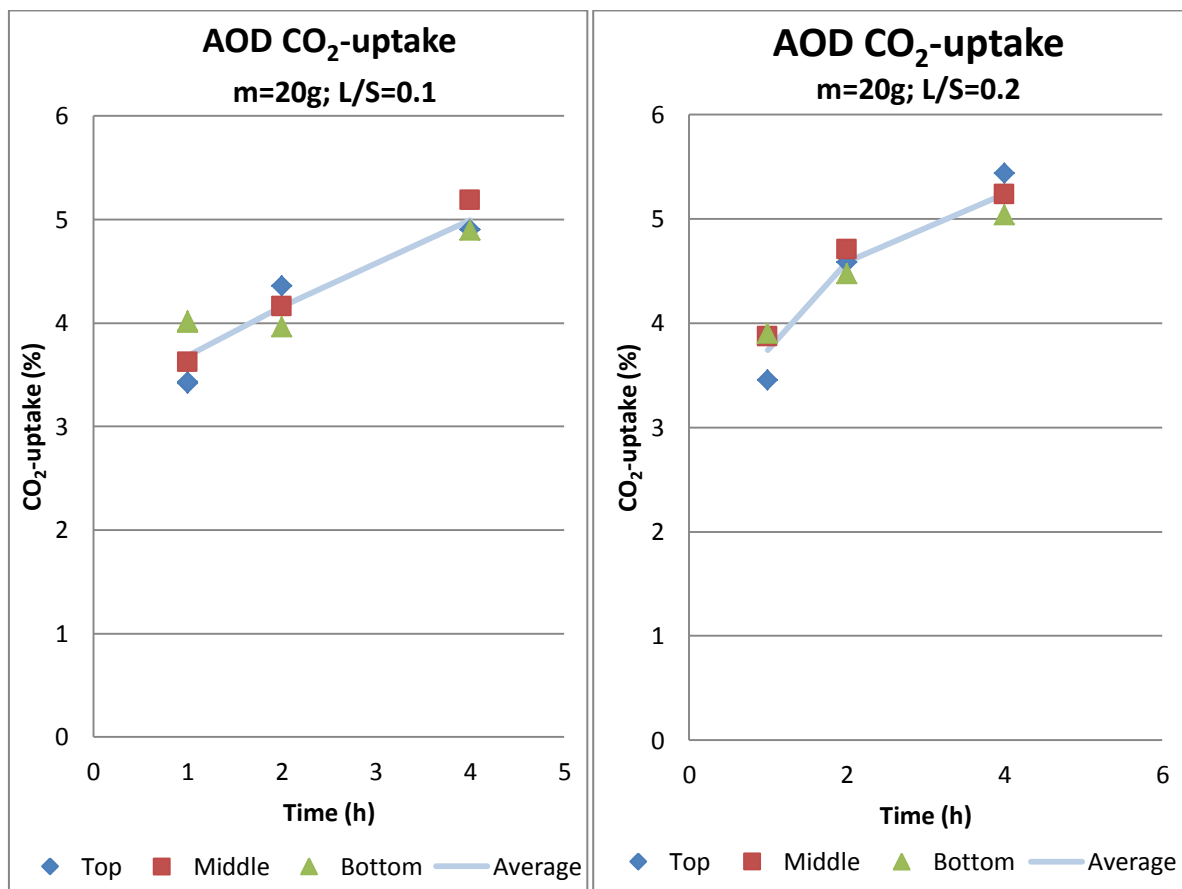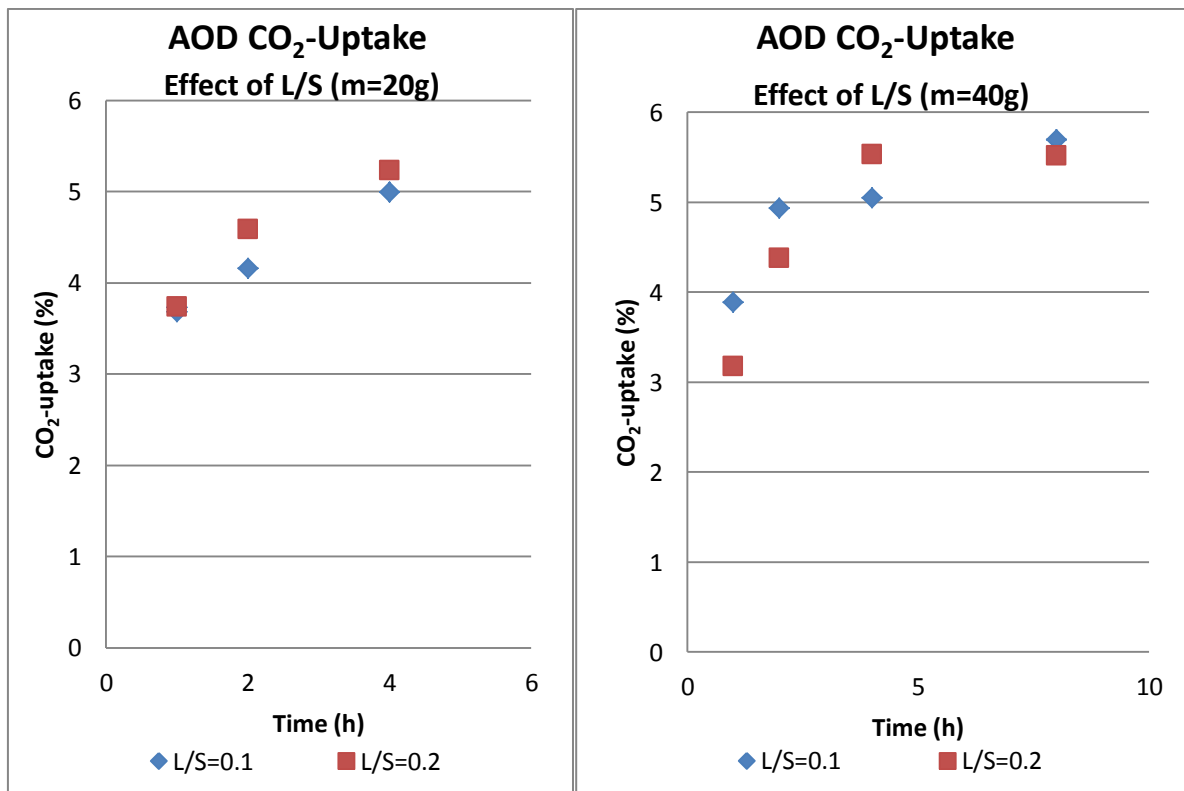

Figure 5.13: Measured CO_2-uptake for the column test with 40g AOD of the intermediate fraction under 22°C and 10.4ml/min of CO_2 for a L/S=0.1 (left) and a L/S=0.2 (right).

The above graphs (Figure 5.13) summarize the effect of the L/S ratio on CO_2-uptake for the column experiments. For the 20g dry mass experiments, CO_2-uptake seems to be higher for the larger L/S. However, for the 40g dry mass experiments, initially (for 1 or 2h reaction time), uptake seems to be higher for the lower L/S whereas for a reaction time of 4h this is the other way around. No real trend seems to persist here, and it should be remarked that the differences in uptake are relatively small, especially with respect to the repeatability of the experiments, treated in Chapter 6 (Figure 6.4). In any case, from this experimental data, the

importance of the L/S ratio on the CO_2-uptake (Figure 5.12 and Figure 5.13) and the total mass (and thus the depth of the material) seems minimal, since the initial significant differences in uptake converge at longer reaction times.

5.4 Carbonation- Change in Material properties

5.4.1 Mineralogy

Following the carbonation experiments, the carbonated material from different selected tests with a high carbonation extent was analysed by XRD again. From the batch experiments, fine and intermediate fraction material carbonated for 24h under 50°C, 10bar CO_2, L/S of 0.4 was analysed (Figure 5.14 and Figure 5.15). From the column experiments, intermediate fraction slag, carbonated for 2 and 8h under 22°C, a CO_2-flow of 10.4ml/min was analysed (Figure 5.16).
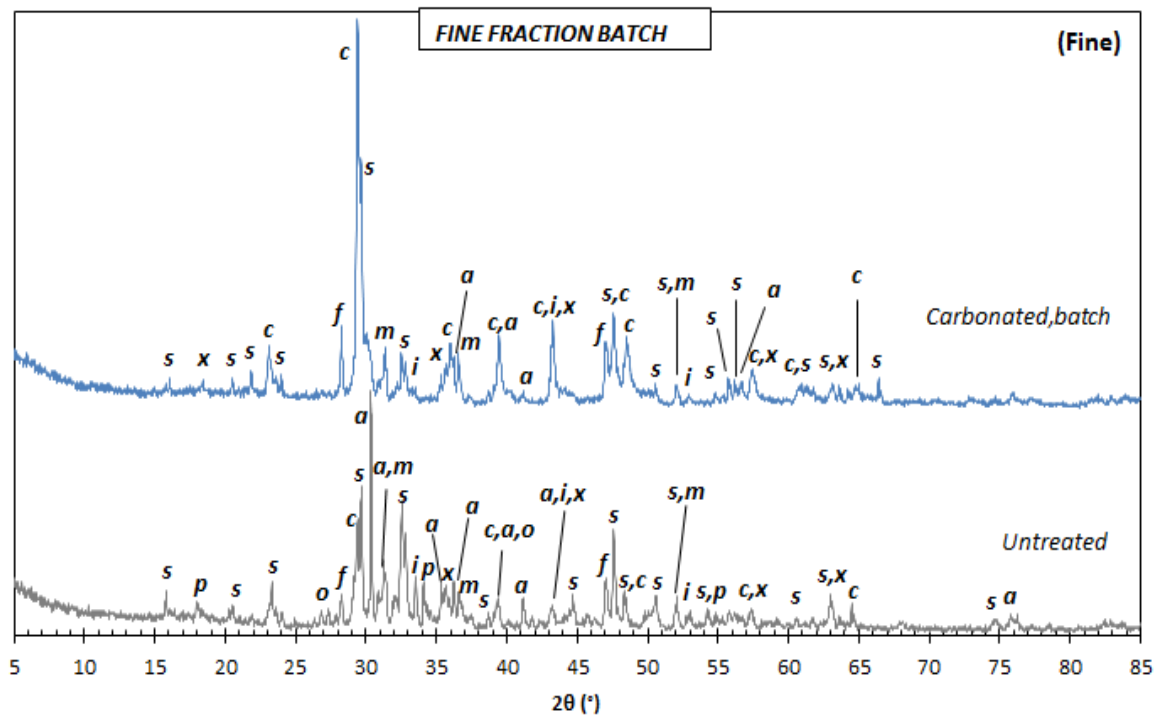
Figure 5.14: Comparison of the mineralogical composition of the fine AOD fraction, untreated and batch carbonated for 24h at 50°C, 10bar CO_2, L/S:0.4. Legend: a) Calcium Aluminum Silicate $CaAl_2SiO_6$; c) Calcite $CaCO_3$; d) Magnetite Fe_3O_4; e) Chromium oxide CrO; f) Calcium fluoride CaF_2; i) Iron Sulfide FeS; m) Melilite $Ca_2(Mg_{0.5}Al_{0.5})(Si_{1.5}Al_{0.5}O_7)$; o) Calcium Oxide CaO; p) Portlandite $Ca(OH)_2$; q) Quarz SiO_2; r) Periclase MgO; s) Calcium Silicate Ca_2SiO_4; x) Iron Oxide $Fe_{21.34}O_{32}$

From Figure 5.14 it shows that batch carbonation of the fine fraction resulted primarily in a reduced signal (thus probably consummation) for calcium aluminium silicate, as well as calcium silicate, portlandite, and calcium oxide together with an increase in the signal for calcite and to a lesser degree of calcium fluoride. The content of melilite seemed fairly constant. This confirms the formation of calcite through the consumption of reactive phases.

Figure 5.15: Comparison of the mineralogical composition of the intermediate AOD fraction, untreated and batch carbonated for 24h at 50°C, 10bar CO$_2$, L/S:0.4. (Legend: see Figure 5.14).

The diffractogram of the batch carbonated intermediate fraction (Figure 5.15) shows a pattern similar to the results for the fine fraction with a significant reduction in the signal for portlandite, calcium silicate and calcium aluminium silicate and an increased signal for calcite and also calcium fluoride. However, it may be observed that for the carbonated material there is still a relatively large signal for the just mentioned reactive species. This matches with the findings of the IC-analysis, where it was found that the CO$_2$-uptake (and thus conversion of reactive species) was about half for the intermediate compared to the fine fraction.

The results of the mineralogical composition of the column carbonated intermediate fraction (Figure 5.16) point in the same direction. 2 Hour carbonation resulted in a lower signal for portlandite, calcium silicate and calcium aluminium silicates with respect to the untreated

slag. Also a slight reduction was recorded in iron sulfide and melilite. The content of calcite (and calcium fluoride) increased. After 8h of reaction, this trend had persisted and a further increase for the signal of calcite can be noted.

Note: On first sight the XRD signal strength for calcite after 8h of carbonation does not seem to be stronger than for 2h. This is however due to the fact that the graphs are not scaled and changes should be observed by looking to relative changes between different mineral species.

It is worth noting that next to the discussed changes in mineralogy, also changes in the physical properties of the material were apparent. Carbonation was found to significantly increase the physical strength and coherence of the material. After both the batch as well as column tests, the initially loose material had been converted into a hard, more agglomerated matrix, which had to be 'cracked' for removal of the slag from the column or batch containers. This was most likely due to the formation of solid carbonates, that had precipitated in the grain voids and thus sticking the matrix together.
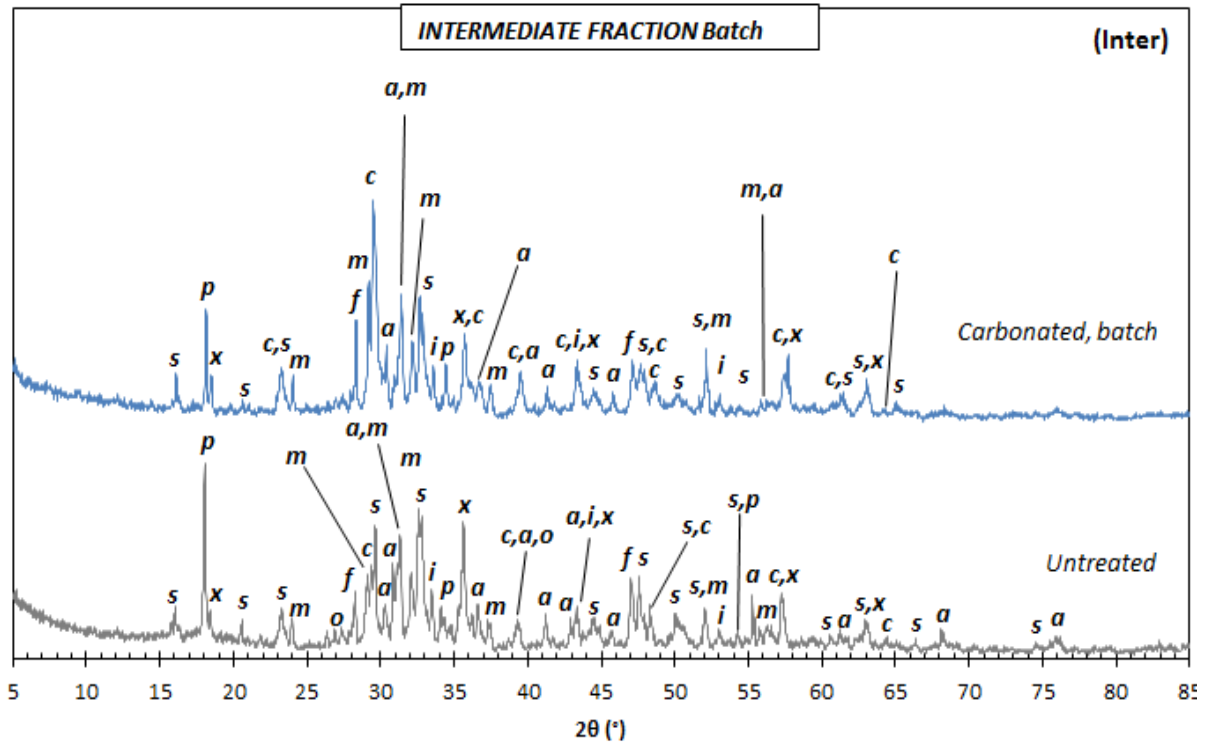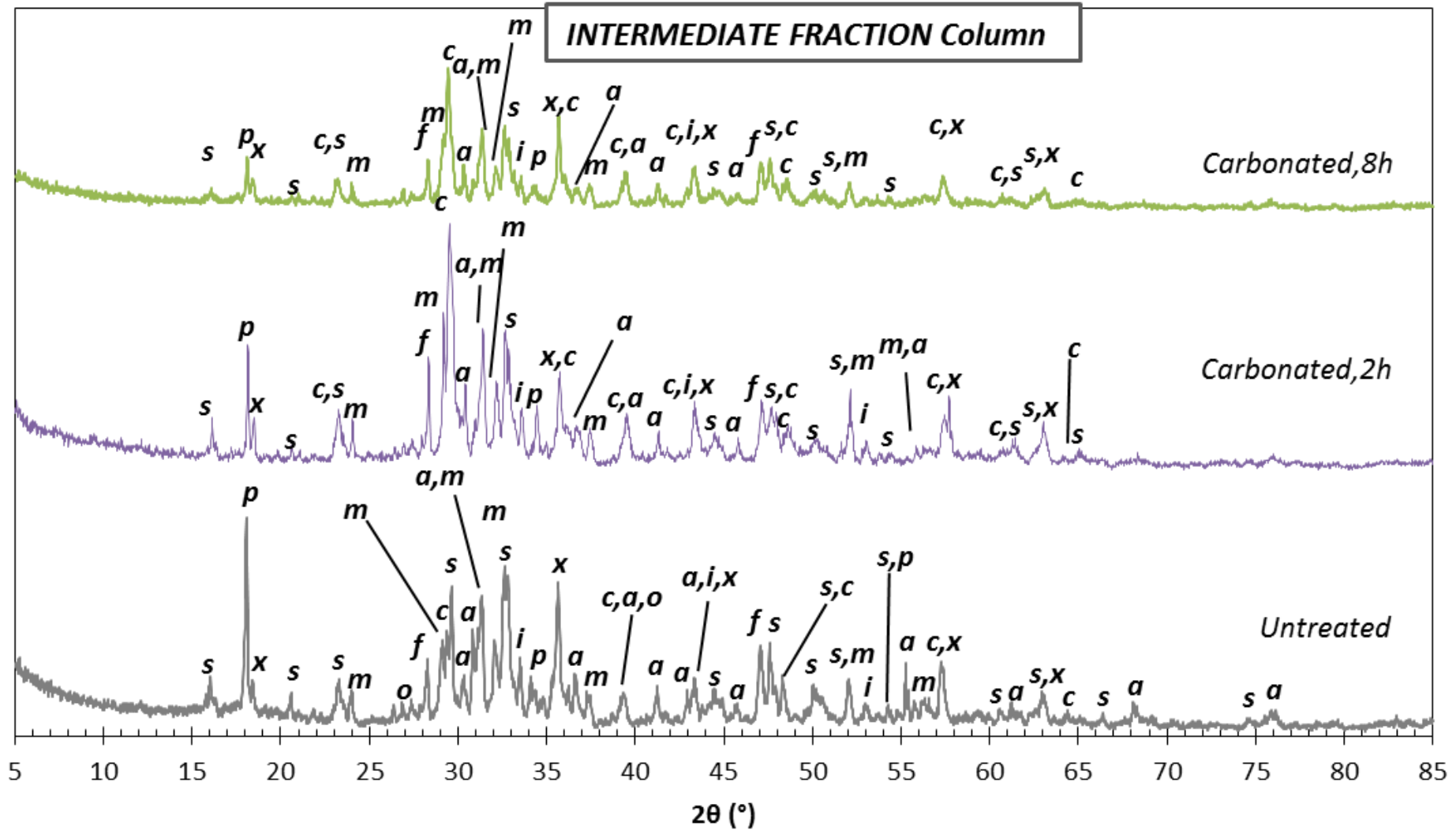
Figure 5.16: Comparison of the mineralogical composition of the intermediate AOD fraction, untreated and column carbonated for 2 and 8h at 22°C, 10.4ml/min CO_2, L/S:0.2. Legend: a) Calcium Aluminum Silicate $CaAl_2SiO_6$; c) Calcite $CaCO_3$; d) Magnetite Fe_3O_4; e) Chromium oxide CrO; f) Calcium fluoride CaF_2; i) Iron Sulfide FeS; m) Melilite $Ca_2(Mg_{0.5}Al_{0.5})(Si_{1.5}Al_{0.5}O_7)$; o) Calcium Oxide CaO; p) Portlandite $Ca(OH)_2$; q) Quarz SiO_2; r) Periclase MgO; s) Calcium Silicate Ca_2SiO_4; x) Iron Oxide $Fe_{21.34}O_3$.

5.4.2   Environmental behavior

After doing the carbonation experiments, further analysis was done on the material (intermediate fraction) from the 2 and 8h column tests with L/S=0.2 which had maximum CO_2-uptake of 4.38 and 5.52% respectively. The scope was to assess the change in environmental behaviour of the studied slag.

5.4.2.1   Standard Leaching

5.4.2.1.1   pH

The eluates pH from the standard leaching test on the 2 and 8h treated material was a first indication for the effect that the carbonation procedure had had.
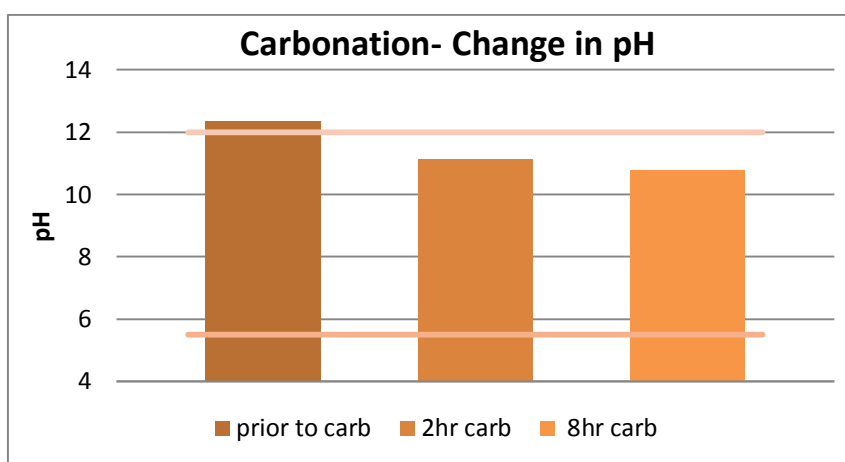
Figure 5.17: Results comparing the pH of the leachates from the 2 and 8h column treated material against the untreated material.

Significant drops in the leachate pH were registered due to column carbonation (Figure 5.17). The initial pH of 12.37 for the untreated material had dropped to 11.12 after 2h and had decreased further to a value of 10.78 after 8h of reaction. This pH decrease with increasing carbonation extent is thought to be due to the formation of carbonates at the expense of alkaline species (hydroxides). Thanks to carbonation, the pH of the eluate of the examined stainless steel slag is within the limits imposed by Italian legislation for material reuse ($5.5 < pH < 12$).
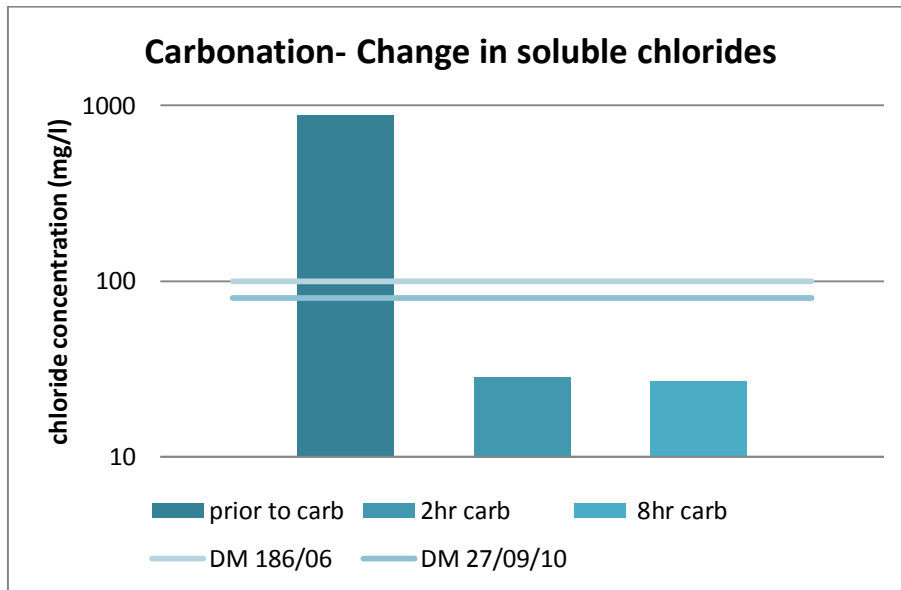
Figure 5.18: Results comparing the soluble chloride content (mg/l) of the leachates from the 2 and 8h column treated material against the untreated material.

Figure 5.18 shows the amount of soluble chlorides detected in the leachates, before and after 2 and 8h during carbonation. A substantial drop in the amount of soluble chlorides is seen to have occurred during carbonation. After 2h, the initial concentration had been cut back with a factor of 31, causing a concentration of 28.41 mg/l compared to the initial value of 885.14 mg/l. For longer carbonation times, the soluble chloride concentration decreased further, at a lower rate, reaching 26.8 mg/l after 8h of reaction. This decrease has also been noted by Apul et al. (2005) and Fällman et al. (2000) and was attributed to the sorption of oxyanions (such as ClO^- upon the surface of precipitated metal (hydr)oxides. Overall, the treatment caused the material to be safely within the limits imposed by Italian legislation for both inert waste landfilling and material reuse (80 and 100 mg/l respectively).

5.4.2.1.2.2   Other elements

After ICP analysis of the eluates (analysed pure, 1:10 and 1:500), a comparison between the treated and untreated leachate was made for the most relevant major (Figure 5.19) and trace (Figure 5.20) elements.

Figure 5.19: Results comparing the content of selected major elements (mg/l) of the leachates from the 2 and 8h column treated material against the untreated material (left). Showing the fraction of the element in the (untreated) solid being leached (%) (right).
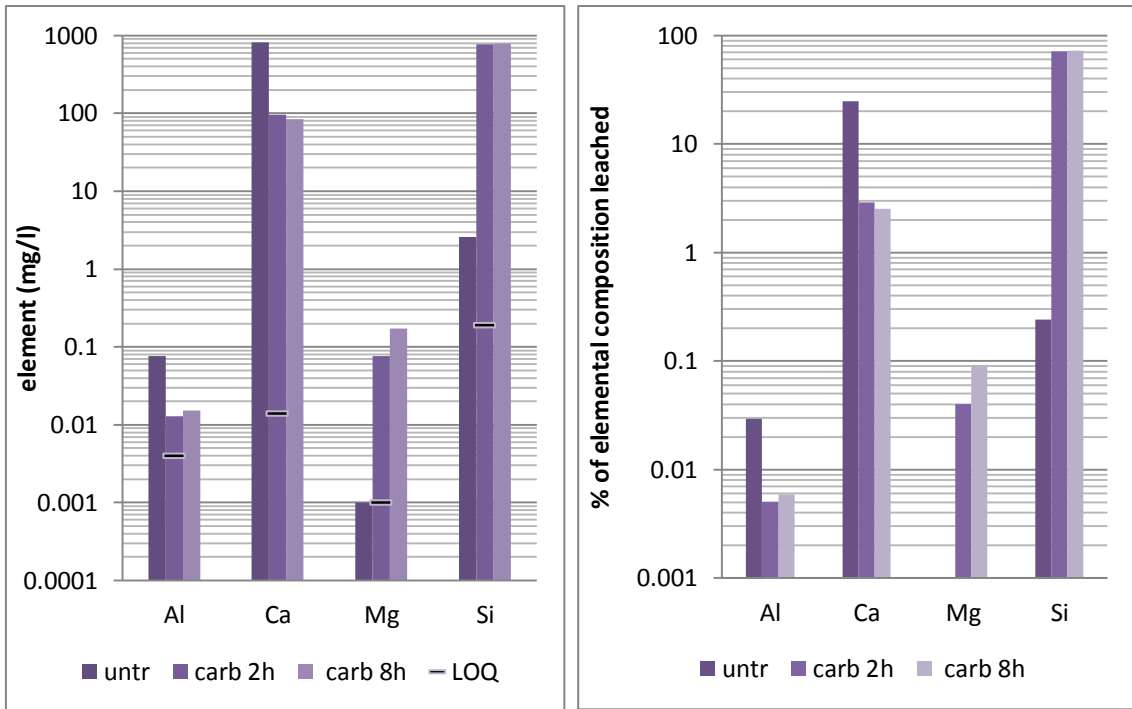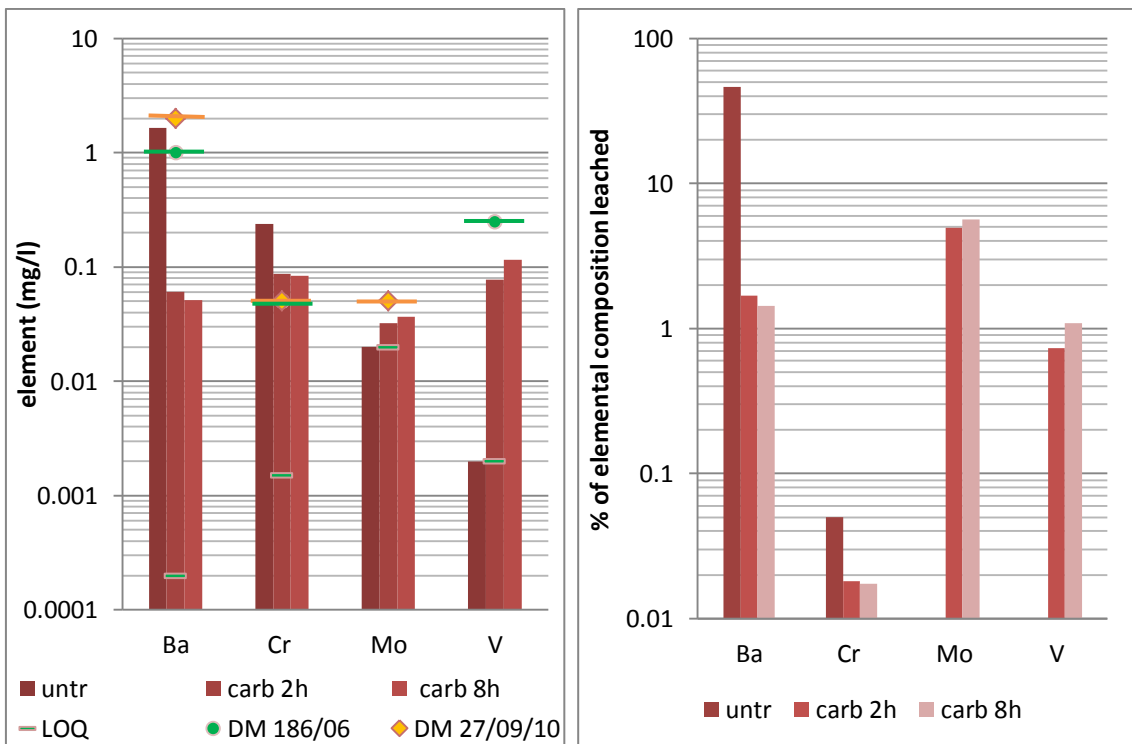

Figure 5.20: Results comparing the content of selected trace elements (mg/l) of the leachates from the 2 and 8h column treated material against the untreated material (left). Showing the fraction of the element in the (untreated) solid being leached (%) (right).

Considering the absolute values, it can be seen that the major elements were subject to significant changes due to carbonation. Ca and Al concentrations showed a pronounced decrease, with their concentration after 2h of carbonation being respectively less than $1/8^{th}$ (12%) and $1/5^{th}$ (20%) of the concentration in the untreated leachate. For longer carbonation times (8h), Ca showed a further but slower decrease in concentration and Al a slight rebound. The former is due to the formation of stable and less soluble carbonates, consuming the more soluble Ca^{2+} bearing phases. The decrease in the Al concentration may possibly be due to the fact that upon carbonation, Al was released due to (partial) dissolution of the reactive phases it was held in and possibly was taken up in less soluble phases. Moreover, the solubility of Al decreased with decreasing pH, causing reduced leaching. On the other hand, Mg and Si showed a notable increase in their leached concentration with carbonation extent: after 2h their concentrations were respectively 75 and 360 times larger than initially and increased further with time. This likely resulted from the dissociation of stable silicates and melilite and the formation of new, more soluble phases upon carbonation.

The effect of carbonation on the leaching of trace elements is of great interest because some of these are environmentally harmful and their maximum concentration in eluates is constrained by legislation. The 2h-treatment already caused a sharp decrease with a factor of over 27 (3.7% of the initial value) in the concentration of Ba in the leachate so it was no longer exceeding the limits of 'reuse' (It. MD 186/06) and 'inert waste landfill' (It. MD 27/09/10). The eluates Cr-concentration was initially significantly above both limits, and were still surpassed after carbonation, despite a decrease with factor 3. However, the trend of a further decreasing concentration with carbonation time indicates the possibility of reaching acceptable values after longer carbonation times. The opposite was found for the trace elements Mo and V: a steady increase for Mo occurred with reaction time, reaching a value 1.6 times (61.1% increase) the initial value after 2h. For V this increase was even more pronounced, its concentration being 38.8 times higher after 2h and further increasing for longer carbonation times (although at a lower rate). Therefore it should be noted that for Mo and V, increasing the carbonation time could lead to an exceedance of the DM 27/09/10 and DM 186/06 limits respectively.

The carbonation effect was also assessed by expressing the leached concentration as a fraction (%) of the total elemental concentration:

$$Fraction\ leached\ (\%) = \frac{c_{X,Leach}(\frac{mg}{kg})}{c_{X,Solid}(\frac{mg}{kg})} * 100 \tag{5.1}$$

From this it was found that the major elements Al as well as Mg leached a negligible small fraction of their total solid concentration before and after treatment. For the untreated material, only Ca initially leached a significant fraction of its total concentration (2.5%), which fell below 0.3% after treatment. On the other hand, over 7% of the total concentration of Si leached after 2 hours of carbonation, while before treatment this was less than 0.025%. Considering the trace elements, initially only Ba leached a significant percentage of its total concentration (4.6%), dropping to values below 0.17% after treatment. The initial percentage of total Cr, Mo and V leached was negligible, but after carbonation the fraction of Mo and V being leached increased to values of 0.5 and 0.07% respectively.

5.4.2.2 Acid Neutralization Capacity
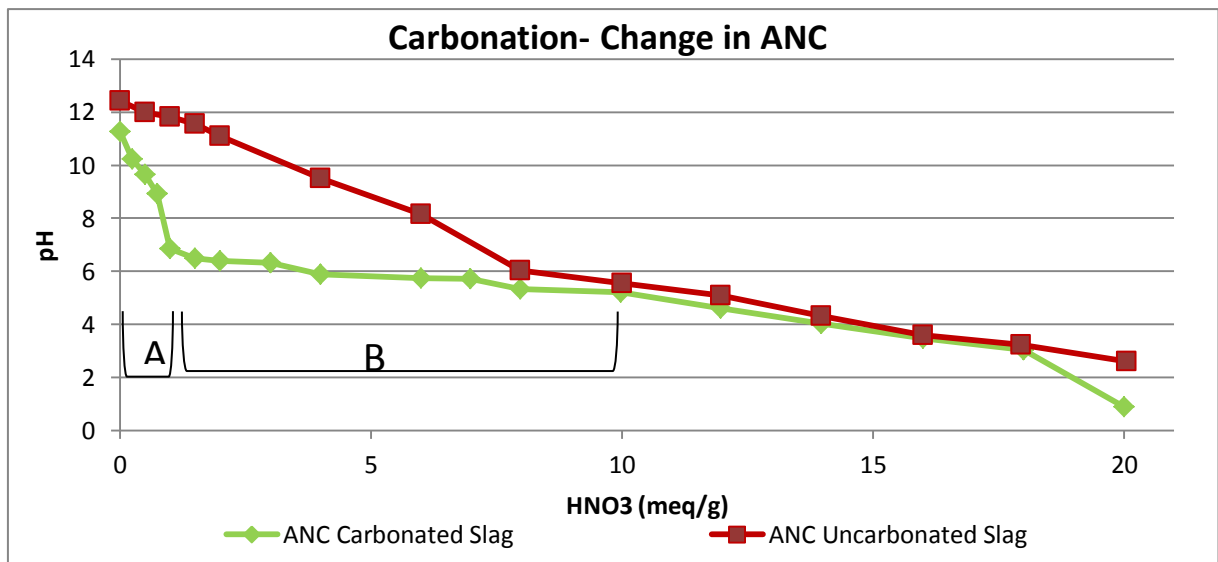
Figure 5.21: Comparison of the results of the ANC test on the treated and untreated intermediate slag fraction.

In the ANC graph for the treated material (Figure 5.21), 2 sections may be identified where the pH evolution was significantly altered compared to the untreated material: A and B. For section A, between 0 and 6.9 meq/g HNO_3, there is now a steep decrease in pH (from 11.28 to 6.86) with the amount of acid added in contrast to the 'plateau' (from 12.43 to 11.55) which was present over the same range for the ANC of the untreated material. This is due to the conversion of the hydroxides in the material as a consequence of carbonation and the

115

formation of carbonates. Therefore, buffering capacity in this range is drastically reduced. As a consequence of the reaction of these hydroxides to form carbonates such as calcite, the buffering capacity in the neutral pH range has been expanded. The latter is indicated as region B, where the decrease in pH is minimal: a change from pH 6.86 to 5.33 is observed for 6.9 to 10.0 meq/g acid addition. The ANC curve beyond this point is fairly identical for the treated and the untreated slag. The data for selected elements is displayed in Figure 5.22.
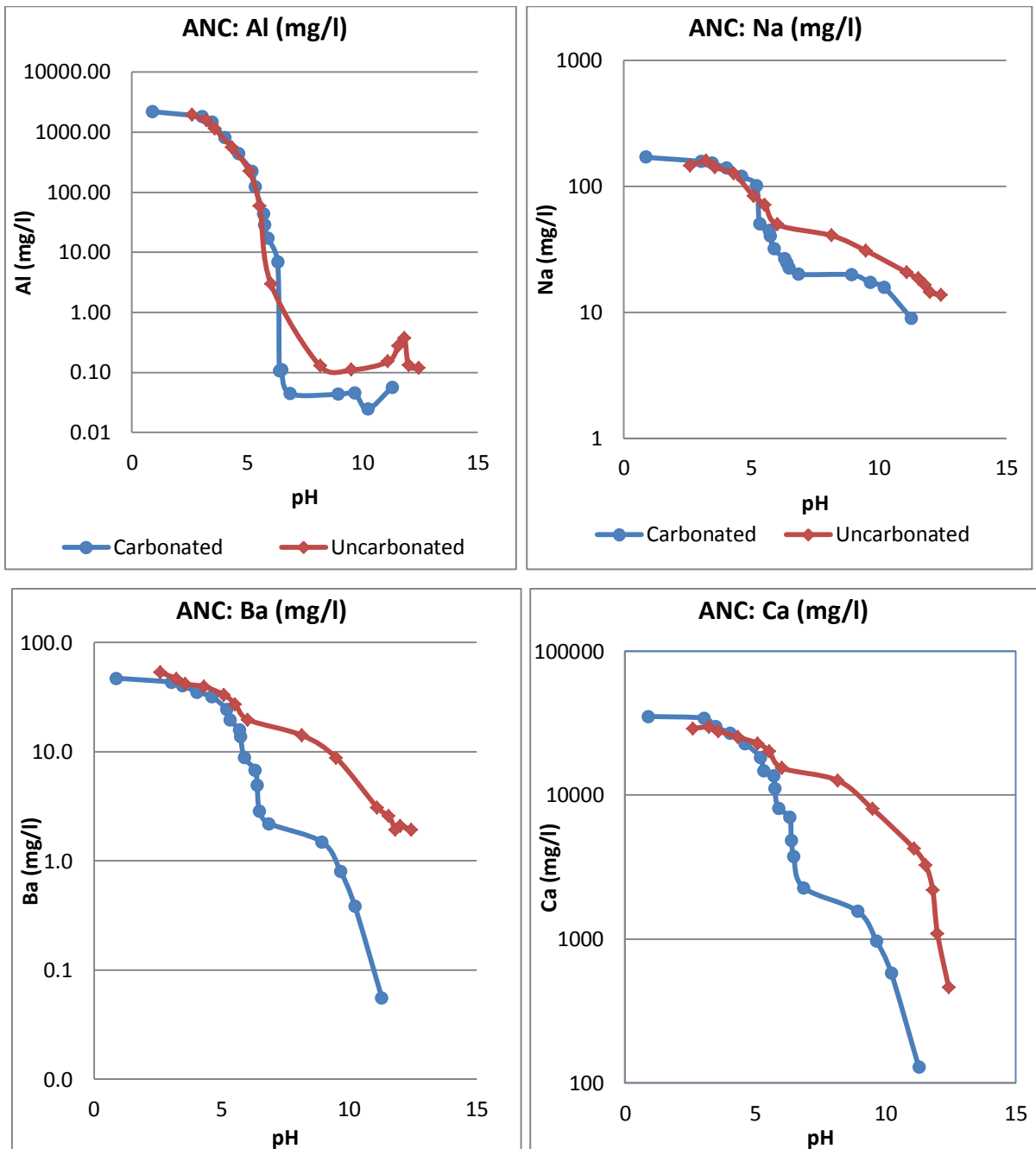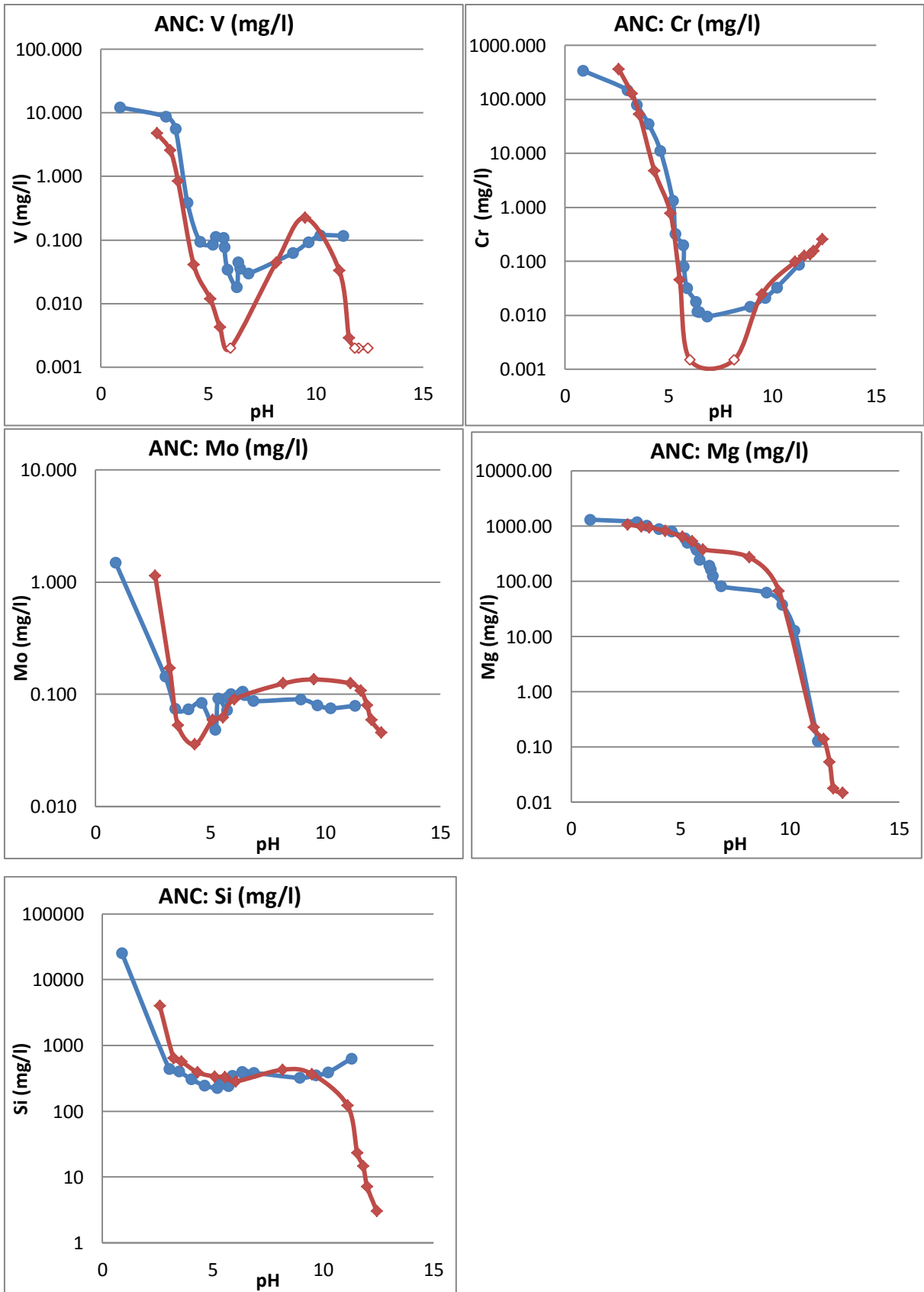
Figure 5.22: Comparison of the results of the ANC test on the treated and untreated intermediate slag fraction for selected elements.

From Figure 5.22, the impact of carbonation on the concentration of several elements with pH can be seen. The elements Al, Ca, Ba and Na have a significant lower concentration over the alkaline pH range for the carbonated slag. This is due to the fact that these elements were present in less soluble phases after treatment. For Ca and Ba, the change in behaviour is similar: carbonation resulted in a lower concentration over the alkaline to neutral pH range. In the case of Ca this is due to the formation of carbonates, possibly Ba and Mg have formed (or have been included in) carbonate species as well. V and Cr are seen to follow the typical behavior of metals with a smaller solubility over a lower near-neutral pH. However, especially V and also Cr showed larger leaching concentrations overall following treatment. The reason for this may not be derived from the XRD analysis since no phases containing these elements were detected. However, a possible explanation for V could be found in the V-bearing di-Ca silicate (C_2S) mineral phase as indicated by van Zomeren et al. (2011) or by the dissolution of Ca-vanadate (Apul et al., 2005; Fällman et al., 2000). The dissolution of this former phase appears to be significantly enhanced due to carbonation, thereby increasing V-leaching. The solubility of Si has been significantly increased at alkaline pH, due to its incorporation into hardly soluble silicates.

6 **DISCUSSION**

6.1 **Material properties**

During and after the characterisation tests of the stainless slag material, which was supplied under the name of 'pure AOD slag', it was remarked that the material possessed deviating properties. This appeared both from the XRD analysis (Figure 5.3), from which it was clear that many more phases were present relative to the AOD that was analysed by Baciocchi et al. (2010). However it must be noted here that the XRD analysis was rather qualitative than quantitative, and that minor phases may not have been displayed due to overlap with major phases, causing a larger response signal. Only mineralogy is however not sufficient to draw conclusion on the nature of a material, as was apparent from para. 3.2.2.1, where different research on the same kind of materials systematically reported a wide range of mineral species. Therefore the results of the elemental composition of the material (Figure 5.2) were analysed and subsequent comparison with the findings of previous research on similar material, may confirm that the investigated material is most likely indeed not pure AOD as illustrated in Table 6.1.

Indeed from this the elemental composition of the material seems to correspond strongly to the range of concentrations generally found for EAF slag (Proctor et al., 2000; Baciocchi et al., 2011; Huiting & Forssberg, 2003), with exception of the concentration of Cr, As and Ni which are significantly higher and the concentrations of Mg and Mn which are lower than usually found for EAF. On the other hand, the observed values of Cr, Mn and Ni are in line with concentrations generally found for AOD (Lopez et al., 1997). Only the value of Mg is somewhat deviating from the standard composition of both materials in the sense that it is lower. This confirmed the presumption that the material provided was not truly 100% AOD taken from the argon decarburization unit, but was probably a mix of AOD and EAF slag (possibly even with other slags).

Table 6.1: Comparison of the elemental composition of the examined slag (AOD 2012) with data from previous research on AOD and EAF slag.

	Current material	Baciocchi et al. (2011)	Lopez et al. (1997)	Huiting & Forssberg (2003)	Baciocchi et al. (2011)	Proctor et al.	Huiting & Forssberg (2003)
El.	Average (mg/kg)	AOD (mg/kg)	AOD	AOD	EAF (mg/kg)	EAF	EAF
Al	24696	6850	-	-	20530	35009	-
As	22	-	-	-	-	1.9	-
Ba	349	-	-	-	-	557	-
Be	0	-	-	-	-	1.1	-
Bi	29	-	-	-	-	-	-
Ca	307197	403300	-	-	352000	250653	-
Cd	0	20	-	-	0.3	7.6	-
Co	0	-	-	-	-	4.8	-
Cr	37725	400	33800	17100	37330	3046	32200
Cu	291	530	850	-	170	178	-
Fe	32064	620	20750	20300	32270	190211	15600
Hg	7	-	-	-	-	0.04	-
K	1360	110	-	-	390	-	-
Mg	17511	14390	-	-	24670	54460	-
Mn	11210	-	-	-	-	39400	-
Mo	54	<2	-	-	230	30	-
Na	1436	730	-	-	3410	-	-
Ni	1041	60	3350	2000	480	30	750
Pb	23	70	450	-	90	27.5	50
Sb	318	-	-	-	-	4	-
Si	98478	141500	-	-	131500	74524	-
Sn	16	-	-	-	-	10	-
Tl	0	-	4050	-	-	11	-
V	850	2	-	-	970	513	-
Zn	107	120	250	100	260	165	110

6.2　Column carbonation

In order to evaluate the functioning of the column setup along with the applicability of the applied procedure, in this section the obtained results will be discussed and put into perspective.

A first means of assessing the functionality of the new column set-up may occur through comparison of the results of the batch and the column test, which both were performed under the same 'column conditions' (Figure 6.1).
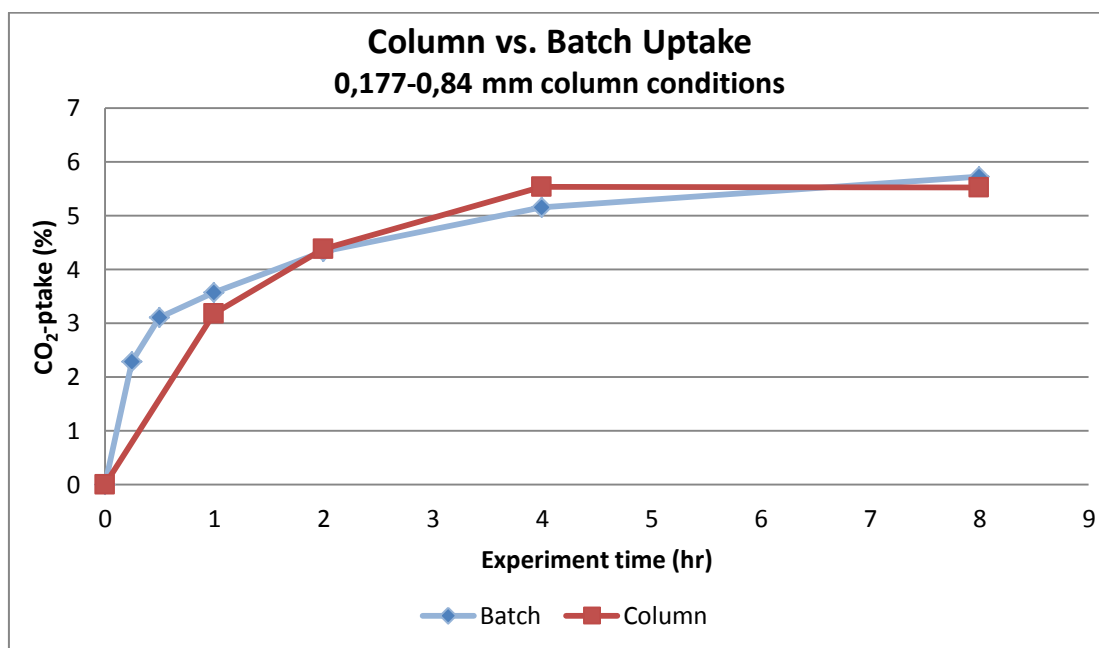
Figure 6.1: Comparison of the CO_2-uptake obtained by using the batch and column setup under the same conditions ($22°C$, 10.4ml/min CO_2, L/S=0.2).

Despite the fact that the 2 methods made use of a completely different setup and while only 3g of slag was used in the batch experiments compared to 40g in the column experiment, it can be seen from Figure 6.1 that the similarity in results is striking. The final CO_2-uptake reached after 8h amounted to 5.5% for the column setup and 5.7% for the batch setup. This result gives confidence and credibility to the applicability of the column set-up to investigate slag carbonation processes.

A remarkable finding during the experiments was that for short reaction times (1h), the 'bottom part' of the material in the column was found to have higher CO_2-uptakes, whereas for longer times (4 or 8h), this trend was reversed. While the cause of the initially higher uptake for the bottom material has already been addressed in para. 5.3.2 to be (probably)

caused by the slow progression of the gas through the medium, it would have been expected that for longer reaction times the values for all sections would converge. As could be seen from Figure 5.11 and Figure 5.12, uptake is lowest for the bottom layer at reaction times of respectively 4 and 8h, and this trend is more apparent for the experiments with L/S of 0.2. This led to the presumption that this phenomenon could be due to changes in the L/S ratio during the test. The initial effective L/S ratio at the beginning of the experiment was known, but not how this L/S ratio evolved during the experiment. Changes in moisture content could occur due to the continuous flow of the gas through the medium (although only 10.4 ml/min), what could potentially affect the carbonation efficiency. Depending on the efficiency of the bubbler in wetting of the gas, slight variations in the L/S were possible.

To assess this, the final effective L/S ratio was determined at the end of some experiments. This was done by putting all material in the oven at 105°C overnight and recording the weight decrease, equal to the amount of water present at the end of the experiment. The change (d) in L/S (%) was then calculated as:

$$d\left(\frac{L}{S}\right) = \frac{\left(\frac{L}{S}\right)_i - \left(\frac{L}{S}\right)_f}{\left(\frac{L}{S}\right)_i} * 100 \; (\%) \qquad (6.1)$$

where the $(L/S)_i$ or $(L/S)_f$ respectively are the initial and final L/S.
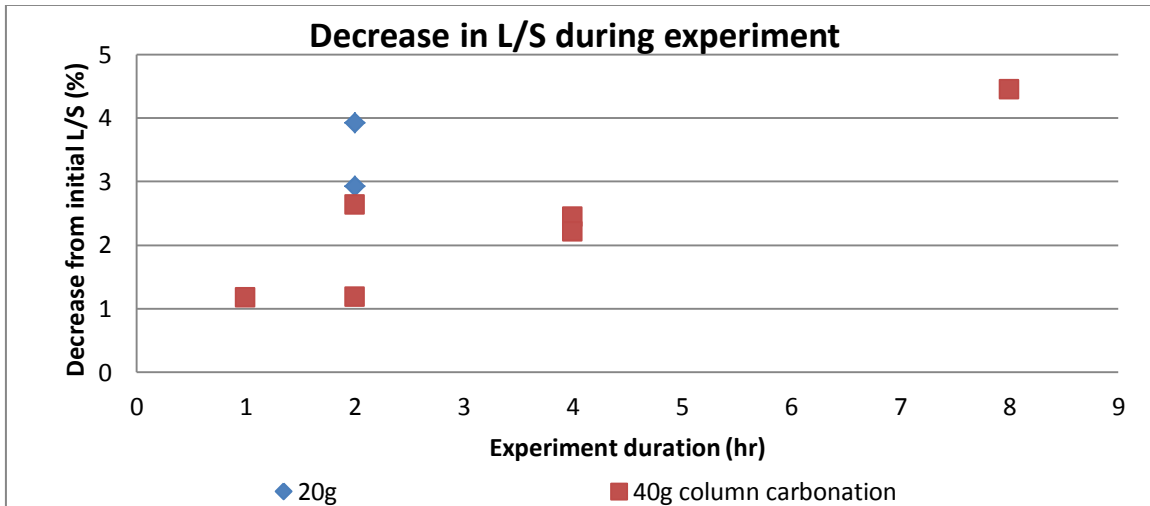
Figure 6.2: Changes observed between the initial and final L/S ratio in function of experiment duration.

The results of this are shown in Figure 6.2. For all examined tests, a decrease in L/S ratio appeared between 1 and 4.5% for the 1 and 8h reaction times respectively. For a given test, the L/S ratio decreased linearly with increasing experiment duration. Indeed, it seemed that for a lower mass of material (20g), the decrease in the moisture content was larger for a given

reaction time compared to the tests with 40g of material. This was to be expected since a lower amount of material and a constant gas flow rate results in a shorter residence time of the gas in the medium. Most likely the gas flow took up a small amount of water while flowing through the column and this water exited the column together with the gas flow (or moved upwards in the column), causing the L/S to gradually but slowly drop, first for the lower part of the column. Thus although this decrease seems small, it was calculated as the average of all layers, and the effective drop in L/S was probably relatively larger for the bottom part, resulting in a decreased carbonation rate. Since the decrease was only minor, the set-up was not changed. However, for tests with a longer duration, this effect could become more important and should be taken into account for example through making changes in the bubbler configuration to increase its efficiency in wetting the gas.

As discussed in para. 4.2.3.2, apart from the standard procedure of wetting the material through mixing, also a different method of wetting through percolation was used. Different procedures were tried out in order to see how the best results could be obtained. Also, the percolation method could yield results more representative for in-situ field-application, since mixing of the material is not attainable in that case. However the mixing method seemed to have the advantage that the moisture distribution of the material was more homogeneous. To assess if the use of both techniques led to different results, data was compared in Figure 6.3.
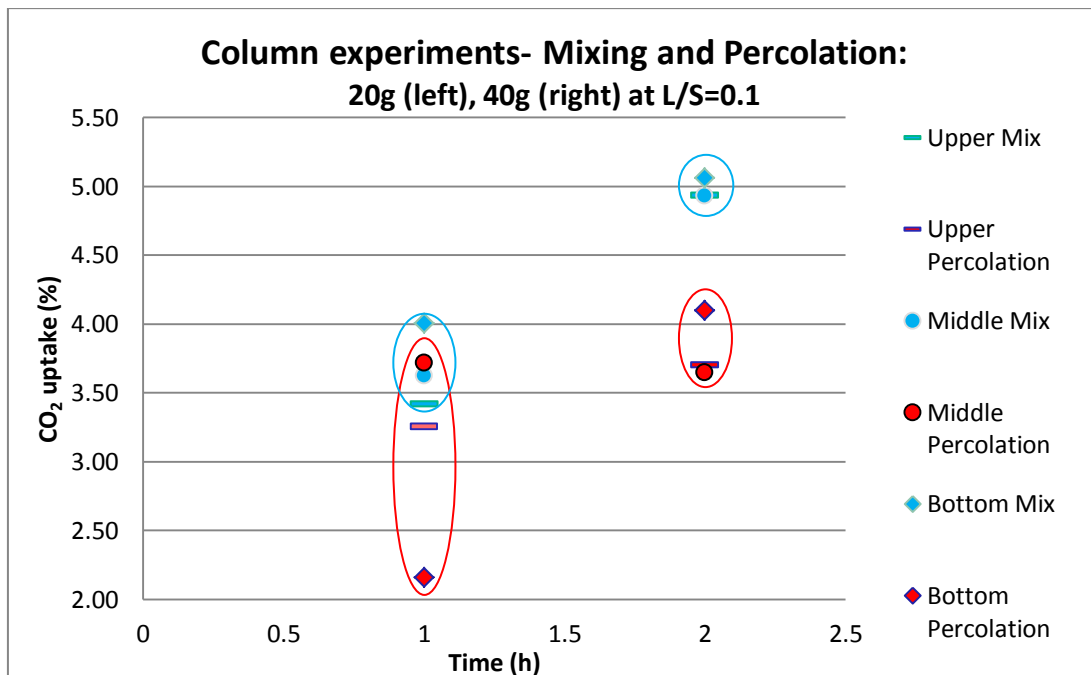
Figure 6.3: CO$_2$-uptake for the column test using the procedures 'Mixing' and 'Percolation' for 20 g (left) and 40g of material (right) under 22°C and 10.4ml/min CO$_2$ for a L/S=0.1.

123

The results demonstrate that the CO_2-uptake values for the distinct layers of material deviate more from one another in experiments when 'percolation' (red) was used than for those where 'mixing' (blue) was applied. Also the absolute column-averaged CO_2-uptake is larger when using the mixing method. The explanation for this is probably as follows: using 'percolation', some areas of the material became well-wetted while others remained dry due to the percolation of the water through the medium along preferential pathways. These dry patches could only achieve a lower carbonation extent due to the lack of water present. In contrary when the material was mixed prior to insertion, the moisture was distributed more homogeneously, leading to a more homogeneous uptake for all material. This was already expected before starting the experiments and was confirmed from the data. Therefore, somewhat lower uptakes could result during field-application, depending on the moisture distribution.

In order to be able to put the differences in CO_2-uptake values between different conditions or different set-ups in perspective, the repeatability of the tests was assessed. This was done by repetition of the same test for 2 or more times, under identical conditions to identify the range of error in the values that might be attributed to the technical aspect of the experiments. The outcomes of this may be seen in Figure 6.4.
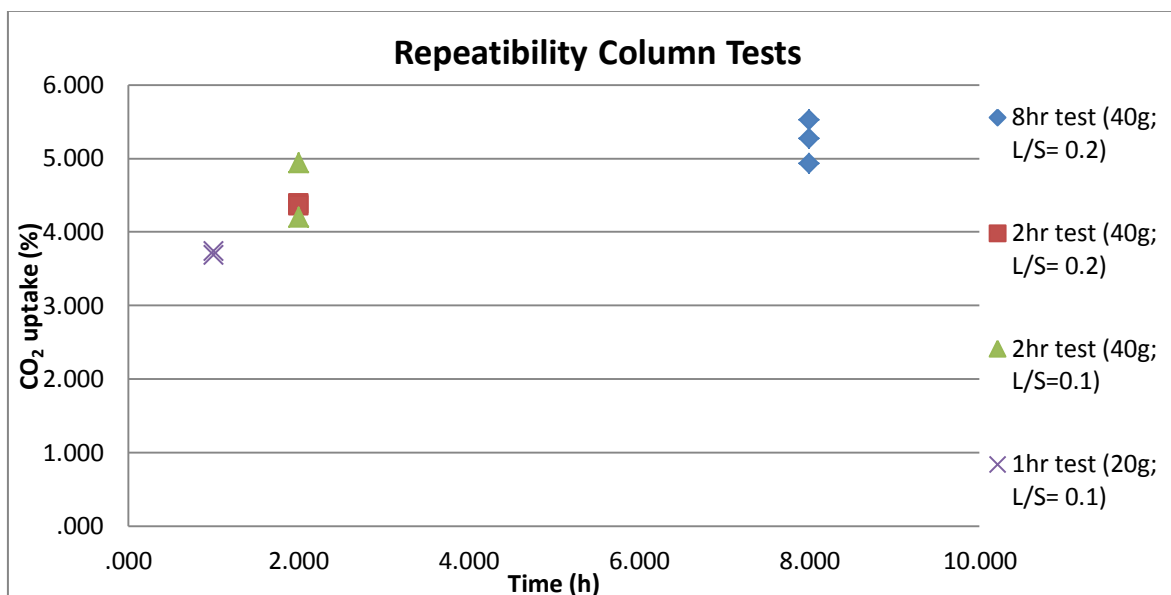
Figure 6.4: Representation of the differences in results, obtained by repeating multiple experiments under identical conditions and procedures to obtain the repeatability value.

The repeatability error was calculated by:

$$(X-\mu)/\mu)*100 \tag{6.2}$$

in which X is the final CO_2-uptake value for an experiment run and μ is the mean of the 2 or 3 runs performed. This repeatability error varied between 0.8% and 8% for the 1h test (20g, L/S=0.1) and the 2h test (40g; L/S=0.1) respectively.

This may be due to e.g. differences in the material, difference in sample preparation for the test, slight differences in test conditions and inaccuracy of the TIC analyser. Differences in material preparation might be residing in the compaction of the material that was performed manually and thus may have led to a slightly different compaction degree for each test. This might vary the effective porosity of -and the CO_2-flow throughout- the medium and thus also the CO_2-uptake. Other possible sources of error could be due to slight differences in test conditions such as slight fluctuations in temperature (what could making the bubbler more or less effective in wetting the CO_2 gas) or slightly different chemical properties of the used material, although the material was well mixed before use. However it is expected that the importance of these factors was minimal.

Finally, the accuracy of the TIC analyser could have affected the measurements: in general the measurement error between 2 or 3 IC analysis results on the same sample was in the order of 2-4% but could be in some cases be 0-11%. The reason for this is not known and is attributed to measurement inaccuracy of the device itself. Thereby it may be concluded that the overall repeatability of the experiments (taking into account the TIC measurement error) was good.

7 **CONCLUSION**

The main aim of this dissertation was to investigate the feasibility of applying in-situ accelerated carbonation upon alkaline industrial (steel) wastes as component of an holistically integrated technology train in the HOMBRE project. In this framework, the two techniques of ECO-GROUT and ACT could be combined to lead to superior results. The final, bigger aim is to enable a faster, more efficient, and more sustainable redevelopment of brownfield areas.

Research on waste carbonation was already quite numerous, with most of the work examining the impact of specific reaction factors such as temperature, CO_2-pressure, grain size, and L/S ratio and the carbonation efficiency of different kinds of alkaline wastes. However, research on direct wet carbonation of stainless steel slags, and subsequently focussing on the effect of different carbonation extents on the (environmental) slag properties, was hardly present. Since in most work the accent is put on achieving maximum CO_2-uptakes under highly enhanced reaction conditions, the resulting energy consummation is superfluous, rendering large-scale application of these techniques unfeasible from an economical point of view. Therefore the current dissertation researched this direct wet carbonation route, by developing a new experimental set-up, operating under ambient conditions in a column tube. This was done in order to simulate field conditions on a lab-scale, to ensure the potential applicability of the method for large-scale remediation. Therefore, emphasis was put on quantifying the effect of treatment on the environmental behaviour of the slag.

The results from the performed batch and column experiments have indicated that this new column carbonation set-up yields carbonation efficiencies that are almost as efficient as the more-widely investigated batch method, when identical conditions are applied. This gives confidence in the method used and also in the applicability at later stage in the field. This is due to the fact that during the column experiment a slow, upward CO_2-flow was generated through the medium; as it could result from CO_2-degassing of the underlying areas where ECO-grouting could be applied. In addition to this, the applied conditions were such that they could be applied during in-situ field treatment as well. Tests were operated under a temperature of 22°C and a L/S ratio of 0.1 or 0.2. Due to the ambient reaction conditions, no

excessive energy-consumption (and related costs) is inherent to the treatment procedure, making field-scale application more apt.

The maximum achieved CO_2-uptake for the 8h column carbonation experiment was 5.7% against a virtually identical value of 5.72% for 8h carbonation in the batch, under similar conditions. For 8h carbonation in batch under enhanced conditions, i.e. 50°C, 10bar CO_2 and L/S of 0.4, an uptake of 6.5% was reached: only less than 1% higher. Therefore it can be stated that the importance of temperature (22-50°C) and CO_2 pressure (<1-10 bar) was limited (Fig. 5.10), and the importance of L/S (0.1-0.2) was nihil. Although the measured CO_2-uptake was not large, it was significant, and the treatment did impact the environmental behaviour of the slag. While the concentration of some potentially harmful compounds such as Al, Ba and Cr decreased, on the other hand increases for Mo and V were found in the leachate. Longer experiment runs should therefore be performed on the material to determine if these trends persist for longer reaction times, what could possibly lead to an exceedance of concentration limits imposed by national or supra-national (EU) laws. The significantly increased buffer capacity of the material upon carbonation may also point out its suitability to be used in other applications such as for the neutralization of acid solutions (acid mine drainage).

In addition to the chemical changes of the material, also changes in physical properties were observed during the tests. Carbonation of the loose material resulted in the formation of a harder, more coherent matrix. Although the increases in strength or durability were not quantified, it seemed as if carbonation also had a positive impact on these properties and thus applying in-situ ACT could help increase matrix stability.

From these findings, it may show that in-situ ACT may be a valuable technique for application in the field of soil-and water pollution, and remediation of brownfield areas. Costs could be reduced by integrating the remediation of the saturated and unsaturated zone. Since remediation may occur in-situ, this (integrated) technique could especially be of interest in situations where the contaminated material is located at/under non-abandoned sites where dig-and-dump options are out of the question, for example in urban areas.

Before proceeding to the implementation of the researched ACT technique, possibly coupled to ECO-GROUT in the framework of the HOMBRE project, it is necessary to perform additional research to better understand the observed patterns. It should be realized that accelerated carbonation would occur over longer time-scales (weeks-months) when applied

in-situ due to the CO_2-degassing from the grouting occurring over a longer period. Therefore on one hand further research may be done by performing accelerated carbonation tests on the material of interest for durations also exceeding 8h, using the same column set-up, preferably with some modifications such as a better wetting of the inflowing gas. This in order to see what the trend in the material property changes would be for longer time-scales and to investigate whether possibly limits for leaching are surpassed by certain elements. The next stage could be to interpret the present and future results through modelling of the carbonation and leaching process, in order to reproduce the observed (mineralogical) changes like: the transformation of Ca-phases into calcite; a negative pH evolution; and changing leaching behaviour. In this way, the conditioned model could be applied to simulate the leaching behaviour under different environmental conditions over longer time scales.

REFERENCES

Adolfsson, D. (2011) *Cementitious Properties of Steelmaking Slags*. Doctoral thesis. Lulea University of Technology, Department of Chemical Engineering and Geosciences, Sweden.

Andrade, J.Á., Augusto, F. & Jardim, I.C.S.F. (2010) Biorremediação de solos contaminados por petróleo e seus derivados. *Eclética química*, 35(3), 17-43.

Angel, S., Bradshaw, K., Clear, C. A., Johnson, D., Kenny, M., Price, B. W. & Southall, M. (2004) *The essential guide to Stabilization/Solidification for the remediation of Brownfield land using cement and lime*. British Cement Association, Camberley.

Antemir, A., Hills, C.D., Carey, P.J., Gardner, K.H., Bates, E.R. & Crumbie, A.K. (2010a) Longterm performance of aged waste forms treated by stabilization/solidification. *Journal of Hazardous Materials*, 181, 65-73.

Antemir, A., Hills, C.D., Carey, P.J., Magnié, M.C. & Polettini, A. (2010b) Investigation of 4 year old stabilized/solidified and accelerated carbonated contaminated soil. *Journal of Hazardous Materials*, 181, 543-555.

Apul, D.S., Gardner, K.H., Eighmy, T.T., Fällman, A.M. & Comans, R.N.J. (2005) Simultaneous application of dissolution/precipitation and surface complexation/surface precipitation. *Environ Sci Technol.,* 39(15), 5736-41.

Baciocchi, R., Costa, G. & Di Bartolomeo, E. (2011) Wet versus slurry carbonation of EAF steel slag. *In Focus: Papers from ACEME10 – The Accelerated Carbonation for Environmental and Materials Engineering conference issue. Greenhouse Gas Science Technology*, 1, 312-319.

Baciocchi, R., Costa, G. Polettini, A. & Pomi, R. (2010a) Carbonation of stainless steel slags at mild operating conditions. *Processes and Technologies for Sustainable Energy*, Ischia, June 27-30.

Baciocchi, R., Costa, G., Di Bartolomeo, E., Polettini, A. & Pomi R. (2012) Wet vs. Slurry carbonation of stainless steel slag. Greenhouse Gases: *Science and Technology*, 4, 312-219.

Baciocchi, R., Costa, G., Di Bartolomeo, E., Polettini, A. & Pomi, R. (2010b) Carbonation of stainless steel slag as a process for CO_2 storage and slag valorization. *Waste Biomass Valor.*, 1, 467–477.

Baciocchi, R., Costa, G., Polettini, A. & Pomi, R. (2009) Influence of particle size on the carbonation of stainless steel slag for CO_2 storage. *Energy Procedia*, 1 (1), 4859-4866.

Baddoo, N.R. (2007) Stainless steel in construction: A review of research, applications, challenges and opportunities. *Journal of Constructional Steel Research,* 64, 1199–1206.

Bastão de Souza, R., Guilherme Maziviero, T., Aparecida Christofoletti, C., Gimenez Pinheiro, T. & Silvia Fontanetti, C. (2013) Soil Contamination with Heavy Metals and Petroleum Derivates: Impact on Edaphic Fauna and Remediation (Chapter 6). In: *Soil Processes and Current Trends in Quality Assessment*. Hernandez Soriano, M.C. (ed.) InTech. pp. 433.

Bertos, M.F., Li, X., Simons, S.J.R., Hills, C.D. & Carey, P.J. (2004) Investigation of accelerated carbonation for the stabilisation of MSW incinerator ashes and the sequestration of CO_2. *Green Chemistry*, 6 (8), 428–436.

Bertos, M.F., Simons, S.J.R., Hills, C.D. & Carey, P.J. (2004) A review of accelerated carbonation-technology in the treatment of cement-based materials and sequestration of CO_2. *Journal of Hazardous Materials*, 112, 193–205.

BIR (2013) *BIR Global Fact & Figures on Ferrous Metals – World Steel Recycling In Figures 2008-2012*. [Online]. Bureau of International Recycling, Ferrous Division. Available from: http://www.bir.org/assets/Documents/publications/brochures/7587FerrousReport2013.pdf [Accessed July, 2013].

Bobicki, E.R., Liu, Q., Xu, Z. & Zeng, H. (2012) Carbon capture and storage using alkaline industrial wastes. *Prog. Energy Combust.*, 38, 302–320.

Bullock, J. (n.d.) *Slag Air-cooled stainless steel slag*. [Online]. MPA, Mineral Products Association. Available from: http://www.mineralproducts.org/prod_slag07.htm [Accessed July, 2013].

C8S, Carbon8 Systems (n.d.) *Case Study Astra pyrotechnics*. [Online] Available from: http://www.c8s.co.uk/pdf/Astra_Pyro_Case_Study.pdf [Accessed July 2013]

Cannon, W.F. & Horton, J.D. (2009) Soil geochemical signature of urbanization and industrialization – Chicago, Illinois, USA. *Applied Geochemistry*, 24 (8), 1590-1601.

Capobianco, O. (2013) Formal personal communication. Tor Vergata University, Rome, Italy.

Cheeseman, C.R. & Virdi, G.S. (2005) Properties and microstructure of lightweight aggregate produced from sintered sewage sludge ash. *Resources, Conservation and Recycling*, 45, 18-30.

Chen, B., Yang, J.X. & Ouyang, Z.Y. (2011) Life Cycle Assessment of Internal Recycling Options of Steel Slag in Chinese Iron and Steel Industry. *Journal of Iron and Steel Research International,* 18 (7), 33-40.

Chen, Q., Johnson, D.C., Zhu, L., Yuan, M. & Hills, C.D. (2007) Accelerated carbonation and leaching behaviour of the slag from iron and steel making industry. *Journal of University of Science and Technology Beijing,* 14, 297-301.

Cioffi, R., Colangelo, F., Montagnaro, F. & Santoro, L. (2011) Manufacture of artificial aggregate using MSWI bottom ash. *Waste Management*, 31, 281-288.

CLA:RE (2006) *Remediation Trial at the Avenue Coking Works Using Stabilisation/Solidification and Accelerated Carbonation.* Case study bulletin, 5 (May 2006).

Colombus Stainless (2013) *Processes Simplified Process for Making Stainless Steel*. [Online]. Available from: http://www.columbusstainless.co.za/processes [Accessed July, 2013].

Colorado Mountain College (2013) *Inductively Coupled Plasma Optical Emission Spectrometer ICP-OES.* [Online]. Available from: http://www.coloradomtn.edu/web/campuses/leadville/timberline_analytical_laboratory/current_equipment/icpoes [Accessed July 2013].

Conner, J.R. (1990) *Chemical Fixation and Solidification of Hazardous Wastes.* Van Nostrand Reinhold, New York.

Connolly, J.R. (2007) *Introduction to X-ray Powder Diffraction*. [Online]. Available from: http://epswww.unm.edu/xrd/xrdclass/01-xrd-intro.pdf [Accessed July 2013].

Costa, G., Baciocchi, R., Polettini, A., Pomi, R., Hills, C.D. & Carey, P.J. (2007) Current status and perspectives of accelerated carbonation processes on municipal waste combustion residues. *Environ Monit Assess*., 135, 55-75.

Das, B., Prakash, S., Reddy, P.S.R. & Misra, V.N. (2007) An overview of utilization of slag and sludge from steel industries. *Resources, Conservation and Recycling,* 50, 40–57.

Deltares (2012) *Holistic Management of Brownfield Regeneration*. [Online] Available from: http://www.deltares.nl/en/expertise/101145/urban-land-and-water-management/811569 [Accessed November 2012].

Deltares (2013) Personal Communication.

DNPM (2007) *Sumário Mineral Brasileiro.* In: Ministério de Minas e Energia, Departamento Nacional de Produção Mineral, Brasília. Brazil.

Domínguez, M.I., Sarria, R.F., Centeno, M.A. & Odriozola, J.A. (2010) Physicochemical characterization and use of wastes from stainless steel mill. *Environmental Progress and Sustainable Energy*, 29, 471–480.

Doucet, F.J. (2010) Effective CO_2-specific sequestration capacity of steel slags and variability in their leaching behaviour in view of industrial mineral carbonation. *Minerals Engineering*, 3, 262-269.

Dri, M., Sanna, A. & Maroto-Valer, M.M. (2013) Dissolution of steel slag and recycled concrete aggregate in ammonium bisulphate for CO_2 mineral carbonation. *Fuel Processing Technology*, 113, 114-122.

EAG (2013) *Materials Characterization ICP-OES vs ICP-MS: A comparison.* [Online]. Available from: http://www.eaglabs.com/mc/icp-oes-vs-icp-ms.html [Accessed July 2013].

EEA (2007) *Progress in management of contaminated sites (CSI 015).* [Online]. Available from: http://www.eea.europa.eu/data-and-maps/indicators/progress-in-management-of-contaminated-sites/progress-in-management-of-contaminated-1 [Accessed March 2013]

EEA (2009) *Remediation Technologies Graphs.* [Online]. Available from: http://www.eea.europa.eu/data-and-maps/figures/remediation-technologies [Accessed June 2013].

EEA (2012a) *Overview of economic activities causing soil contamination in some WCE and SEE countries* (pct. of investigated sites). [Online]. Available from: http://www.eea.europa.eu/data-and-maps/figures/overview-of-economic-activities-causing-soil-contamination-in-some-wce-and-see-countries-pct-of-investigated-sites [Accessed June 2013].

EEA (2012b) *Detailed analysis of industrial and commercial activities causing soil contamination by country*. [Online]. Available from: http://www.eea.europa.eu/data-and-maps/figures/detailed-analysis-of-industrial-and-commercial-activities-causing-soil-contamination-by-country [Accessed June 2013].

EEA (2012c) *Overview of contaminants affecting soil and groundwater in Europe*. [Online]. Available from: http://www.eea.europa.eu/data-and-maps/figures/overview-of-contaminants-affecting-soil-and-groundwater-in-europe [Accessed June 2013].

Eloneva, S., Teir, S., Salminen, J., Fogelholm, C.J. & Zevenhoven, R. (2008a) Fixation of CO_2 by carbonating calcium derived from blast furnace slag. *Energy*, 33, 1461– 1467.

Eloneva, S., Teir, S., Salminen, J., Fogelholm, C.J. & Zevenhoven R. (2008b) Steel converter slag as a raw material for precipitation of pure calcium carbonate. *Industrial and Engineering Chemistry Research,* 47(18), 7104-7111.

ENEA, European Network of Environmental Authorities (2006) *The contribution of structural and cohesion funds to a better environment. European Commission.* [Online]. Available from: http://ec.europa.eu/environment/integration/pdf/preliminary_stocktaking.pdf [Accessed May 2013].

Environment Canada (2002) TAB #22 and #23: I*n-Situ and Ex-Situ Remediation Technologies for Contaminated Sites.* [Online]. Available from: http://www.on.ec.gc.ca/pollution/ecnpd/tabs/tab22-e.html [Accessed August 2013]

EPA (2000) *Solidification/Stabilization use at superfund sites*. Cincinnati. EPA/542/R00/010.

EPA (2006) *National Slag Association Presentation: Iron & Steel Slag, The Ultimate Renewable Resource.* [Online] Available from: http://www.epa.gov/wastes/conserve/imr/irc-meet/06-slag.pdf [Accessed July 2013]

Euroslag (2010) *Products – Statistic Data 2010*. [Online]. Available from: http://www.euroslag.com/ [Accessed July, 2013].

Fällman, A.M. (2000) Leaching of chromium and barium from steel slag in laboratory and field tests: a solubility controlled process. *Waste Manag*., 20, 149-154.

Forteza, R., Far, M., Seguí, C. & Cerdá, V. (2004) Characterization of bottom ash in municipal solid waste incinerators for its use in road base. *Waste Management*, 24, 899-909.

Gahan, C.S., Cunha, M.L. & Sandström, Å. (2009) Comparative study on different steel slags as neutralising agent in bioleaching. *Hydrometallurgy*, 95, 190–197.

Geldenhuis, J.M.A. (2002) Recovery of valuables from flue dust fines. *Mineral Eng*., 15, 95–98.

Goyer, R., Golub, M., Choudhury, H., Hughes, M., Kenyon, E. & Stifelman, M. (2004) *Issue Paper on the Human Health Effects of Metals* [Online]. U.S. Environmental Protection Agency. Available from: http://www.epa.gov/raf/publications/pdfs/HUMANHEALTHEFFECTS81904.PDF [Accessed July 2013]

Grotenhuis, T., Baciocchi, R., Hartog, N., Irminski, W., Malina, G., Menger, P., Smit, M. & Torres, N.N. (2012) *HOMBRE, Holistic Management of Brownfield Redevelopment: In Depth Analysis and Feasibility of the Technology Trains.* Report Number: D 4.1.

Halliday, A. (2012) *Essar illegally dumping hot iron slag, activist writes to minister. [Online]. The Indian EXPRESS.* Available from: http://www.indianexpress.com/news/essar-illegally-dumping-hot-iron-slag-activist-writes-to-minister/941279/ [Accessed July 2013].

Hills C. (1997) *Patent WO9713735* (ACT). Hazardous Waste Treatment.

HOMBRE (2010) *Urban redevelopment – Brownfield regeneration Brochure*. Available from:
http://www.zerobrownfields.eu/HombreMainGallery/Docs/Project/uBGS%20037%20A3EN%20december2010%20Duijne.pdf

HOMBRE (2012a) *HOMBRE HOlistic Management of Brownfield Regeneration: Urban redevelopment – Brownfield regeneration NEWS.* [Online] Available from: http://www.zerobrownfields.eu/HombreMainGallery/Docs/HOMBRE_Newsletter_01_2012_final.pdf [Accessed November 2012].

HOMBRE (2012b) Hand-out Brochure on the HOMBRE project.

HOMBRE Homepage (n.d.) *Aims and Project Description*. [Online] Available from: http://www.zerobrownfields.eu/ [Accessed November 2012].

Hou, X. & Jones, B.T. (2000) Inductively Coupled Plasma/ Optical Emission Spectrometry. In: Meyers, R.A. (Ed.). *Encyclopedia of Analytical Chemistry*, 9468-9485.

Huijgen, W. & Comans, R. (2005) *Mineral CO_2 Sequestration by Carbonation of Industrial Residues – Literature Overview and Selection of Residue*. Energy Research Centre of The Netherlands. Petten, The Netherlands (ECNC05074).

Huijgen, W. & Comans, R. (2006) Carbonation of Steel Slag for CO_2 Sequestration: Leaching of Products and Reaction Mechanisms. *Environm. Sci. Technol*., 40, 2790-2796.

Huijgen, W., Comans, R. & Witkamp, G.J. (2007) Cost evaluation of CO_2 sequestration by aqueous mineral carbonation. *Energy Convers. Manage*., 48, 1923–1935.

Huijgen, W., Comans, R. (2003) *Carbon dioxide sequestration by mineral carbonation, literature review; ECNC03016*. Energy Research Centre of The Netherlands. Petten, The Netherlands.

Huijgen, W., Witkamp, G.J. & Comans, R. (2005) Mineral CO_2 sequestration by steel slag carbonation. *Environ Sci Technol*., 39 (24), 9676–9682.

Huijgen, W., Witkamp, G.J. & Comans, R. (2006) Mechanisms of aqueous wollastonite carbonation as a possible CO_2 sequestration process. *Chemical Engineering Science*, 61, 4242-51.

Huntzinger, D.N., Gierke, J.S., Sutterc, L.L., Kawatrad, S.K. & Eisele, T.C. (2009) Mineral carbonation for carbon sequestration in cement kiln dust from waste piles. *Journal of Hazardous Materials*, 168 (1), 31-37.

ICDA (2007) *Health safety and environment guidelines for chromium*. ICDA, Paris.

IEA (2000) *CO_2 storage as carbonate minerals (PH3/17)* Newall, P.S., Clarke, S.J., Haywood, H.M., Scholes, H., Clarke, N.R., King, P.A. (eds.). IEA GHG. Cheltenham, U.K.

IEA (2012) *CO_2 emissions from fuel combustion Highlights*. [Online]. IEA Statistics. Available from: http://www.iea.org/co2highlights/co2highlights.pdf [Accessed August 2013].

IMD (2004) *World Competitiveness Centre International Institute for Management Development (IMD)- Brownfield competitiveness and redevelopment*. [Online]. Available from: http://www01.imd.ch/wcc/online/ [Accessed December 2013]

IPCC (2005) *IPCC Special Report on Carbon Dioxide Capture and Storage*. Prepared by Working Group III of the Intergovernmental Panel on Climate Change. Metz, B., Davidson, O., de Coninck, H.C., Loos, M. & Meyer, L.A. (eds.). Cambridge University Press, Cambridge, UK and New York, NY, USA. 442 pp.

IPCC (2007) *Climate Change 2007: Mitigation. Contribution of Working Group III to the Fourth Assessment Report of the Intergovernmental Panel on Climate Change*. Metz, B., Davidson, O., Bosch, P.R., Dave, R. & Meyer, L.A. (eds). Cambridge University Press, Cambridge, UK and New York, NY, USA.

Jiang, L.A. (2011) Review of physical modeling and numerical simulation of long term geological storage of CO_2. *Appl Energy*, 88, 3557–3566.

Johnson, D.C. (2000) *Accelerated Carbonation of Waste Calcium Silicate Materials*. SCI, Lecture Papers Series: 108/2000.

Johnson, D.C., Macleod, C.L. & Hills, C.D. (2003) Solidification of stainless steel slag by accelerated carbonation. *Environ. Technol*., 24, 671−678.

Kakizawa, M. Yamasaki, A. & Yanagisawa, Y. (2001) A new CO_2 disposal process via artificial weathering of calcium silicate accelerated by acetic acid. *Energy*, 26 (4), 341-354.

Karamalidis, A.K. & Voudrias, E.A. (2007) Cement-based stabilization/solidification of oil refinery sludge: leaching behavior of alkanes and PAHs. *Journal of Hazardous Materials*, 148, 122-135.

Khan, S., Cao, Q., Zheng, Y.M., Huang, Y.Z. & Zhu, Y.G. (2008) Health risks of heavy metals in contaminated soils and food crops irrigated with wastewater in Beijing, China. *Environmental Pollution*, 152 (3), 686-692.

Kim, Y. & Worrell, E. (2002) CO_2 emission trends in the cement industry: an international comparison. *Mitigation and Adaptation Strategies for Global Change*, 7, 115-133.

Kodama, S., Nishimoto, T., Yogo, K., & Yamada, K. (2006). *Design and evaluation of a new CO_2 fixation process using alkaline earth metal wastes.* In Proceedings of the 8th International Conference on Green House Gas Technology. Trondheim, Norway.

Kunzler, C., Alves, N., Pereira, E., Niencezewski, J., Ligabue, R., Einloft, S. & Dullius, J. (2011) CO_2-Storage with Indirect Carbonation Using Industrial Waste. *Energy Procedia*, 4, 1010-1017.

Lackner, K.S., Butt, D.P. & Wendt, C.H. (1997) Progress on binding CO_2 in mineral substrates. *Energy Convers. Manage.,* 38, 259-264.

Lackner, K.S., Wendt, C.H., Butt, D.P., Joyce, E.L. & Sharp, D.H. (1995) Carbon dioxide disposal in carbonate minerals. *Energy,* 20 (11), 1153-1170.

Laforest, G. & Duchesne, J. (2006) Characterization and leachability of electric arc furnace dust made from remelting of stainless steel. *J. Hazard. Mater*., B135, 156–164.

Lekakh, S.N., Rawlins, C.H., Robertson, D.G.C., Richards, V.L. & Peaslee, K.D. (2008) Kinetics of aqueous leaching and carbonization of steelmaking slag. *Metallurgical and Materials Transactions B*, 39B, 125-134.

Li, C.L. & Tsai, M.S. (1993) Mechanism of spinel ferrite dust formation in electric arc furnace steelmaking. *ISIJ Int*., 33, 284–290.

Lopez, F.A., Lopez Delgado, A. & Balcazar, N. (1997) *Physicochemical and mineralogical properties of EAF and AOD slag*. In: EOSC97: 2nd European oxygen steelmaking congress. pp. 417–426.

Ma, G. & Garberscraig, A.M. (2006) A review on the characteristics, formation mechanism and treatment processes of Cr (VI)-containing pyrometallurgical wastes. *The Journal of Southern African Institute of Mining and Metallurgy*, 106, 753–763.

Majuste, D. & Mansur, M.B. (2008) Characterization of the fine fraction of the argon oxygen decarburization with lance (AOD-L) sludge generated by the stainless steelmaking industry. *J. Hazard. Mater.,* 153, 89–95.

Majuste, D. & Mansur, M.B. (2009) Leaching of the fine fraction of the argon oxygen decarburization with lance (AODL) sludge for the preferential removal of iron. *Journal of Hazardous Materials*, 162, 356–364

Majuste, D. (2007) *Tratamento da lama fina gerada na lavagem de gases do convertedor AOD-L, na produção do aço inoxidável, visando a recuperação de cromo e níquel*. (M.Sc. Thesis). UFMG, Brazil, pp. 173.

Manso, J.M., Polanco, J.A., Losanez, M. & Gonzales, J.J. (2006) Durability of concrete made with EAF slag as aggregate. *Cement & Concrete Composites*, 28, 528-534.

Medici, F., Piga, L. & Rinaldi, G. (2000) Behaviour of polyaminophenolic additives in the granulation of lime and fly ash. *Waste Management*, 20, 491-498.

Meehl, G.A., Stocker, T.F., Collins, W.D., Friedlingstein, P., Gaye, A.T., Gregory, J.M., Kitoh, A., Knutti, R., Murphy, J.M., Noda, A., Raper, S.C.B., Watterson, I.G., Weaver, A.J. & Zhao, Z.C. (2007) *Global Climate Projections*. In: Climate Change 2007: The Physical Science Basis. Contribution of Working Group I to the Fourth Assessment Report of the Intergovernmental Panel on Climate Change. Solomon, S., Qin, D., Manning, M., Chen, Z., Marquis, M., Averyt, K.B., Tignor, M. & Miller, H.L. (eds.). Cambridge University Press, Cambridge, UK and New York, NY, USA.

Mehta, P.K. (1987) Natural pozzolans: Supplementary cementing materials in concrete. *CANMET Special Publication*, 86, 1–33.

Meima, J.A., van der Weijden, R.D., Eighmy, T.T. & Comans, R.N.J. (2002) Carbonation processes in municipal solid waste incinerator bottom ash and their effect on the leaching of copper and molybdenum. *Appl. Geochem.*, 17 (12), 1503-1513.

Miklos, P. (2000) *The utilization of electric arc furnace slags in Denmark*. In: Proceedings of 2nd European Slag Conference, Düsseldorf.

Mirsal, I.A. (2008) *Soil Pollution: Origins, Monitoring & Remediation*. Springer, Berlin.

Motz, H. & Geiseler, J. (2001) Products of steel slags an opportunity to save natural resources. *Waste Manage*, 21, 285-293.

Muchuweti, M., Birkett, J.W., Chinyanga, E., Zvauya, R., Scrimshaw, M.D. & Lester, J.N. (2006) Heavy metal content of vegetables irrigated with mixture of wastewater and

sewage sludge in Zimbabwe: implications for human health. *Agriculture, Ecosystem and Environment*, 112, 41-48.

Mukherjee, C. (2011) HC raps Tata Steel for slag dump. [Online]. *The Telegraph*, 2/08/2011. Available from: http://www.telegraphindia.com/1110802/jsp/jharkhand/story_14320949.jsp [Accessed July 2013].

Mulligan, C.N., Yong, R.N. & Gibbs, B.F. (2001) Remediation technologies for metal contaminated soils and groundwater: an evaluation. *Engineering Geology*, 60 (1–4), 193-207. Available from: http://www.sciencedirect.com/science/article/pii/S0013795200001010 [Accessed July 2013]

NASA (n.d.) *Earth Observatory Features: World of Change: Global Temperatures*. [Online]. Available from: http://earthobservatory.nasa.gov/Features/WorldOfChange/decadaltemp.php [Accessed June 2013].

National Slag Association (1998) *Steelmaking Slag: A Safe and Valuable Product*. [Online] Available from: http://www.nationalslag.org/archive/nsa_risk_assessment_summary.pdf [Accessed May 2013].

NineSigma (2011) *Request for Proposal Milled Stainless Steel Slag Application Adapted, Improved or New.* [Online]. Available from: https://www.myninesigma.com/_layouts/RFPs/NineSigma_RFP_67518.pdf [Accessed July 2013].

Nippon Slag Association (2003) Characteristics and applications of iron and steel slag. [Online]. Available from: http://www.slg.jp/e/slag/usage.html [Accessed July 2013].

NOAA (2012) *Climate at a Glance Time Series.* [Online]. Available from: http://www.ncdc.noaa.gov/cag/time-series/global [Accessed July, 2013]

Nolasco-Sobrinho, P.J., Espinosa, D.C.R. & Tenorio, J.A.S. (2003) Characterisation of dusts and sludges generated during stainless steel production in Brazilian industries. *Ironmak. Steelmak.*, 30, 11–17.

O'Connor, W. K., Dahlin, D. C., Rush, G. E., Gerdemann, S. J., Penner, L. R. & Nilsen, D. N. (2005) *Aqueous mineral carbonation (Final Report)- Mineral availability, pretreatment, reaction parametrics, and Process Studies*. Department of Energy, US.

Oldeman, L.R. (1992) *Global extent of soil degradation*. ISRIC Bi-Annual Report 1991-1992. pp. 19-36. Wageningen.

Oliver, L., Ferber, U., Grimski, D., Millar, K. & Nathanail, P. (n.d.) *The Scale and Nature of European Brownfields.* [Online] Available from: http://www.cabernet.org.uk/resourcefs/417.pdf [Accessed January 2013]

Orhan, G. (2005) Leaching and cementation of heavy metals from electric arc furnace dust in alkaline medium. *Hydrometallurgy*, 78 (3), 236-245.

Page, G.W. & Berger, R.S. (2006) Characteristics and land use of contaminated brownfield properties in voluntary cleanup agreement programs. *Land Use Policy*, 23 (4), 551-559, Available from: http://www.sciencedirect.com/science/article/pii/S0264837705000359 [Accessed March 2013].

Palencia, I., Romero, R., Iglesias, N. & Carranza, F. (1999) Recycling EAF Dust Leaching Residue to the Furnace: A Simulation Study. *JOM*, 51 (8), 28-32.

Pasetto, M. & Baldo, N. (2010) Experimental evaluation of high performance base course and road base asphalt concrete with electric arc furnace steel slags. *Journal of Hazardous Materials*, 181, 938-948.

Proctor, D.M., Fehling, K.A., Shay, E.C., Wittenborn, J.L., Green, J.J., Avent, C., Bigham, R.D., Connolly, M., Lee, B., Shepker, T.O. & Zak, M.A. (2000) Physical and chemical characteristics of blast furnace, basic oxygen furnace, and electric arc furnace steel industry slags. *Environmental Science and Technology*, 34 (8), 1576–1582.

Qian, G.R., Sun, D.D., Tay, J.H. & Lai, Z.Y. (2002a) Hydrothermal reaction and autoclave stability of Mg bearing RO phase in steel slag. *British Ceramic Transactions*, 101 (4).

Qian, G.R., Sun, D.D., Tay, J.H., Lai, Z.Y. & Xu, G. (2002b) Autoclave properties of kirschsteinite-based steel slag. *Cement and Concrete Research*, 32 (9), 1377–1382.

Rao, S.R. (2006) Chapter 8: *Metallurgical slags, dust and fumes.* Waste Management Series: Resource Recovery and Recycling from Metallurgical Wastes, 269–327.

Reddy, K.J., Gloss, S.P. & Wang, L. (1994) Reaction of CO_2 with alkaline solid wastes to reduce contaminant mobility. *Water Res.*, 28(6), 1377-1382.

Rögener, F., Sartor, M., Bán, A., Buchloh, D. & Reichardt, T. (2012) Metal recovery from spent stainless steel pickling solutions. *Resources, Conservation and Recycling*, 60, 72–77.

Roskill Information Services (2005) *The Economics of Precipitated Calcium Carbonate*. Roskill Information Services Limited. West Hartford, CT, USA.

Sampling Method MD2 (n.d.) *Division of a sample by quartering*. [Online]. Available from: http://asphalt.csir.co.za/tmh/tmh5/MD2%20%20Division%20of%20a%20sample%20by% 20quartering.pdf [Accessed December 2012].

Sanna, A., Dri, M., Hall, M.R. & Maroto-Valer, M. (2012) Waste materials for carbon capture and storage by mineralisation (CCSM) – A UK perspective. *Applied Energy*, 99 (11), 545-554.

Santos, R.M., Ling, D., Sarvaramini, A., Guo, M., Elsen, J., Larachi, F., Beaudoin, G., Blanpain, B. & Van Gerven, T. (2012) Stabilization of basic oxygen furnace slag by hotstage carbonation treatment. *Chemical Engineering Journal*, 203, 239-250.

Santos, R.M., Van Bouwel, J., Vandevelde, E., Mertens, G., Elsen, J. & Van Gerven, T. (2013) Accelerated mineral carbonation of stainless steel slags for CO_2 storage and waste valorization: Effect of process parameters on geochemical properties. *International Journal of Greenhouse Gas Control*, 17, 32-45.

Shen, D.H., Wu, C.M. & Du, J.C. (2009) Laboratory investigation of basic oxygen furnace slag for substitution of aggregate in porous asphalt mixture. *Construction and Building Materials,* 23, 453-461.

Shen, H. & Forssberg, E. (2003) An overview of recovery of metals from slags. *Waste Manage.*, 23 (10), 933-949.

Shen, H. & Forssberg, E. (2004) Physicochemical and mineralogical properties of stainless steel slag oriented to metal recovery. *Resourse Conserv. Recycl.*, 40, 245–271.

Shen, H., Forssberg, E. & Nordström, U. (2004) Physicochemical and mineralogical properties of stainless steel slags oriented to metal recovery. *Resources, Conservation and Recycling*, 40 (3), 245–271.

Shi, C. (2002) Characteristics and cementitious properties of ladle slag fines from steel production. *Cement Concrete Res.*, 32, 459–462.

Shimadzu (n.d. a) *Products TOC Analyzers*. [Online]. Available from: http://www.shimadzu.com/an/toc/lab/toc-l4.html [Accessed February 2013].

Shimadzu (n.d. b) SSM5000A User Manual.

Škrbic, B. & Mladenovic, N. (2010) Chemometric interpretation of heavy metal patterns in soils worldwide. *Chemosphere,* 80 (11), 1360-1369.

Sora, I.N., Pelosato, R., Botta, D. & Dotelli, G. (2002) Chemistry and microstructure of cement pastes admixed with organic liquids. *Journal of the European Ceramic Society*, 22, 1463-1473.

Sorlini, S., Abbà, A. & Collivignarelli, C. (2011) Recovery of MSWI and soil washing residues as concrete aggregates. *Waste Management*, 31, 289-297.

Steelworld (2008) *An Overview on Refining Technologies for Stainless Steel.* [Online]. Available from: http://www.steelworld.com/tehnology0108.pdf [Accessed July 2013].

Stefanova, A., Aromaa, J. & Forsen, O. (2013, in press) Alkaline leaching of zinc from argon oxygen decarbonization dust from stainless steel production. *Physicochem. Probl. Miner. Process*., 49(1).

Stefanova, A. & Aromaa, J. (2012) *Alkaline leaching of iron and steelmaking dust*. Aalto University publication series. Science + Technology 1/2012. Helsinki, Finland. pp. 72.

Steinour, HH. (1959) Some effects of carbon dioxide on mortars and concrete- discussion. *J. Am. Concr. Inst.*, 30 (2), 905-907.

Tang, M.T., Peng, J., Peng, B., Yu, D. & Tang, C.B. (2008) Thermal solidification of stainless steelmakingdust. *T. Nonferr. Metal Soc.,* 18, 202–206.

Tawfic, T.A., Reddy, K.J., Gloss, S.P. & Drever, J.I. (1995) Reaction of CO_2 with clean coal technology ash to reduce trace element mobility. *Water, Air, Soil Pollut.,* 84, 385-398.

Teir, S., Eloneva, S. & Zevenhoven, R. (2005) Production of precipitated calcium carbonate from calcium silicates and carbon dioxide. *Energy Conversion and Management*, 46 (18–19), 2954-2979.

Teir, S., Eloneva, S., Fogelholm, C.J. & Zevenhoven, R. (2007a) *Carbonation of minerals and industrial by-products for CO_2 sequestration.* In: Proceedings of the 3rd international green energy conference, June 17–21, Västerås, Sweden.

Teir, S., Eloneva, S., Fogelholm, C.J. & Zevenhoven, R. (2007b) Dissolution of steelmaking slags in acetic acid for precipitated calcium carbonate production. *Energy*, 32(4), 528–539.

Teng, Y., Yang, J., Xu, Z. & Zhao, H. (2012) The Leaching of Heavy Metals from Steel Slag in Panzhihua Region. Goldschmidt 2012 Conference Abstracts. Mineralogical Magazine.

Toshiyuki, K. & Akio, K. (1994) *Treatment of Cooling Steelmaking Slag*. Japan Patent, JP06184610, 05 July 1994.

U.S. Department Of The Interior (2005) *Mineral Commodity U.S. Geological Survey*. [Online]. Available from: http://minerals.usgs.gov/minerals/pubs/mcs/2005/mcs2005.pdf [Accessed January 2013].

U.S. Geological Survey (2013) *Mineral Commodity Summaries Iron and Steel Slag.* [Online]. Available   from:

http://minerals.usgs.gov/minerals/pubs/commodity/iron_&_steel_slag/mcs2013fesla.pdf [Accessed July 2013].

UNFCCC, *UN Framework Convention On Climate Change* (1992) Article 2: Objective. [Online]. Available from: http://unfccc.int/essential_background/convention/background/items/1350.php [Accessed May 2013].

US Davis Chemwiki (n.d.) *Powder Xray Diffraction.* [Online]. Available from: http://chemwiki.ucdavis.edu/Analytical_Chemistry/Instrumental_Analysis/Diffraction/Powder_Xray_Diffraction [Accessed July 2013].

US Department of Transportation (1998)*User guidelines for waste and by-product materials in pavement construction.* Federal Highway Administration. Publication No. FHWA-RD-97-148.

USGS (1998) *Survey: Slags Iron and Steel.* Mineral Industry Surveys 1997 Annual Review. U.S. Department of Interior USGS Slag (DOI).

van Oss, H.G. (2003) *Slag Iron and Steel.* [Online]. U.S. Geological Survey Minerals Yearbook 2003. Available from: http://minerals.usgs.gov/minerals/pubs/commodity/iron_&_steel_slag/islagmyb03.pdf [Accessed July 2013].

van Zomeren, A., van der Laan, S.R., Kobesen, H.B.A., Huijgen, W.J.J. & Comans, R.N.J. (2011) Changes in mineralogical and leaching properties of converter steel slag resulting from accelerated carbonation at low CO_2 pressure. *Waste Management*, 31 (11), 2236-2244.

Wahlström, M., Laine-Ylijoki, J., Kaartinen, T., Hjelmar, O. & Bendz, D. (2009) *Acid neutralization capacity of waste – Specification of requirement stated in landfill regulations.* Norden, Nordic Council of Ministers, Copenhagen.

Wedding, C.G. & Brown, C.D. (2007) Measuring site-level success in brownfield redevelopments: A focus on sustainability and green building.[Online]. *Journal of Environmental Management*, 85 (2), 483-495. Available from: http://www.sciencedirect.com/science/article/pii/S0301479706003239.

World Bank (2010) *The management of Brownfield Redevelopment- A Guidance Note.* [Online]. World Bank, Europe and Central-Asia Region, Sustainable Development Department. Available from: http://www-wds.worldbank.org/external/default/WDSContentServer/WDSP/IB/2010/06/14/00033303

7_20100614004032/Rendered/PDF/550090WP0P118011PUBLIC10brownfields.pdf [Accessed November 2013].

World Steel Association (2010) Statistics Archive. [Online] Available from: http://www.worldsteel.org/statistics/statistics-archive.html [Accessed July, 2013].

Wu, L. & Themelis, N.J. (1993) The flash reduction of electric arc furnace dusts. *JOM*, 44, 35–39.

Wuana, R.A. & Okieimen, F.E. (2011) Heavy Metals in Contaminated Soils: A Review of Sources, Chemistry, Risks and Best Available Strategies for Remediation. International Scholarly Research Network (ISRN) *Ecology*, 2011, number 402647. pp. 20.

Xia, D.K. & Pickles, C.A. (1999) Caustic roasting and leaching of electric arc furnace dust. *Canadian Metallugical Quarterly*, 38 (3), 175–186.

Xue, Y., Wu, S., Hou, H. & Zha, J. (2006) Experimental investigation of basic oxygen furnace slag used as aggregate in asphalt mixture. *Journal of Hazardous Materials*, B138, 261-268.

Ye, G., Burström, E., Kuhn, M. & Piret, J. (2003) Reduction of steelmaking slags for recovery of valuable metals and oxide materials. *Scandinavian Journal of Metallurgy*, 32, 7–14.

Yeung, A.T. & Gu, Y.Y. (2011) A review on techniques to enhance electrochemical remediation of contaminated soils. *Journal of Hazardous Materials*, 195, 11-29.

Yi, H., Xu, G., Cheng, H., Wang, J., Wan, Y. & Chen, H. (2012) An Overview of Utilization of Steel Slag. *Procedia Environmental Sciences*, 16, 791-801.

Yildirim, I.Z. & Prezzi, M. (2011) Chemical, Mineralogical, and Morphological Properties of Steel Slag. *Advances in Civil Engineering*, 2011, number: 463638. pp. 13. Available from: http://www.hindawi.com/journals/ace/2011/463638/ [Accessed July 2013].

Youcai, Z. & Stanforth, R. (2000) Integrated hydrometallurgical process for production of zinc from electric arc furnace dust in alkaline medium. *J. Hazard. Mater.,* B80, 223–240.

Zevenhoven, R., Eloneva, S. & Teir, S. (2006) Chemical fixation of CO_2 in carbonates: Routes to valuable products and longterm storage. *Catalysis Today*, 115 (1-4), 73-79.

Zhang, H. & Hong, X. (2011) An overview for the utilization of wastes from stainless steel industries. *Resources, Conservation and Recycling*, 55, 745–754.

Zhang, X.Y., Zhang, H., He, P.J., Shao, L.M., Wang, R.Y. & Chen, R.H. (2008) Beneficial reuse of stainless steel slag and its heavy metals pollution risk. *Res. Environ. Sci*., 21 (4), 33–37 (in Chinese).

Ziock, H.J., Lackner, K.S. & Harrison, D.P. (2000) *Zero emission coal power, a new concept*. In: Proceedings of the 1st US National Conference on Carbon Dioxide Sequestration. DOE Publications, Washington DC.

Zovko, M. & Romic, M. (2011) *Soil Contamination by Trace Metals: Geochemical Behaviour as an Element of Risk Assessment, Earth and Environmental Sciences*. Dr. Imran Ahmad Dar (Ed.). Available from: http://www.intechopen.com/books/earth-and-environmental-sciences/soil-contamination-by-trace-metals-geochemical-behaviour-as-an-element-of-risk-assessment [Accessed July 2013]

Zunkel, D. (1996) What to do with your EAF dust. *Steel Times Int.,* 20, 46–50.

Front page pictures

http://i.ehow.com/images/a04/rs/8r/soil-pollution-4.1-800X800.jpg

http://www.africancolours.com/african-art-news/614/congo,%20(drc)/picha_encounters_2010_lubumbashi_biennal.htm

http://oxideclass.mushriquiart.com/

http://www.panoramio.com/photo/17129774

http://www.airphotona.com/image.asp?imageid=11210

http://www.personal.psu.edu/lhs126/StainlessSteelSensitizationPics.html

http://www.ceholt.com/service/refurbishing-equipment

APPENDIX

Table A: Limits of quantification (LOQ) of the ICP-OES for specific elements (mg/l).

Element	LOQ
Al	0.004
As	0.04
Ba	0.00024
Be	0.00026
Bi	0.022
Ca	0.014
Cd	0.0015
Co	0.0036
Cr	0.0015
Cu	0.0025
Fe	0.0027
Hg	0.0026
K	0.04
Li	0.019
Mg	0.001
Mn	0.001
Mo	0.02
Na	0.0016
Ni	0.0045
Pb	0.0015
Sb	0.035
Se	0.11
Si	0.2
Sn	0.02
Tl	0.048
V	0.002
Zn	0.001

Table B: Data on the elemental composition obtained through alkaline fusion.

Element	fine	interm	coarse	LOQ
Al	17317.48	26925.79	29845.86	0.004
As	21.50	20.48	24.13	0.041
Ba	297.06	359.19	389.27	0.00024
Be	0.00	0.00	0.00	0.022
Bi	25.74	30.80	30.01	0.014
Ca	310376.57	315633.16	295579.84	0.0015
Cd	0.00	0.00	0.00	0.0015
Co	0.00	0.00	0.00	0.0036
Cr	29878.62	43117.88	40177.20	0.0015
Cu	305.57	157.30	410.93	0.0025
Fe	19918.74	38619.00	37654.13	0.0027
Hg	11.25	5.46	3.63	0.0026
K	833.38	1206.94	2038.27	0.04
Mg	16382.54	18389.32	17761.40	0.001
Mn	8987.49	12770.01	11871.61	0.001
Mo	31.79	64.93	65.37	0.02
Na	1046.59	1454.17	1806.95	0.016
Ni	518.30	1291.15	1313.67	0.0045
Pb	20.95	22.17	24.44	0.0015
Sb	276.89	348.30	327.54	0.035
Si	91607.84	102875.88	100949.31	0.2
Sn	24.89	13.28	10.87	0.021
Tl	0.00	0.00	0.00	0.048
V	630.16	1009.11	911.47	0.002
Zn	80.52	105.81	133.38	0.001

Table C: Detailed data of the ANC test.

Sample #	VH2O (ml)	VHNO3 (ml)	m AOD (g)	HNO3 (meq/g)	pH	T
1,00	40,00	0,00	4,05	0,00	12,43	24,30
2,00	39,00	1,00	4,00	0,50	12,00	24,20
3,00	38,00	2,00	4,01	1,00	11,82	24,30
4,00	37,00	3,00	4,02	1,49	11,55	24,20
5,00	36,00	4,00	4,01	2,00	11,10	24,30
6,00	32,00	8,00	4,00	4,00	9,50	24,10
7,00	28,00	12,00	4,00	6,00	8,16	23,90
8,00	24,00	16,00	4,01	7,98	6,03	24,30
9,00	20,00	20,00	4,00	10,00	5,54	24,30
10,00	16,00	24,00	4,01	11,97	5,09	24,40
11,00	12,00	28,00	4,01	13,97	4,32	23,90
12,00	8,00	32,00	4,00	16,00	3,59	24,00
13,00	4,00	36,00	4,01	17,96	3,23	23,90
14,00	0,00	40,00	3,99	20,05	2,60	24,10